DEVELOPMENT OF IMMUNOASSAYS FOR SPECIFIC CLASSICAL AND LECTIN PATHWAY ACTIVATION MARKERS

PhD Thesis for a double Doctor of Philosophy degree under the
Marie Skłodowska-Curie Action European Doctorate Program "CORVOS"

Lisa Hurler

Doctoral School of Theoretical and Translational Medicine
Semmelweis University, Budapest, Hungary
and
Institute of Hygiene and Medical Microbiology,
Medical University of Innsbruck, Innsbruck, Austria

Supervisors:	Zoltán Prohászka, MD, DSc
	Reinhard Würzner, MD, PhD
Official reviewers:	Tamás Németh, MD, PhD
	Doris Wilflingseder, PhD

Head of the Complex Examination Committee:	Alán Alpár, MD, DSc
Members of the Complex Examination Committee:	Miklós Kellermayer, MD, DSc
	Mihály Kovács, DSc

Budapest and Innsbruck

April 2023

EXPLANATION OF THE DOUBLE DEGREE & DOCTORAL PROGRAMME CORVOS

CORVOS, for COmplement Regulation and Variations in Opportunistic infectionS is an ambitious pan-European initiative of 10 European universities, five research institutes/public health bodies, three biomedical companies and two hospitals that comprises an interdisciplinary doctoral programme including cross-sectoral secondments and training in transferable skills. CORVOS is/was funded by the EU Marie Skłodowska Curie action (MSCA, 860044) from 2019 until 2024.

Thirteen internationally renowned multidisciplinary scientists lead CORVOS and the plan is that 15 highly motivated Early-Stage-Researchers (ESRs) widely recruited in 2020 and 2021 publicly defend their scientific discoveries in the understanding of the role of complement in opportunistic infections in 2023 and 2024 (Figure 1).

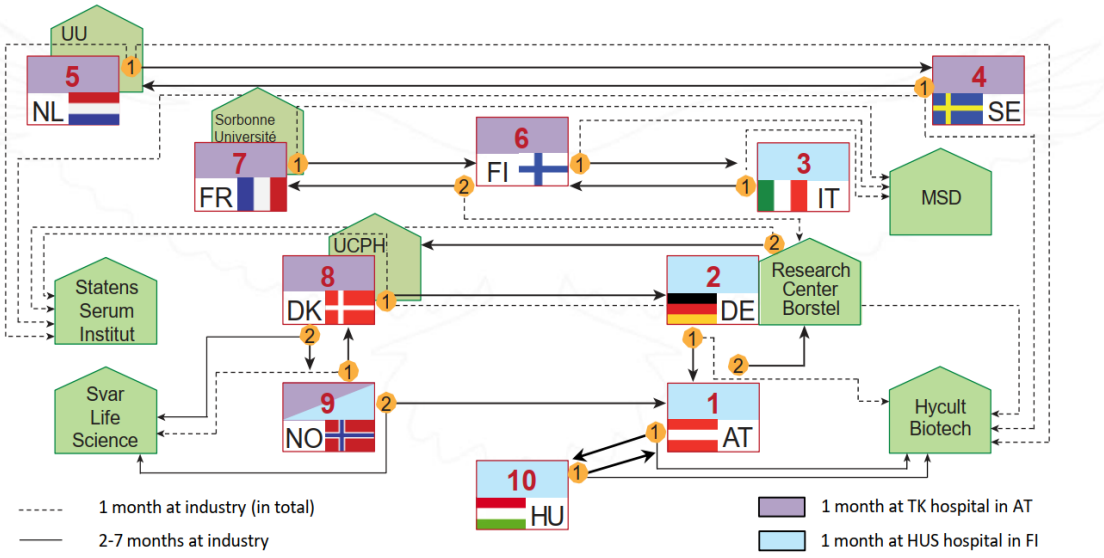

Figure 1: CORVOS Secondment Plan.

As inspired alumni, these ESRs will be jointly awarded a "Double PhD degree" from two European universities and, equipped with entrepreneurial and clinical skills, prepared for their future careers in a constantly changing society.

The ESR HU-1, **Lisa Hurler**, has

- performed the majority of her scientific work at **Semmelweis University, Budapest** under the supervision of Prof. Zoltán Prohászka (01.03.-02.10.20, and 01.04.-21.11.21, and 18.12.21-12.06.22, and 10.01-28.02.23);
- stayed for 6 months during her **academic secondment at Med. University Innsbruck** under the supervision of Prof. Reinhard Würzner (10.07.22-09.01.23),
- did her **clinical training at the University Hospital of Helsinki** (22.11.-17.12.21),
- her **industrial entrepreneurship at Hycult Biotech** (13.06.-08.07.22), and
- her **industrial secondment at Hycult Biotech** (03.10.20-31.03.21).

After a successful defence of her PhD thesis in Budapest, obeying the rules of both universities, **Lisa Hurler** will obtain

-a **"Double PhD degree"** from **Semmelweis University Budapest, and Medical University of Innsbruck**

which is summarized and written in a single PhD thesis. Therefore, it is considered as one (!) degree (one doctorate) issued together by two universities.

Reinhard Würzner, Medical University of Innsbruck, Speaker of CORVOS.

STATEMENT OF ORIGINALITY

I, Lisa Hurler, declare that I have authored this thesis independently, that I have not used other than the declared sources/resources, and that I have explicitly marked all material which has been quoted either literally or by content from the used sources.

This work has not previously been submitted for a degree or diploma in any university.

EIDESSTATTLICHE ERKLÄRUNG

Ich, Lisa Hurler, erkläre an Eides statt, dass ich die vorliegende Arbeit selbstständig verfasst, andere als die angegebenen Quellen/Hilfsmittel nicht benutzt, und die den benutzten Quellen wörtlich oder inhaltlich entnommenen Stellen als solche kenntlich gemacht habe.

Diese Arbeit wurde bisher bei keiner Hochschule oder Universität zur Erlangung eines akademischen Abschlusses oder Diploms eingereicht.

TABLE OF CONTENTS

LIST OF FIGURES

LIST OF EQUATIONS

LIST OF TABLES

KEY WORDS

C1-INH complexes • early complement activation • C1s/C1-INH complex • classical pathway activation • MASP-1/C1-INH complex • lectin pathway activation • assay development and validation • coronavirus infection • COVID-19 • severe acute respiratory syndrome coronavirus 2 • mannose binding lectin • Sepsis

LIST OF ABBREVIATIONS

%CV	coefficient of variation
aHUS	Atypical hemolytic uremic syndrome
AP	Alternative pathway
APC	antigen-presenting cell
BSA	bovine serum albumin
C1-INH	C1 esterase inhibitor
C4BP	C4b binding protein
CCP	Complement control protein
COVID-19	Coronavirus Disease 2019
CP	Classical pathway
CR1	Complement receptor type 1
CRP	C-reactive protein
DAF	Decay Accelerating Factor
DAMP	Damage-associated molecular pattern
EBV	Epstein-Barr-virus
EDTA	Ethylendiamintetraacetat
EGF	Epidermal-growth factor
EGTA	ethylene glycol-bis(β-aminoethyl ether)-N,N,N′,N′-tetraaceticacid
ELISA	enzym-linked immunosorbent assay
FACS	Fluorescence Activated Cell Sorting
FB	Factor B
FD	Factor D
FH	Factor H
FI	Factor I
FXII	Factor XII
HAE	Hereditary angioedema
HC	Healthy controls
HIV	Human immunodeficiency virus
HRP	Horseradish peroxidase
IFN-γ	Interferon gamma
Ig	immunoglobulin

IL	Interleukin
LloQ	Lower limit of quantification
LP	Lectin pathway
LPS	lipopolysaccharide
LRP	Low Density Lipoprotein Receptor-related Protein
mAb	monoclonal antibody
MAC	Membrane attack complex
MASP-1/-2/-3	Mannan-binding lectin serine protease 1 / 2 / 3
MBL	mannose-binding lectin
MCP	Membrane cofactor protein
MERS-CoV	middle east respiratory syndrome coronavirus
MHC	Major Histocompatibility Complex
MIS-C	Multisystem Inflammatory Syndrome in Children
N protein	SARS-CoV-2 nucelocapsid protein
NA	Not available
NET	Neutrophil extracellular traps
NHS	Normal human serum
NK	Natural Killer
ns	Non-significant
OD	Optical density
PAMP	Pathogen-associated molecular pattern
PBS	phospate-buffered saline
PRR	Pattern Recognition Receptor
PTX3	Pentraxin 3
R	correlation coefficient
R^2	coefficient of determination
RA	Rheumatoid arthritis
S protein	SARS-CoV-2 spike protein
SAP	Serum amyloid protein
SARS-CoV	severe acute respiratory syndrome coronavirus
SARS-CoV-2	Severe acute respiratory syndrome coronavirus 2
SD	Standard deviation

SDS	sodium dodecyl sulfate
SLE	systemic lupus erythematosu
SNP	Single nucleotide polymorphism
SP	Serine protease
TBS	Tris-buffered saline
TCC	terminal complement complex
TLR	Toll-like receptor
TMB	3,3′,5,5′-Tetramethylbenzidin
TNF-α	Tumor necrosis factor alpha
TP	Terminal pathway
UloQ	Upper limit of quantification
VBS	Veronal-buffered saline
WB	Western blot
ZAS	Zymosan-activated serum

SUMMARY

Assessing complement activation typically involves measurement of split products downstream of C3, indicating activation of all three complement pathways. Although C4d can distinguish CP/LP from AP activation, no validated assays were available commercially to differ between early classical and early lectin pathway activation.

C1 esterase inhibitor (C1-INH) is tightly regulating classical and lectin pathway activation via formation of covalent complexes with the respective activated serine proteases (C1r and C1s for the CP, MASP-1 and MASP-2 for the LP), making C1-INH complexes promising biomarkers to monitor early CP and LP activation.

Within the scope of this thesis, immunoassays measuring levels of C1s/C1-INH complex and MASP-1/C1-INH complex in human serum and plasma were therefore developed and characterized. In *in vitro* activation experiments, the use of C1-INH complexes as suitable markers for early classical and early lectin pathway activation was validated, and the complex levels were analysed in healthy individuals (n = 96) to define a first reference range. In addition, C1-INH complex levels were investigated in pathological samples of infectious diseases, where C1-INH complex concentrations were significantly increased *in vivo* in COVID-19 (n = 343), and associated with disease severity. Besides that, lectin pathway activation was mainly independent of the genetic variants of its key pattern recognition molecule MBL, although SARS-CoV-2 had an effect on MBL levels during the infection. Furthermore, genetic variations in *MBL2* were not associated with susceptibility to SARS-CoV-2, mortality, or the development of Long COVID.

The C1s/C1-INH and MASP-1/C1-INH complex assays were further validated in a cohort of sepsis patients (n = 70), where both complexes were significantly increased in the pathological samples when compared to healthy controls.

In conclusion, it was shown that C1s/C1-INH and MASP-1/C1-INH complexes are specific biomarkers to measure early classical and early lectin pathway activation, respectively. Measurement of C1-INH complex levels in the future can thereby provide valuable information about specific early classical or lectin pathway activation *in vitro* and *in vivo*.

ZUSAMMENFASSUNG

Die Beurteilung von Komplementaktivierung umfasst typischerweise die Messung von Produkten nach der Spaltung von C3 oder C5, was auf die Aktivierung aller drei Komplementwege hinweist. Obwohl mittels C4d CP/LP von AP-Aktivierung unterschieden werden kann, waren keine validierten Assays kommerziell erhältlich, um zwischen der Aktivierung des frühen klassischen und des frühen Lektinwegs zu unterscheiden. C1-Inhibitor (C1-INH) reguliert die Aktivierung des CP und LP durch die Bildung kovalenter Komplexe mit entsprechenden aktivierten Serinproteasen (C1r und C1s für den CP, MASP-1 und MASP-2 für den LP), was C1-INH-Komplexe zu vielversprechenden Biomarkern zur Überwachung der frühen CP- und LP-Aktivierung macht.

Aus diesem Grund wurden im Rahmen dieser Arbeit Immunoassays entwickelt und charakterisiert, die die Messung des C1s/C1-INH-Komplexes und des MASP-1/C1-INH-Komplexes in menschlichem Serum und Plasma erlauben. In *in vitro* Aktivierungsexperimenten wurde die Verwendung von C1-INH-Komplexen als geeignete Marker für frühe klassische und Lektinwegs-Aktivierung validiert, und zur Definition eines ersten Referenzbereiches die Komplex-Konzentrationen in gesunden Personen (n = 96) analysiert. Darüber hinaus wurden die C1-INH-Komplexspiegel in pathologischen Proben von Individuen mit Infektionskrankheiten untersucht. Hierbei wurde gezeigt, dass C1-INH-Komplexkonzentrationen *in vivo* in COVID-19 (n = 343) signifikant erhöht und mit der Schwere der Erkrankung assoziiert waren. Dennoch war die Aktivierung des Lektinwegs größtenteils unabhängig von den genetischen Varianten seines wichtigsten Pattern Recognition Rezeptors (PRRs) MBL, obwohl SARS-CoV-2 im Laufe der Infektion einen Einfluss auf die MBL-Spiegel haben kann. Darüber hinaus waren genetische Varianten in *MBL2* auch nicht mit Suszeptibilität für SARS-CoV-2, Mortalität, oder der Entwicklung von Long COVID assoziiert. Desweiteren wurden die neuen Immunoassays in Sepsispatienten (n = 70) validiert, wo Level beider Komplexe in den pathologischen Proben signifikant erhöht waren.

Zusammenfassend konnte gezeigt werden, dass C1s/C1-INH- und MASP-1/C1-INH-Komplexe spezifische Biomarker zur Bestimmung der Aktivierung des klassischen bzw. Lektinwegs sind, und deren Messung in Zukunft wertvolle Informationen über die spezifische Aktivierung der beiden Signalwege *in vitro* und *in vivo* liefern kann.

1 INTRODUCTION

1.1 The Immune System

The immune system comprises two distinct lines of defense: the innate and the adaptive immunity (see Figure 2), while there is also much interaction between the two of them (1, 2).

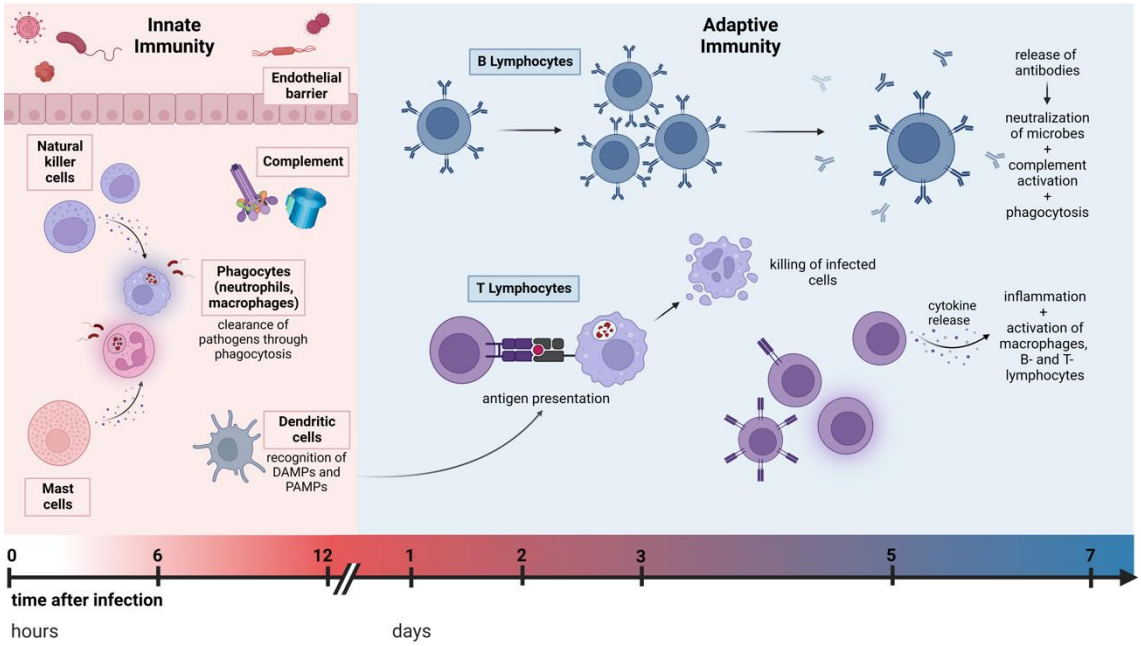

Figure 2: Overview of key players and effector functions of the innate and adaptive immune system. Innate immunity is always present and the main functions are to act as a barrier against pathogens, as well as to recognize and eliminate damaged cells and pathogens. Later on during an infection, adaptive immunity develops as a response to invading pathogens, triggered by the activation of lymphocytes. B lymphocytes expand and secrete antibodies, which are able to neutralize infected cells, activate the complement system and are involved in phagocytosis. T lymphocytes recognize antigens from antigen-presenting cells, which leads to the direct killing of infected cells as well as to the release of cytokines, which subsequently enhances inflammation and activates macrophages, B and T lymphocytes. For more details see chapter 1.1. Figure created with BioRender.com.

1.1.1 Innate Immunity

Innate immunity, also referred to as native or natural immunity due to its constant presence without any triggers, is the initial, antibody-independent defense mechanism against invading pathogens and tissue injury, active in the first few hours of encountering an infection. It is therefore crucial for host defense before adaptive immunity can develop. Innate immunity has three major functions: acting as a barrier against invading microorganisms, detecting damaged cells and pathogens in host tissue via damage-associated molecular patterns (DAMPs) and pathogen-associated molecular patterns

(PAMPs), and eliminating them through various effector functions (reviewed in detail in (1, 3)).

The humoral arm of the innate immune system is the complement system, which will be explored in further detail in chapter 1.2. Alongside the humoral immune response, there is also the cellular part in innate immunity (3). Acting as the primary interface between the external environment and the host, epithelial barriers serve mainly as a physical barrier, protecting the skin, respiratory tract, as well as the gastrointestinal tract from the invasion of external pathogens (4). Besides that, they can produce and secrete antimicrobial molecules (5) and contain lymphocytes that secrete cytokines, activate phagocytes, and thereby kill infected cells (4). Additionally, the epithelial barrier, in conjunction with connective tissues, also contains mast cells that release proinflammatory cytokines upon tissue injury or infection (6).

Pathogens able to breach epithelial barriers are eliminated through phagocytosis by phagocytes, which can sense DAMPs and PAMPs through their pattern-recognition receptors (PRRs) (7). One of the most important pattern recognition receptors of the innate immune system are toll-like receptors (TLRs) (8). Although there are at least ten different TLRs in humans, the most profound roles during microbial infections have TLR4, recognizing mainly LPS, and TLR2, having a very broad range of PAMPs (8). Activation of TLRs and other PRRs triggers downstream transcriptional stimulation, ultimately resulting in the expression of several proinflammatory cytokines such as IL-6, IL-1β, TNF-α, and type I interferons (9). Those specific signals, sent from the site of infection or injury, recruit phagocytes like neutrophils, dendritic cells (DCs), natural killer cells (NKs), and macrophages (10, 11). Neutrophils make up around half of the circulating leukocytes, and in addition to phagocytosis and the secretion of cytokines, they were also shown to form neutrophil extracellular traps (NETs), physical barriers containing DNA and granule proteins, which can trap pathogens (12). Natural killer cells primarily destroy viral and bacterial infected cells and secrete IFN-y, which triggers phagocytosis by macrophages (13). Dendritic cells, located in host tissues, are also involved in the recognition of invading pathogens via several pattern recognition receptors (14, 15). Furthermore, DCs serve as a bridge between the innate and adaptive immune system by presenting antigens to lymphocytes (15, 16).

1.1.2 Adaptive immunity

Adaptive immunity, also called acquired immunity, develops as a response to infections, and hence takes several days or weeks to become fully active (17). In contrast to innate immunity, the adaptive immune response is highly specific (17). As triggers, antigens, derived from the microbe or altered host-cell, are presented to lymphocytes by antigen-presenting cells (APCs) and activate them. The most specialized APCs are DCs (15, 18), but monocytes and macrophages also participate in antigen presentation via major histocompatibility complex (MHC) I or II proteins (19). To keep pace with rapidly increasing pathogen amounts during an infection, lymphocytes undergo clonal expansion, resulting in an enhanced number of cells deriving from one single clone and hence expressing identical receptors for the given antigen (17).

There are two major groups of lymphocytes, namely B and T lymphocytes. The latter (around 80-90 % of lymphocytes circulating in human blood) play a crucial role in cell-mediated immune response, while B lymphocytes (10-20 %) account for the humoral part of adaptive immunity (20). When activated, B lymphocytes proliferate and secrete antibodies recognizing specific antigens (21). Those antibodies help in neutralizing and eliminating pathogens or their toxins, which are located outside of cells.

On the other hand, T lymphocytes are specifically designed to target infected host cells, when the pathogens are not accessible for circulating antibodies directly (17). Through antigen-presentation of infected cells or pathogens in phagocytes, cytotoxic T lymphocytes ($CD8^+$) recognize them and can thereby immediately kill infected cells (22). Besides that, activation of helper T lymphocytes ($CD4^+$) results in the release of cytokines, which not only triggers inflammation but also activates macrophages, further strengthening the immune response (23). Additionally, proliferation and differentiation of other T and B lymphocytes can also be triggered or suppressed by regulatory T lymphocytes (24). Besides the development of a specific response towards antigens, the adaptive immune system is also in charge of the generation of an immunologic memory. Long-lived memory B and T cells develop upon first contact with an antigen, and can be activated rapidly when the host is challenged with the same pathogen in the future, which enables a very quick and robust immune response (25). The release of specific antibodies can also give rise to the activation of the complement system, as described below.

1.2 Overview of the Complement System and its Biological Roles

The complement system is an important player of the immune system in the interface between innate and adaptive immunity, and acts as a first-line defence in the elimination of invading pathogens, circulating immune complexes and apoptotic cells. It is composed of more than 50 plasma proteins, mainly expressed in the liver (26, 27). While most of those proteins circulate in an inactive (zymogen) form, the system acts in a cascade-like manner and can be activated via three different pathways: the classical (CP), the lectin (LP) and the alternative pathway (AP) (reviewed in (28-31)). An overview of the three different pathways, ultimately converging in the common terminal pathway (TP), is displayed in Figure 3. The different steps thereof are discussed in the following chapters. Activation of all three pathways results in the formation of a C3 convertase, able to cleave C3 into C3a and C3b. C3a acts as an anaphylatoxin and mediates inflammation, while C3b binds to target structures, initially triggering complement activation (32). C3b-opsonized structures are recognized by complement receptor 1 (CR1), expressed on erythrocytes, and subsequently transported to the liver for phagocytosis. Additionally, C3b can also bind to the C3 convertase, leading to the formation of the C5 convertase (33). The C5 convertase is responsible for cleaving C5 into C5a and C5b. Similar to the C3 split products, C5a is an anaphylatoxin recruiting phagocytes to the site of inflammation, while C5b binds non-covalently to target structures, initiating the terminal complement pathway. The complement components C6, C7, C8, and C9 then associate with the bound C5b, ultimately leading to the assembly of the terminal complement complex (TCC/C5b-9) (34). Called the membrane attack complex (MAC complex) when formed on a target membrane, C5b-9 is generating a pore able to osmotically lyse or opsonize the targeted cell (35).

Initially, the complement system was discovered for its capability to lyse cell membranes upon pathogen recognition via PAMPs (36). Nevertheless, protection against invading microbes via opsonisation and lytic killing is not the only biological function of the complement system. While the targeting of modified host cells is happening through the recognition of DAMPs, the complement system can furthermore distinguish between self and non-self and clear the host from damaged self-structures (37).

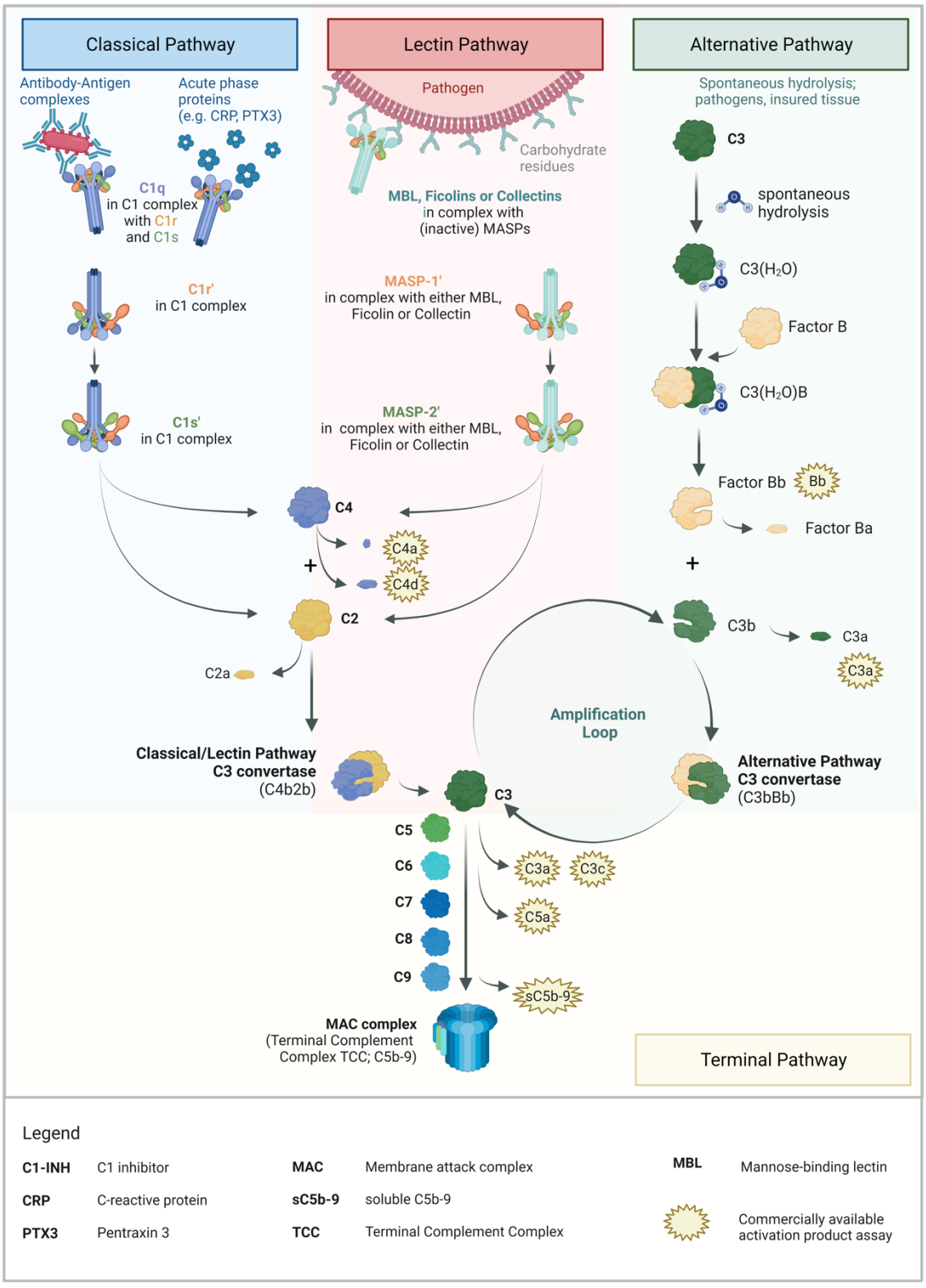

Figure 3: Overview of the complement system. For explanations and further details see chapters 1.2.1, 1.2.2 and 1.2.3. Commercially available assays measuring complement activation products are highlighted on the figure. Figure created with BioRender.com. Figure taken and adapted with permission from Hurler *et al.* (38), under the terms of the Creative Commons Attribution License (CC BY), https://creativecommons.org/licenses/by/4.0/.

Additionally, anaphylatoxins such as C3a and C5a act as chemoattractants to recruit neutrophils (39), mast cells (40), as well as activated T and B lymphocytes (41, 42) to the site of inflammation, thereby bridging innate and adaptive immune responses. When it comes to tissue homeostasis, the complement system can control tissue differentiation as well as regeneration (43, 44). Some functions only discovered in recent years are the participation in the regulation of reproduction and pregnancy (45) and the involvement in aging via the *Wnt* signaling pathway (46). Recently, the complement system has also been linked to different pathological conditions, such as neurodegenerative diseases (47) and cancer (48, 49).

1.2.1 The Alternative Pathway (and its Regulation)

The alternative pathway is the most abundant pathway under physiological circumstances and was originally discovered in the 1950s by Pillemer *et al.* (50). Unlike the classical and lectin pathways, which are activated through specific interactions between either two proteins or proteins and carbohydrates (for the detailed mechanism see chapters 1.2.2 and 1.2.3), the alternative pathway is activated through spontaneous hydrolysis of C3, also called the „tickover mechanism" (51, 52). This autoactivation causes conformational changes in C3, leading to the formation of the bioactive form C3(H_2O) (53). The altered C3 associates with Factor B (FB), followed by conformational changes in FB. The substrate is then cleaved by the serine protease Factor D (FD), leading to the two split fragments Ba and Bb (54). The latter stays associated with the C3 complex, forming the fluid phase C3 convertase C3(H_2O)Bb, which can cleave additional C3 molecules into C3a and C3b (55-57). Generated C3b does associate with Factor B, thereby increasing the amount of C3 convertase. This effect is further enhanced by properdin, which stabilizes the protein-protein interactions (58).

Besides the spontaneous activation through hydrolysis, the alternative pathway can also act as an „amplification loop", activated through fixed C3b generated during CP or LP activation (59). Downstream activation occurs similar to the just described tickover mechanism through binding of Factor B to C3b and enhancement of the alternative C3 convertase concentration (60).

Although the C3 convertase irreversibly decays within minutes after formation (61), huge amounts of C3b can still be generated during the short life-span, which could cause

damage to host cells. To prevent this, membrane-associated regulators are specifically important in protecting unaltered host cells from being targeted by the complement system and in keeping complement activation in check (62).

The decay-accelerating factor (DAF, CD55) dissociates the C3 convertase by binding to C4b and C3b fragments (63, 64). The membrane cofactor protein (MCP, CD46), on the other hand, decreases AP activation by degrading C3b/C4b in the presence of factor I (FI), a fluid phase regulator, as a cofactor (65, 66). Furthermore, complement receptor 1 (CR1, CD35) acts as a cofactor for these two regulators and can also lead to dissociation of the convertase (67), while CD59 acts on the terminal pathway by preventing the formation of the MAC complex through binding to C8 and C9 (68, 69).

Whereas membrane-associated regulators only protect the host cells, soluble regulators are additionally effective against invading pathogens. Factor I (FI) for instance is able to cleave C3b into an inactive form (iC3b), where the cleavage rate can further be enhanced by factor H (FH) (70). FH, the most important regulator of the alternative pathway, has an important role in marking self surfaces via glycan markers in order to avoid complement activation (71). Additionally, it can stimulate fragment Bb to dissociate from C3 convertases, slowing down the consumption of C3 and *de novo* generation of AP C3 convertases (72). Similarly, classical C3 convertases can be dissociated into C2b and C4b through the C4 binding protein (C4BP) (73, 74). Further down in the cascade, MAC assembly on target membranes can be prevented through the binding of clusterin or vitronectin (75, 76).

1.2.2 The Classical Pathway (and its Association with Immune Complexes)

The classical pathway is mainly activated through the binding of its sole pattern recognition molecule C1q to the Fc-region of IgG- or IgM-containing circulating antibody-antigen complexes. Of note, only antibodies associated with antigens give rise to CP activation, while circulating free antibodies cannot activate the classical pathway due to reduced affinity to C1q (77). Besides that, there are significant differences in the capability to activate complement between different immunoglobulin isotypes (78). Whereas classical pathway activation is highest by IgG1, IgG3 and IgM are also very effectively fixing complement. Weak complement activation is observed by IgG2, while IgG4 and other immunoglobulins (IgA, IgE, IgD) are not able to activate the classical pathway (78).

Immune-complex independent activation is also possible through direct interaction between C1q and acute phase proteins such as the C-reactive protein (CRP), serum amyloid P component (SAP) or Pentraxin 3 (PTX3) (79-83). Additionally, C1q was also shown to directly bind to lipopolysaccharides on the surface of bacteria (84), surface proteins from viruses such as EBV and HIV-1 (85), and apoptotic cells (86, 87).

C1q, which is mainly produced extra-hepatically by monocytes, macrophages, and dendritic cells (88, 89), is a hexameric molecule. Each subunit of C1q is consisting of polypeptide chains A, B and C, encoded by *C1QA, C1QB* and *C1QC*, respectively (90).

The pattern recognition molecule is associated with complement components C1r and C1s in a calcium-dependent manner, making up the C1 complex ($C1qC1r_2C1s_2$), comprising of one C1q and two pairs of serine proteases C1r and C1s (91). Binding of the C1q globular heads to a target surface or an activating agent causes structural changes in the C1q, allowing activation of the serine protease domain of C1r through auto-cleavage (92, 93). Active C1r (C1r') is then able to activate zymogen C1s, followed by proteolytic cleavage of C4 and C2, formation of the classical C3 convertase (C4b2b), and complement activation downstream of C3, as illustrated in Figure 3.

1.2.3 The Lectin Pathway (and its Key Pattern Recognition Molecule MBL)

The lectin pathway was only discovered in 1987 and shows high similarities with the classical pathway (94). However, in contrast to the classical pathway, lectin pathway activation can occur through a variety of pattern-recognition molecules, including collectins mannan-binding lectin (MBL), collectin-10 and collectin-11, as well as ficolins (ficolin-1, ficolin-2 and ficolin-3) (94-97). Those pattern-recognition molecules are associated with MBL-associated serine proteases (MASP-1 to -3), the small MBL-associated protein (sMAP or MAp19) (98), and the MBL/ficolin-associated protein-1 (MAP-1/MAp44) (99, 100). After recognition of foreign carbohydrate structures or acetyl groups on the surface of pathogens such as bacteria, viruses, or funghi, zymogen MASP-1 can autoactivate and subsequently cleave MASP-2 (101). While active MASP-2 (MASP-2') can cleave both C4 and C2, active MASP-1 (MASP-1') is only able to cleave C2 of the central complement components (102). Nevertheless, MASP-1' is converting zymogen MASP-2, thereby further enhancing the proteolytic cleavage of C2 and C4, C3 convertase formation and downstream complement activation (103, 104).

MASP-3, MAp19 and MAp44, resulting from alternative splicing of *MASP1* and *MASP2* (98, 99), are not capable to directly activate the lectin pathway. While MASP-3 is speculated to play a role in alternative pathway initiation through activation of Factor B and D (105), the two non-enzymatic proteins MAp19 and MAp44 are proposed to have a regulatory role during lectin pathway activation (99, 100, 106), although still debated (98).

The key pattern recognition molecule of the lectin pathway is mannan-binding lectin (MBL). MBL acts as an acute phase protein (107) and belongs to the collectin family (108). In accordance with other pattern recognition molecules of the complement system, MBL is a multimeric protein, consisting of identical polypeptide chains (108). The single polypeptide chains comprise of a cystein-rich crosslinking region, a collagen-like region, a short hydrophobic neck region and a C-terminal, Ca^{2+}-dependent carbohydrate-recognition domain (see Figure 4A) (109).

The protein is encoded by the *MBL2* gene located on chromosome 10q11.2-p21, and the functional concentration of MBL in serum is mainly determined genetically. The *MBL2* gene consists of four exons (see Figure 4B) and may contain several promoter and structural gene polymorphisms (reviewed in (109-111)).

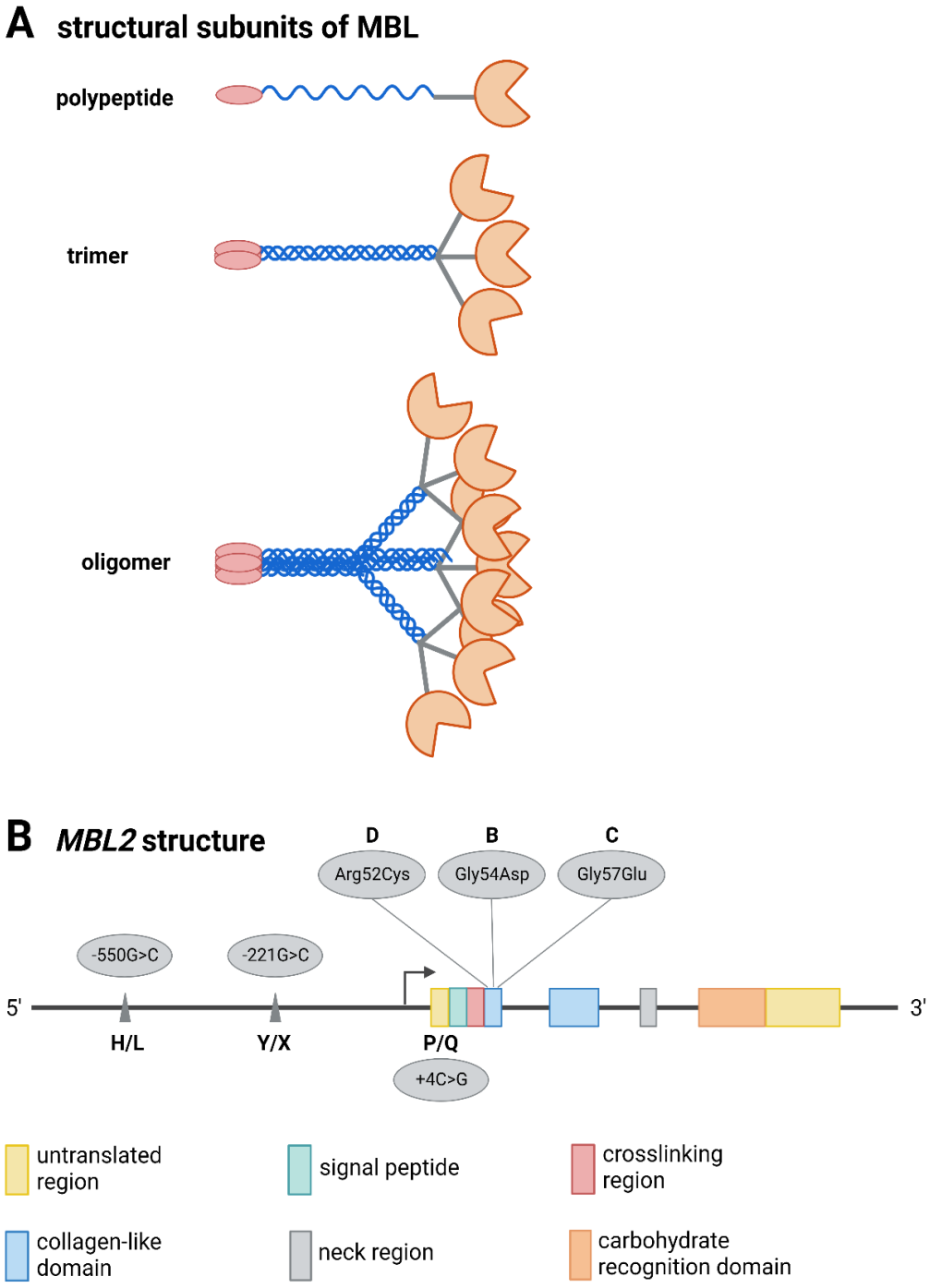

Figure 4: Overview of MBL protein subunits and *MBL2* gene structure. (A) Overview of MBL protein subunits, consisting of single polypeptides, combined to trimers and finally to oligomers (mostly hexamers). (B) Overview of the *MBL2* gene, comprising of 4 exons. Locations of the 6 common SNPs are indicated in the gene structure in grey circles. The exons contains untranslated regions (yellow), a signal peptide (green), a cystein-rich crosslinking region (red), a collagen-like region (blue), a short hydrophobic neck region (grey), as well as the carbohydrate recognition domain (orange). Figure created with BioRender.com and partially taken with permission from supplementary material of Hurler *et al.* (112), under the terms of the Creative Commons Attribution License (CC BY), https://creativecommons.org/licenses/by/4.0/.

In the first exon of *MBL2*, three missense polymorphisms in codons 54 (Gly54Asp; rs1800450; variant allele B), 57 (Gly57Glu; rs1800451; variant allele C) and 52 (Arg52Cys; rs5030737; variant allele D) are described (113-115). While the wildtype is termed allele A, the variant alleles are named B, C, or D, respectively. These variant alleles (B, C, and D) are often combined and referred to as allele 0. In all variant alleles, functional MBL concentrations and lectin pathway activity are decreased, caused by changes in the collagen-like domain structure due to amino acid substitutions and therefore diminished stability of higher-order oligomers. In addition to the three exonic single nucleotide polymorphisms (SNPs), three polymorphisms of the promoter/5'-UTR region (-550C/G: L/H, rs11003125; -221G/C: Y/X, rs7096206; +4C/T: P/Q, rs7095891) are common, which can also have an effect on MBL levels. There is a strong linkage disequilibrium, leading to seven common haplotypes with high (HYPA, LYQA), intermediate (LYPA), low (LXPA) or deficient (LYPB, HYPD, LYQC) functional activity (109-111). An overview of the six common SNPs is provided in Table 1.

Table 1: Overview of the six common *MBL2* single nucleotide polymorphisms. Table taken with permission from supplementary material of Hurler *et al.* (112).

SNP	GENE POSITION	RS ID	CHROMOSOME POSITION	AMINO ACID SUBSTITUTION
X → Y	promoter	rs7096206	chr10:52771925:G:C	
A → B	exon 1	rs1800450	chr10:52771475:C:T	Gly54Asp
A → C	exon 1	rs1800451	chr10:52771466:C:T	Gly57Glu
A → D	exon 1	rs5030737	chr10:52771482:G:A	Arg52Cys
H → L	promoter	rs11003125	chr10:52772254:G:C	
P → Q	5' UTR	rs7095891	chr10:52771701:G:A	

Combination of low or deficient haplotypes (XA/0 and 0/0) results in functional MBL deficiency, which is defined as either MBL protein levels < 500 ng/mL (116) or MBL function < 0.2 U/µL, as measured by C4b deposition (117). MBL deficiency, accounting for around 10-30 % of the general population, is one of the most prevalent immunodeficiencies, and was associated with a higher susceptibility to infections, particularly in immunocompromised individuals and during childhood (118).

1.2.4 Serine Proteases of the CP and LP Pathway

As described before, the classical and the lectin pathway require activation of pathway-specific serine proteases. The general modular structure of such proteases is demonstrated in Figure 5.

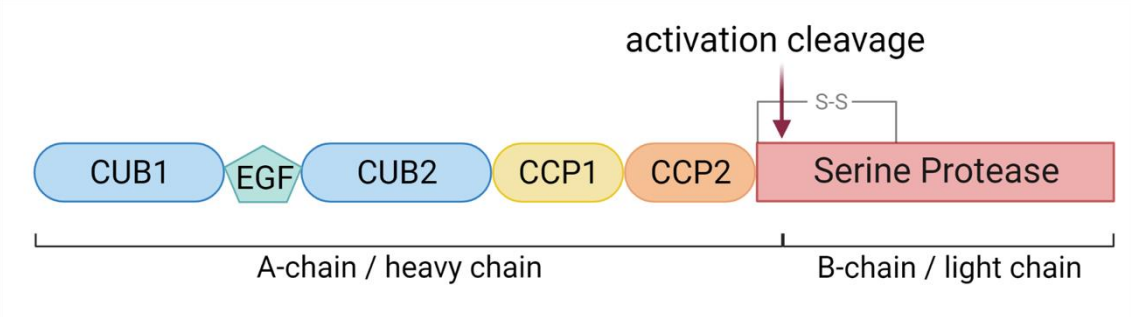

Figure 5: Domain organization of CP and LP serine proteases. Serine proteases of the classical (C1r and C1s) and the lectin pathway (MASP-1 and MASP-2) consist of six different domains: two CUB domains (CUB1 and CUB2) enclosing one EGF-like region, complement control protein 1 and 2 (CCP1 and CCP2), as well as the catalytically active serine protease (SP) domain at the C-terminus. The proteases are organized in a heavy/A-chain, as well as a light/B-chain. Abbreviations: CUB, complement C1r/C1s, Uegf, Bmp1; EGF, epidermal-growth factor; CCP, complement control protein. Figure created with BioRender.com.

Common components of the serine proteases are two Ca^{2+}-binding 'complement C1r/C1s, Uegf, Bmp1' (CUB) domains (119) enclosing an Ca^{2+}-binding epidermal-growth factor (EGF)-like domain (120) at the N-terminal site, which enables binding of pattern recognition molecules such as C1q or MBL. This N-terminal region is followed by the two complement control protein (CCP1 and CCP2) domains (121) and a chymotrypsin-like serine protease domain at the C-terminal end (122).

The proteases are synthesized as polypeptides and are made up of two chains (A-/heavy chain and B-/light chain), which are held together by a disulfid bridge under physiological conditions. Once the respective pathways are activated, the zymogen proteases are cleaved on specific activation cleavage sites, followed by C4 and C2 cleavage and the formation of the C3 convertase as discussed before.

1.2.5 Regulation of CP and LP Activation by C1-INH and Formation of C1-INH Complexes

Both, the classical (C1r and C1s) as well as the lectin pathway serine proteases (MASP-1 and MASP-2) are tightly regulated by the C1 esterase inhibitor (C1-INH). Whereas the lectin pathway can also be controlled by additional regulators, C1-INH is the only known molecule able to inhibit classical pathway activation (123). C1 esterase inhibitor is a highly glycosylated protein primarily expressed in the liver (124). The protein is encoded by *SERPING1* and organized into a C-terminal serpin domain, responsible for the inhibition of serine proteases, and an N-terminal domain, whose function is not yet fully understood (125-127). Nonetheless, studies suggest that the N-terminal domain may be involved in protein folding and processing (128) or in altering the affinity between serine proteases C1r and C1s and the C1q upon binding of C1-INH (126). Next to its role in complement regulation, C1-INH also has profound roles in the regulation of the coagulation, the contact, as well as the fibrinolytic system (129), as summarized in Table 2.

Table 2: Overview of biological systems regulated by C1-INH.

INHIBITION BY C1-INH	TARGET PROTEASES	RESULTS	REF.
COMPLEMENT SYSTEM	C1r, C1s	Classical pathway inhibition (only known inhibitor)	(130, 131)
	MASP-1, MASP-2	Lectin pathway inhibition	(132, 133)
CONTACT SYSTEM	Plasma kallikrein, Factor XIIa (FXIIa)	Primary regulator of the contact system	(134-136)
COAGULATION SYSTEM	Thrombin, Factor XI (FXI)	Inhibition of blood coagulation	(137)
FIBRINOLYTIC SYSTEM	Tissue plasminogen activator (tPA), plasmin	Regulation of fibrinolysis	(136, 138)

During classical pathway regulation, C1-INH can covalently bind to the catalytic centers of either activated C1r or C1s (139). Besides that, binding can also occur to either MASP-1' or MASP-2' in the MBL/ficolin/collectin complexes of the lectin pathway in a similar manner. Binding of C1-INH blocks the function of the serine proteases and hence limits consumption of C4 and C2 (140). Regulation of complement activation by C1-INH (with CP regulation as an example) is illustrated in Figure 6. Covalent binding of C1-INH leads to a dissociation of the C1 complex, releasing covalent C1s/C1-INH and C1r/C1-INH complexes as well as free C1q (141). The regulation of the lectin pathway works in a similar way (132), while MASP-1/C1-INH and MASP-2/C1-INH complexes are released.

Shortly after release into the circulation, the low density lipoprotein receptor-related protein (LRP) is internalizing and degrading the newly generated C1-INH complexes (142).

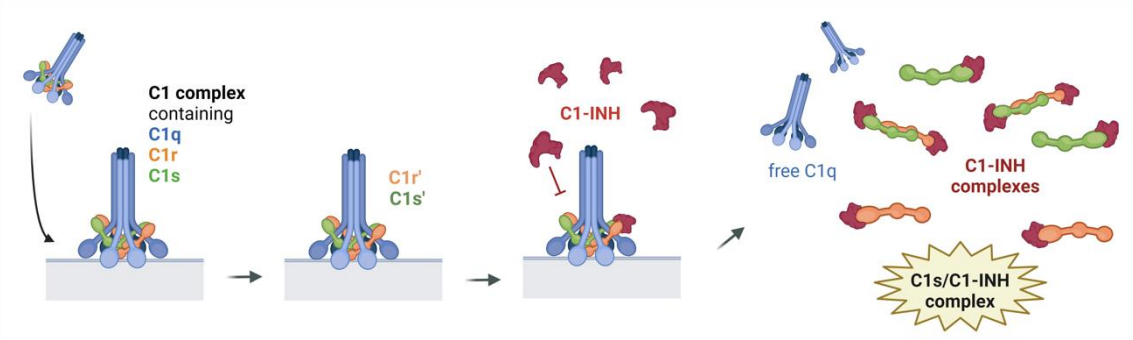

Figure 6: Proposed mechanism of C1-INH complex formation during regulation of classical and lectin pathway activation(with CP regulation as an example). After binding of C1q to an activating target, the PRM-associated serine proteases (CP: C1r and C1s, LP: MASP-1 and MASP-2) are activated, allowing downstream complement activation. Circulating C1-INH can covalently bind to the active serine proteases, which then prevents further complement activation. Upon binding of C1-INH, the C1 complex dissociates and releases free C1q, C1r/C1-INH and C1s/C1-INH complexes. Similarly, during lectin pathway regulation, MASP-1/C1-INH and MASP-2/C1-INH complexes are released. Abbreviations: C1r', active C1r; C1s', active C1s; C1-INH, C1 esterase inhibitor. Figure created with BioRender.com. Figure taken and adapted with permission from Hurler et al. (38), under the terms of the Creative Commons Attribution License (CC BY), https://creativecommons.org/licenses/by/4.0/.

1.3 Complement Activation in Disease

1.3.1 Overview of Diseases Associated with Complement Dysregulation and Activation

The complement system plays a vital role in the immune response, but when it is not functioning properly, it can lead to various diseases. Alterations in the complement system can be caused by a wide range of factors such as infections, autoimmune diseases, or deficiencies in complement components. Some common examples for complement-associated diseases or conditions are listed in Table 3.

Table 3: Common diseases and conditions associated with altered complement protein levels or function.

DISEASE	DISEASE PRESENTATION	MECHANISM	ALTERED COMPLEMENT	REF.
Atypical hemolytic uremic syndrome (aHUS)	microangiopathic hemolytic anemia, thrombocytopenia, and renal impairment	Genetic variants in complement genes (*C3, CFB, CFH, CFHR, CFI, CD46*)	CP activity ↓ AP activity ↓ C3↓ sC5b-9 ↑	(143, 144)
Glomerular dieseases	Various presentations ranging from asymptomatic to severe illness, finally resulting in renal failure	autoantibodies (C3NeF) preventing AP regulation, Genetic variants (*C3, CFB CFH, CFI*)	C3↓ C3a ↑ C5a ↑ sC5b-9 ↑ glomerular deposits of complement	(145)
Hereditary Angioedema (HAE)	Recurrent attacks of severe swelling	Genetic variants in C1-INH	C1-INH antigen↓ C1-INH function↓	(146)
Rheumatoid Arthritis (RA)	Synovial inflammation and swelling, followed by cartilage and bone destruction	Autoantibodies against antigens in the joint	C2 ↑ C3a ↑ C3d ↑ C4d ↑ sC5b-9 ↑	(147)

Systemic Lupus erythematosus (SLE)	Widespread inflammation and tissue damage due to autoimmunity	Genetic variations in complement genes (*C1Q, C2, C4, CR2, CR3*), Autoantibodies against C1q	C3 ↓ C4 ↓ CH50 ↓ sC5b-9 ↑	(148)
Thrombotic thrombocyto-penic purpura (TTP)	Multiple organ failure due to platelet-rich thrombi in the microvasculate	ADAMTS13 deficiency	C3a ↑ sC5b-9 ↑	(149)
Viral and bacterial infections	Various presentations, depending on pathogens	Pathogens activate complement either directly or upon antibody release in the host	sC5b-9 ↑ several other complement activation products (depending on pathogen) ↑	(150)

While the list of diseases associated with complement abnormalities/changes is constantly getting longer, only a few infectious diseases will be discussed in the scope of this thesis more in detail, namely COVID-19 and Sepsis.

1.3.2 Complement and COVID-19

The novel coronavirus, officially named Severe Acute Respiratory Syndrome Coronavirus 2 (SARS-CoV-2), is responsible for coronavirus disease 2019 (COVID-19). The virus is a single-stranded RNA virus and belongs to the family of *Coronaviridae*, capable of causing disease in animal species and humans (151). The virus was first described in December 2019 in Wuhan, a city located in the Hubei province of China, followed by a rapid spread worldwide (152). The resulting pandemic caused more than 762 million registered COVID-19 cases, and a total of over 6.8 million deaths globally as of April 2023 (153).

The clinical presentation of SARS-CoV-2 infections can be highly heterogenous, ranging from an asymptomatic disease course to mild flu-like symptoms to severe respiratory failure with acute respiratory distress syndrome (ARDS) and even death (154).

The virus can enter the human body through interaction of the viral spike (S) protein with the host receptor angiotensin-converting enzyme 2 (ACE2), highly expressed on alveolar lung epithelial cells (155). Upon binding, the transmembrane serine protease TMPRSS2 is able to cleave the spike protein, thereby allowing fusion of the virus and host lipid bilayers (156). Once inside the host cell, SARS-CoV-2 is able to directly start producing viral proteins and virus replication. This process also activates innate immunity, leading to the production of IFNs and subsequently the release of proinflammatory cytokines, such as IL-1, IL-6, IL-8 and TNF (157).

The complement system is also a major defense mechanism against viruses, and previous outbreaks of coronaviruses such as SARS-CoV in 2002/2003, as well as Middle East respiratory syndrome coronavirus (MERS-CoV) in 2012, have shown complement activation and dysregulation being associated with the disease course (158-160). Thus, extensive research regarding complement activation and dysregulation in COVID-19 started soon after SARS-CoV-2 was discovered.

As known today, the complement system can be activated via all three pathways upon infection with SARS-CoV-2, as summarized in Figure 7.

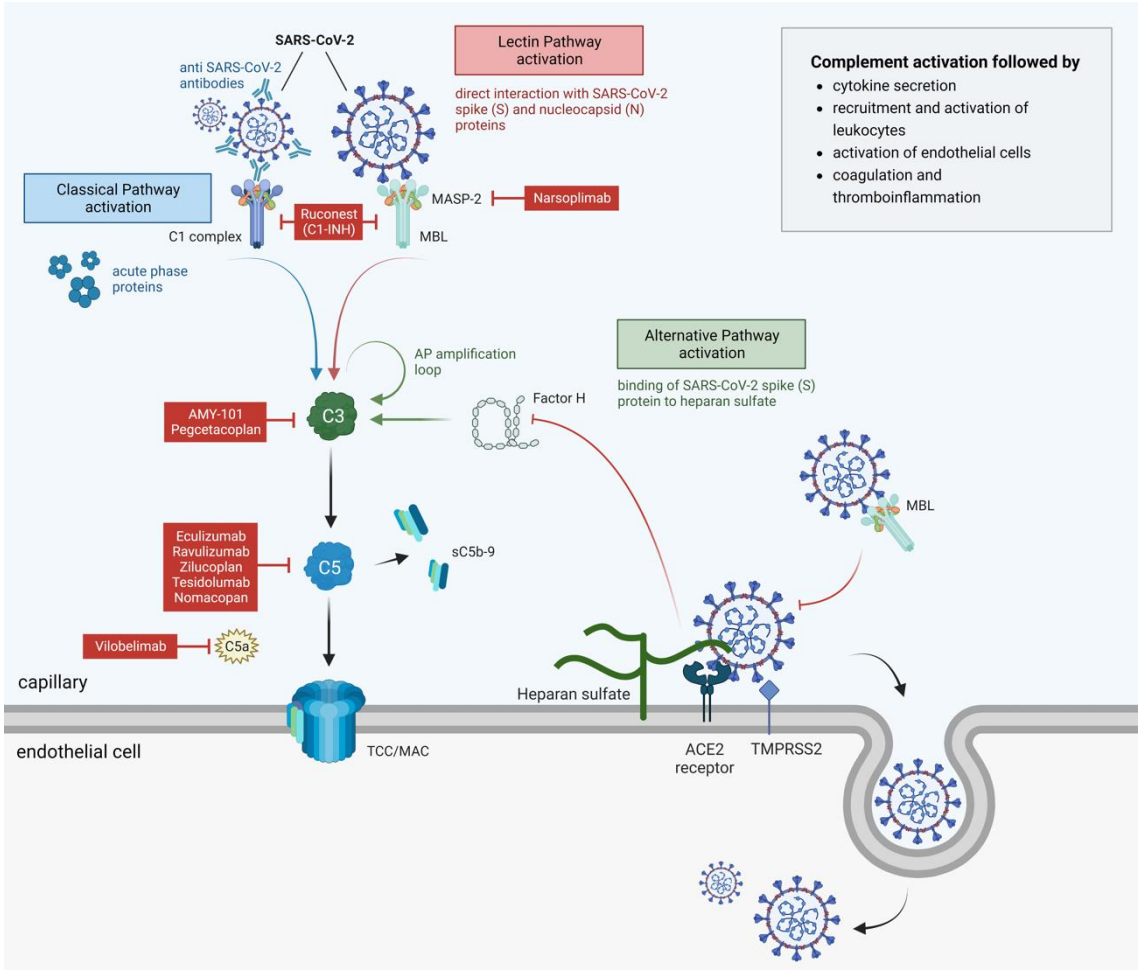

Figure 7: Overview of currently known complement involvement and targeting in COVID-19. Lectin pathway activation in COVID-19 can occur through direct interaction of viral proteins (spike (S) and nucelocapsid (N) with MBL. Besides that, binding of MBL is also suggested to inhibit viral entry into the cells. The classical pathway is activated through acute phase proteins, while later on CP activation can also occur thorugh anti SARS-CoV-2 antibody antigen complexes, following formation of the C3 convertase and downstream complement activation. This can further be enhanced by the alternative pathway, while the AP was also shown to directly be activated through the virus, where SARS-CoV-2 spike protein can bind to heparan sulfat and thereby inhibiting Factor H. Subsequently the AP cannot be regulated by Factor H anymore, resulting in over-activation of the complement system. Complement activation can result in the release of cytokines, recruitment and activation of B and T cells, activation of endothelial cells and the activation of coagulation and thromboinflammation. Complement inhibitors used in clinical studies in COVID-19 are indicated next to their target proteins in red. Figure created with BioRender.com.

Directly after an infection, the lectin pathway is activated through direct binding of MBL or other LP PRMs to viral proteins or surface structures (161, 162). Later in the disease course, C1q can bind to circulating SARS-CoV-2 specific IgG or IgM antibody-antigen complexes, leading to the activation of the classical pathway (163, 164). Besides that, classical pathway activation can further be enhanced by acute phase proteins such as CRP

and PTX3, which have both been shown to be elevated in COVID-19 (165, 166). Last, but not least, the alternative pathway can either act as an amplification loop for LP and CP activation, or AP activation can further be increased through the competition of factor H and SARS-CoV-2 for heparan sulfate binding sites (164, 167, 168).

Although several studies investigated complement activation in COVID-19, there is still much uncertainty regarding how SARS-CoV-2 infection leads to complement over-activation and how exactly complement participates in the pathology of COVID-19.

In initial studies, which mainly focused on the lectin pathway due to previous findings in other coronaviruses (158, 159), researchers could show deposition of LP- and TP-associated proteins such as MBL, MASP-2, C4d, and C5b-9 in lungs and kidneys of SARS-CoV-2 infected patients (169-171). While others could also see deposition of C4d and C5b-9 in lung tissue of COVID-19 patients (164), they could further detect deposits of classical pathway initiator C1q, IgG and IgM, as well as alternative pathway proteins C3d and Factor H, strongly suggesting activation of all three complement pathways.

Besides that, high levels of circulating anaphylatoxins C3a and C5a, as well as the terminal activation fragment sC5b-9, were not only found in COVID-19 patients, but also correlated significantly with disease severity (163, 172, 173).

After all this evidence pointed towards involvement of all three complement pathways in the disease progression of severe COVID-19, the aim was therefore to utilize the new C1-INH complex assays in a first proof-of-concept study, showing that C1s/C1-INH and MASP-1/C1-INH complex levels are also increased *in vivo* during SARS-CoV-2 infections. The new C1-INH complex assays, in combination with several other complement measurements, might shed further light on complement activation in COVID-19. During the investigations, a special focus was placed on the genetic background of the key pattern recognition molecule of the lectin pathway, MBL, and potential associations of *MBL2* genetic variations with disease severity and outcome (development of Long COVID and COVID-19 related mortality).

1.3.3 Complement Activation in Sepsis

Sepsis, organ dysfunction caused by dysregulated immune responses due to infections, is a leading cause of death worldwide, with an incidence rate between 270-437/100.000 persons per year (174). Clinical presentation of sepsis is very divers and depends on the underlying cause as well as of the host's immune response. Common symptoms include fever, hypotension, fast breathing, as well as mental implications, such as loss of consciousness, confusion, dizziness or fainting (175, 176). If not diagnosed and treated in time, sepsis can progress to multiple organ dysfunction (severe sepsis) or even death (177).

While complement is involved in the clearance of invading pathogens, complement activation has also been shown to be harmful in the course of sepsis, followed by multiorgan failure (178). Several studies showed a more profound role of complement activation in patients deceased from sepsis compared to sepsis survivors (179, 180). With respect to the pathways involved in sepsis, most complement studies focus on C3 split products such as C3a, C3b and C3d, and C5a, generated by all three complement pathways (181-184). Systemic levels of C3a, C5a as well as sC5b-9 were found to be increased in septic patients, while the hemolytic activity of the classical pathway was shown to be reduced (180, 184, 185). Besides that, in animal studies $C4^{-/-}$, $C3^{-/-}$ and immunoglobulin-deficient mice were shown to be more sensitive to endotoxin when compared to wildtype mice, indicating contribution of the classical pathway in endotoxin clearance (186, 187). However, lectin pathway activation probably has the most profound role in sepsis, in combination with AP amplification (188). Activation of the LP, caused by direct interactions between MBL and glycosylated residues on the pathogen surfaces or by the release of LPS from gram-negative bacteria into the circulation, was shown to be associated with rapid shock in mice (189). On the other hand, C3 and Factor B levels were suggested as prognostic markers for survival in septic shock patients, indicating participation of the alternative pathway in sepsis development (190).

Measurement of C1-INH complexes might help to uncover complement activation in sepsis, as well as serve as an additional proof-of-concept study for the new immunoassays *in vivo*.

1.4 Complement Testing

Since complement is getting more and more important in many different diseases (see Table 3), one aspect that is also getting more attention is the testing of complement. There are several different ways of how the complement system, or components thereof, can be analysed, which will be described in the following chapters.

1.4.1 Measurement of Complement Protein Levels

A decrease of given complement components indicates activation and hence consumption of the respective proteins. Methods widely used to quantify proteins such as C3, C4, C5, C1-INH or FB are nephelometry or turbidimetry (191). Through the addition of polyconal antibodies, targeting the protein of interest, to a patients sample, immune complexes are formed that will alter the detection of light beams passing through the samples. Measurement of the intensity of scattered light (nephelometry) or the intensity of transmitted light (turbidimetry) in a detector will provide information about the protein concentration (191).

Another method widely used is radial immunodiffusion, also known as the Mancini technique (192). Here, antibodies against the protein to be measured are added to agar and the mixture is poured onto glass slides. Standard and samples are added and incubated for 24-72 h, while antigens can diffuse out of the wells and percipitate after immune complex formation with the antibodies in the agar, leading to the formation of rings surrounding the wells. The more antigen is present in the samples, the wider the formed ring will be (192). A modification thereof is the Ouchterlony method (double immunodiffusion), where antibodies are not included in the agar gel, but in neighboring wells instead (193). Through the diffusion of the antigen to be measured and the antibody, precipitation occurs at the point of antibody-antigen equivalence (14, 193). This method also allows the comparison of different antibody-antigen combinations.

Furthermore, complement proteins can also be quantified using immunoelectrophoresis, a combination between electrophoresis and immunoprecipitation (194). First, serum proteins are seperated according to size and charge in agar gel using electrophoresis, before an antibody-containing solution is added, leading to diffusion of antibody and antigen into the gel and the formation of immunoprecipitation (194).

Semi-quantitative measurements can be done using Western Blot or immunostaining. Additional methods quantifying individual complement components are FACS, ELISAs for specific components and complement deposition assays (195, 196). A comparison of different techniques is shown in Table 4.

Table 4: Comparison of different methods used in complement diagnostics.

METHOD	ADVANTAGES	DISADVANTAGES
Radial immunodiffusion	- very few equipment - simple and specific - robust	- long reaction times
Double immunodiffusion	- very few equipment - very specific	- long reaction times - potentially low sensitivity
Turbidimetry/ Nephelometry	- very high sensitivity - fast - automation possible	- high costs for equipment and reagents - hard to set up - particles/molecules can impair measurement (e.g. lipemic samples)
ELISA	- most commonly employed immuno-precipitation method in complement analysis - high sensitivity - automation possible - diverse applications	- relatively time-consuming - usage of 2 antibodies can be problematic, especially when detecting small molecules (targeting of 2 different epitopes) - sometimes too sensitive
Western Blot	- simultaneous visualization of proteins and activation fragments/complexes	- labor-intensive - not suitable for clinical practice (automation difficult)

Some upcoming methods of the recent years are multiplex assays, allowing quantification of several complement components in a single run either by flow-based laser detection or by magnetic beads (197), or mass spectrometry based methods (198, 199).

1.4.2 Functional Testing of Complement

Traditionally, hemolytic assays are performed in order to aquire information about the functional activity of the classical and the alternative pathway. Those functional tests are specifically valuable to gain information about potential deficiencies of complement components. Hemolytic functionality tests are still based on the original protocols for measuring CP functionality established by Mayer in 1967 (200), but in the meantime many modifications thereof exist.

According to the original method, serial dilutions of the sera to be tested are incubated with antibody-sensitized sheep erythrocytes, while the serum acts as a source of complement and ultimatively is lysing the erythrocytes. After incubation, the readout is the amount of patient serum necessary to lyse 50 % of the red blood cells, also known as the CH_{50} (201). Another method utilizes liposomes containing enzymes, which are released upon classical pathway activation and react with an added substrate, allowing the quantification of released enzyme (202, 203). Determination of alternative pathway activation (AH_{50}) works in a similar manner, but rabbit or guinea pig erythrocytes are used, since they activate the AP spontaneously and do not require specific coating (204, 205). However, addition of EGTA is necessary when investigating AP function in order to inhibit the influence of the CP and LP (206).

Measurement of the activity of all three pathways can also be done by performing a functional ELISA. Hereby, multiwell plates are coated with reagents known to activate the respective pathways (IgM for CP, mannan for LP, LPS for AP). After incubation with serum samples, the functional activity is measured on the level of a C9 neo-epitope generated during TCC formation upon activation (207, 208). Readout of functional complement on ELISA plates can not only be done on the level of C9, but deposition of proteins covering several steps of the complement cascade (e.g. C1q, C4, C3, FB) can be detected, as already described in 1989 by Zwirner *et al.* (209). In all methods investigating complement pathway functionality, it is required to use complement-preserved serum samples (210).

Besides functional tests of whole complement pathways, it is also possible to analyse the activity of single complement components. The easiest way to do so is through the usage of serum deficient or depleted of the protein of interest. Upon titration of the given sample, which includes the protein to be tested, the capability to reconstitute hemolytic

activity or C5b-9 deposition can be measured (211). For some proteins, functionality can also be tested via chromogenic assays (212) or their binding capacity to target structures (213, 214).

1.4.3 Measurement of Complement Activation Products

Complement activation can occur either in the circulation or locally, e.g. in infected tissues or organs (215). In order to get information about the activation state of the complement system at the timepoint of sampling, complement activation products need to be measured. Those activation products are for example split products of C4 (C4a, C4d), C3 (C3a, C3b, C3c, C3d), C5 (C5a) or Factor B (Ba, Bb), as well as complement complexes formed upon activation. Through the development of neoepitope-specific monoclonal antibodies or utilization of antibodies detecting different components of formed complexes, those activation fragments or complexes can be distinguished from native forms of the respective proteins (216-218).

The most established markers used to assess complement activation are split products downstream of C3/C4, indicating activation of all three pathways. Besides that, the sC5b-9 complex (also known as sTCC or the soluble MAC (sMAC)), results from the activation of all three complement pathways (219), while formation of the C3bBbP complex is quantified as a measure for alternative pathway activation (220).

2 OBJECTIVES

2.1 Development and Characterization of Immunoassays Detecting C1s/C1-INH and MASP-1/C1-INH complex concentrations

No validated tools existed to measure early classical and early lectin pathway activation. Covalent C1-INH complexes, formed upon activation of the respective serine proteases (C1s and C1r for the classical pathway (CP), MASP-1 and MASP-2 for the lectin pathway (LP)) might be suitable markers to distinguish between early CP and early LP activation. The first aim of the project was therefore to develop and characterize two immunoassays, one measuring the C1s/C1-INH complex as a marker for early classical pathway activation, and one measuring the MASP-1/C1-INH complex as an indicator for early lectin pathway activation.

2.2 Validation of C1s/C1-INH and MASP-1/C1-INH complexes as markers for early classical and early lectin pathway activation

While C1/C1-INH complexes were investigated as a measure of classical pathway activation in several studies (221-225), no data was published about the use of MASP-1/C1-INH complexes as a marker of lectin pathway activation. For that reason, the second aim was to proof that C1-INH complexes are suitable markers to assess early classical and early lectin pathway activation *in vitro*.

2.3 Investigation of C1-INH complexes in health and disease

C1/C1-INH complex levels have been shown to be increased in several diseases where CP activation is known to be involved in the disease course, such as HIV, SLE, RA as well as HAE (221-225). In contrast, MASP-1/C1-INH complexes were only investigated in HAE patients before (222, 226). In order to validate the use of C1-INH complexes as early CP and LP activation markers also *in vivo*, the third aim was to investigate C1s/C1-INH and MASP-1/C1-INH complex levels in

a. healthy controls,
b. COVID-19 patients (with focus on lectin pathway activation and the genetic background of its key pattern recognition molecule MBL), and
c. sepsis patients.

3 MATERIAL AND METHODS

3.1 Materials

3.1.1 Chemical reagents

Chemical reagents used during the project are listed in Table 5.

Table 5: Chemical reagents used during the project.

REAGENT	CAT#	MANUFACTURER/SOURCE
Zymosan A aus *Saccharomyces cerevisiae*	Z4250	Merck KGaA, Darmstadt, Germany
Ethylenediaminetetraacetic acid tetrasodium salt hydrate (EDTA)	E5391	Merck KGaA, Darmstadt, Germany
Ethyleneglycol-bis(β-aminoethyl)-N,N,N′,N′-tetraacetic Acid (EGTA)	324626	Merck KGaA, Darmstadt, Germany
Sodium chloride (NaCl)	3957.1	Carl Roth, Karlsruhe, Germany
Potassium chloride (KCl)	104936	Merck KGaA, Darmstadt, Germany
Sodium phosphate dibasic dihydrate (Na_2HPO_4 x $2H_2O$)	71643	Merck KGaA, Darmstadt, Germany
Potassium dihydrogen phosphate (KH_2PO_4)	104873	Merck KGaA, Darmstadt, Germany
Calcium chloride dihydrate ($CaCl_2$ x $2H_2O$)	C8106	Merck KGaA, Darmstadt, Germany
Tris-HCl	9090.3	Carl Roth, Karlsruhe, Germany
Tween 20	1706531	BioRad Laboratories Inc., California, USA
Sodium dodecylsulfate polyacrylamide (SDS)	2326.2	Carl Roth, Karlsruhe, Germany
Glycerol	3783.1	Carl Roth, Karlsruhe, Germany
Bromophenol blue sodium salt ($C_{19}H_9Br_4O_5SNa$)	A512.1	Carl Roth, Karlsruhe, Germany

3.1.2 Buffers and solutions

Composition of buffers and solutions used during the experiments are summarized in Table 6.

Table 6: Overview of buffers used and their composition.

BUFFER	COMPONENTS	QUANTITY
Phospahte-buffered saline (PBS), 10x (pH: 7.2)	NaCl	80.0 g
	KCl	2.0 g
	Na_2HPO_4 x $2H_2O$	11.5 g
	KH_2PO_4	4.0 g
	MilliQ water	Up to 1000 mL
Tris-buffered saline (TBS), 10x (pH: 7.6)	Tris	24.2 g
	NaCl	80.0 g
	MilliQ water	Up to 1000 mL
Tris-buffered saline with Tween (TBST) (pH: 7.6)	TBS (10x)	100 mL
	Tween 20	1 mL
	MilliQ water	Up to 1000 mL
TBST-Ca^{2+}, 10x (pH: 7.5)	Tris-HCl	100.0 mL
	NaCl	88.0 g
	$CaCl_2$	2.9 g
	Tween 20	10.0 mL
	MilliQ water	Up to 1000 mL
Electrophoresis buffer, 8x (pH: 8.5)	Tris	24.0 g
	Glycin	115.4 g
	SDS (20 %)	20.0 mL
	MilliQ water	Up to 1000 mL
Western Blot blocking buffer	TBS (10x)	10.0 mL
	Tween 20	0.1 mL
	BSA	5.0 g
	MilliQ water	89.9 ml
Western Blot Primary antibody dilution buffer	Western Blot blocking buffer	1.0 mL
	TBST	9.0 mL

Loading Dye, 2x (non-reducing)	Tris (0.5M)	1 mL
	SDS (10 %)	1.6 mL
	Glycerol	800 µL
	PBS	400 µL
	Bromphenol blue (4 %)	200 µL
Veronal-buffered saline (VBS), 5x (pH: 7.4)	1,3-Diethylbarbituric acid	2.9 g
	NaCl	42.5 g
	Sodium 5,5-diethylbarbiturate	1.9 g
	MilliQ water	Up to 1000 mL
VBS^{++}, 1x	VBS 5x	1.0 mL
	Mg^{2+}/Ca^{2+} mix (75mM Mg^{2+}, 500mM Ca^{2+})	10.0 µL
	MilliQ water	Up to 5.0 mL
Bicarbonate buffer, 1x	Bicarbonate ($NaHCO_3$)	8.401 g
	MilliQ water	1000 mL

3.1.3 Proteins and antibodies

Proteins and antibodies used for the experiments are compiled in Table 7 and Table 8.

Table 7: Recombinant and commercially available proteins used for the experiments.

PROTEIN	CAT#	MANUFACTURER/SOURCE
Recombinant C1s, CCP1-CCP2-SP fragment	NA	Peter Gál *et al.*, as described in (222)
Recombinant MASP-1, CCP1-CCP2-SP fragment	NA	Peter Gál *et al.*, as described in (227)
Recombinant MASP-2, CCP1-CCP2-SP fragment	NA	Peter Gál *et al.*, as described in (101)
Recombinant MASP-3, CCP1-CCP2-SP fragment	NA	Peter Gál *et al.*, as described in (228)
Recombinant C1r, CCP1-CCP2-SP fragment	NA	Peter Gál *et al.*, as described in (229)
Recombinant human MBL (rMBL)	NA	Steffen Thiel *et al.*, as described in (230)

Purified C1-INH, obtained from Berinert® concentrate	NA	Peter Gál *et al.*, as described in (222)
MASP-1/C1-INH complex (*in-house*)	NA	Produced *in-house*, as described in (222)
C1s/C1-INH complex	C1040	CompTech Complement Technology Inc., Texas, USA
C1s/C1-INH complex (*in-house*)	NA	Produced *in-house*, as described in (222)
Purified C1s enzyme	A104	CompTech Complement Technology Inc., Texas, USA
Purified C1q	A400	Quidel, San Diego, USA
SARS-CoV-2 S protein, His Tag, Super stable trimer	SPN-C52H9	AcroBioSystems, Newark, USA

Table 8: Overview of commercially availabe and *in-house* developed antibodies used during the project.

ANTIBODY	CAT#	MANUFACTURER/SOURCE
Mouse anti human C1s	NA	Developed and produced *in-house*, as described in (38)
Mouse anti human MASP-1	NA	Developed and produced *in-house*, as described in (38)
Mouse anti human C1-INH	NA	Developed and produced *in-house*, as described in (38)
Goat anti mouse - HRP	1010-05	Southern Biotech, Birmingham, US
Mouse anti MBL (human)	HYB 131-01	Statens Serum Institut, Copenhagen, Denmark
Rabbit anti mouse IgG (H+L) - HRP	31450	Invitrogen GmbH, Lofer, Austria

3.1.4 Lab consumables and instruments

Lab consumables and instruments are listed in Table 9.

Table 9: Overview of lab consumables and instruments.

LABWARE/INSTRUMENT	MANUFACTURER
Nunc Maxisorp 96-well plates (microplates and strip plates)	Thermo Scientific Fisher, California, USA
Eppendorf tubes (0.5 mL, 1.5 mL, 2.0 mL)	Eppendorf SE, Hamburg, Germany
Falcon tubes (15 mL, 50 mL)	Greiner Bio-One, Frickenhausen, Germany
Pipet tips	Greiner Bio-One, St. Gallen, Switzerland
Glassware	DWK Life Science, Wertheim, Germany
Microplate reader Tecan infinite M1000 Pro	Tecan Trading AG, Männedorf, Switzerland
Microplate reader BioRad 680	BioRad Laboratories Inc., California, USA
Pipets	Eppendorf SE, Hamburg, Germany Sartorius AG, Göttingen, Germany Thermo Scientific Fisher, California, USA
Biosan Thermo shaker PST-60HL-4	Biosan Laboratories, Michigan, USA
Biosan Dry Blot Thermostat Bio TDB-100	Biosan Laboratories, Michigan, USA
Incubator	Heraeus, Hanau, Germany
Mini TransBlot system	BioRad Laboratories Inc., California, USA
TransBlot SD Semi-Dry Transfer Cell	BioRad Laboratories Inc., California, USA
Vortex Thermo Denley Vibramix	Thermo Scientific Fisher, California, USA
Microcentrifuge Eppendorf 5415D	Eppendorf SE, Hamburg, Germany
ChemiDoc XRS+ System	BioRad Laboratories Inc., California, USA

3.1.5 Assays, Kits and commercially available reagents

Commercially available assays and reagents are summarized in Table 10.

Table 10: Commercially available assays, kits and reagents used during the project.

ASSAY/KIT/REAGENT	CAT#	MANUFACTURER
Trans-Blot Turbo Midi 0.2 µm PVDF Transfer Packs	1704157	BioRad Laboratories Inc., California, USA
10 % Mini-PROTEAN® TGX Stain-Free™ Protein Gels, 12 well, 20 µl	4568035	BioRad Laboratories Inc., California, USA
Precision Plus Protein™ Kaleidoscope™ Prestained Protein Standards	1610375	BioRad Laboratories Inc., California, USA
Clarity™ Western ECL Substrate, 200 mL	1705060	BioRad Laboratories Inc., California, USA
WIESLAB® Complement System Classical Pathway - RUO	COMPLCP310RUO	SVAR Life Science, Malmö, Sweden
WIESLAB® Complement System MBL Pathway - RUO	COMPLMP320RUO	SVAR Life Science, Malmö, Sweden
MBL, human, ELISA	HK323	Hycult Biotech, Uden, The Netherlands
TCC, human, ELISA	HK328	Hycult Biotech, Uden, The Netherlands
C1s/C1-INH complex, human, ELISA*	HK399	Hycult Biotech, Uden, The Netherlands
MASP-1/C1-INH complex, human, ELISA*	HK3001	Hycult Biotech, Uden, The Netherlands
C1-INH, human, ELISA	HK396	Hycult Biotech, Uden, The Netherlands
MicroVue C4d Fragment EIA Kit	A009	Quidel, San Diego, USA
MicroVue sC5b-9 Plus EIA Kit	A020	Quidel, San Diego, USA

* developed in cooperation with Hycult Biotech as part of the PhD project

3.1.6 Software

Table 11: Software used for data analysis and visualization.

SOFTWARE	MANUFACTURER/SOURCE
Graphpad Prism 9	GraphPad Inc., San Diego, USA
Statistica 13.5	Tibco Softwares Inc., California, USA
BioRender	BioRender, Toronto, Canada
Plink 1.9	https://www.cog-genomics.org/plink/

3.2 Patient and sample collection

3.2.1 Human samples

Blood samples (Citrate plasma, Heparin plasma, EDTA plasma and serum) from healthy human donors for the assay development were purchased from BioIVT (BioIVT, New York, USA). Besides that, healthy individuals were enrolled in Budapest as described elsewhere (231), while the study was approved by the Scientific and Research Ethics Committee of the Medical Research Council (ETT TUKEB) in Budapest, Hungary (8361-1/2011-EKU).

For investigation of complement activation in COVID-19, samples of SARS-CoV-2 infected individuals and healthy controls were sampled and processed as described before (173, 232, 233). Cohorts were collected at two tertiary care hospitals in Budapest, Hungary (173), at the Addenbrooke's hospital in Cambridge, UK (232), and at the tertiary care Hospital St. Vinzenz in Zams, Austria (233). Ethical approval was obtained from the Hungarian Ethical Review Agency (ETT-TUKEB; No. 8361-1/2011-EKU and IV/4403-2/2020/EKU), the Government Office of the Capital City Budapest (31110-7/2014/EKU (481/2014)), the East of England – Cambridge Central Research Ethics Committee („NIHR BioResource" REC ref 17/EE/0025, and „Genetic variation AND Altered Leucocyte Function in health and disease – GANDALF" REC ref 08/H0308/176), as well as from the Ethics Committee of the Medical University of Innsbruck (1144/2020).

Collection of blood samples from healthy individuals and sepsis patients in Austria was approved by the ethical committee of the Medical University of Innsbruck

(ECS1021/2019), while whole blood was collected as approved by the Ethics Committee of the Medical University of Innsbruck (ECS1166/2018) and the Ethical Review Board of the Danube University Krems. The samples have been collected and processed as described elsewhere (234).

Complement-preserved normal human serum (NHS) pools were prepared freshly from serum of at least 12 healthy individuals, while aliquots were stored at -80°C until further usage.

In all studies and sample collections, written informed consent was given by the healthy or diseased individuals, or their closest relative available. All investigations were conducted according to the guidelines of the Declaration of Helsinki.

3.2.2 Sera of animal origin

Blood samples of animal origin were used for testing of cross-reactivity in the C1-INH complex assays. Some murine, pig, and dog sera were bought from Innovative (Innovative Research Inc., Michigan, USA), while horse and rat sera were obtained from Harlan (Harlan Bioproducts for Science Inc., Maryland, USA). Besides that, additional animal samples, already present at the Medical University Innsbruck and sampled in the frame of a past study (235), were included in the experiments. Those samples covered sera from mouse, rat, rabbit, guinea pig, bovine, sheep, horse, pig, wild boar, dog, orang utan, spider monkey, chicken, tiger, bear, fox, sea lion, and rhino.

3.3 Generation of *in-house* C1-INH complexes

C1s/C1-INH and MASP-1/C1-INH complexes were produced *in-house* following the method described elsewhere (222). In brief, C1-INH and the active serine protease (recombinant CCP1-CCP2-SP fragment of either C1s or MASP-1), diluted in PBS, were incubated in a 1:1 molar ratio for 2 hours at 37 °C on a shaker (250 RPM). After incubation, samples were diluted and stored in aliquots in 1 % BSA in PBS at -80 °C until further usage.

3.4 Methods for antibody characterization

3.4.1 Direct ELISA to test specificity of the antibodies

Specificity of *in-house* produced antibodies (developed by coworkers as described in (38)) was tested in a direct ELISA. Proteins to be tested were coated over night at 4 °C on Nunc Maxisorp 96 well plates (Thermo Fisher Scientific) in a concentration of 1 µg/mL in bicarbonate buffer. After coating, wells were blocked for 1.5 hours at room temperature with 2 % BSA in PBS (200 µL/well). Plates were then washed with wash buffer WB21 (Hycult Biotech), before primary antibodies (anti C1-INH, anti C1s or anti MASP-1) were incubated in the wells at a concentration of 3 µg/mL in dilution buffer DB107 (Hycult Biotech) for 1 h at room temperature. Following 4x washing with WB21, HRP-conjugated goat anti-mouse antibody (Southern Biotech) was incubated 1:4000 in DB107 for 1 h at room temperature. Wells were washed again (4x), before 50 % TMB in H_2O was added. After 5 min, the reaction was stopped by adding stop solution (Hycult Biotech), and absorbance at 450 nm was measured on a plate reader (reference: 620 nm). All measurements were done in duplicates, while the experiment was performed in biological replicates (n = 3). If not stated otherwise, the working volume was 100 µL/well. Specificity of the antibodies was analysed based on the measured OD values.

3.4.2 Western blot

Western blots were performed in order to test the antibodies for their specificity and usability in WB applications. To separate the proteins according to their size, precast 10 % gels (BioRad) were used. Normal human serum (complement-preserved, NHS), zymosan-activated serum (3 h, ZAS) or control proteins and complexes (purified or recombinant, depending on availability) were mixed with non-reducing loading dye (2x), heated for 5 min at 95 °C, and electrophoresed at 200 V for 45 min. Afterwards, proteins were transferred to a polyvinylidene fluoride membrane using the Trans-Blot Semi-Dry Transfer Cell (BioRad). The membrane was blocked for 1.5 h at room temperature using 2 % BSA in PBS (Western Blot blocking buffer), before overnight incubation with 1 µg/mL mouse anti-human C1-INH, mouse anti-human C1s or mouse anti-human MASP-1 (*in-house* monoclonal antibodies (mAbs) used for assay development) in primary antibody dilution buffer at 4 °C. The next day, the membrane was washed

3x 15 min with TBST, before bound antibodies were detected adding HRP-labelled goat anti-mouse IgG (1:2000 dilution; Southern Biotech) in primary antibody dilution buffer for 1 h at room temperature. After incubation, the membrane was washed 3x again using TBST, followed by development using enhanced chemiluminescence (ECL) substrate (BioRad) in the ChemiDoc XRS+ System.

3.5 Development of C1s/C1-INH and MASP-1/C1-INH complex assays and assay performance

Two immunoassays measuring C1s/C1-INH (cat #HK399) and MASP-1/C1-INH (cat #HK3001) complex levels were developed in cooperation with Hycult Biotech (Uden, The Netherlands).

Wells were coated with monoclonal antibodies detecting either C1s or MASP-1, before samples (plasma (EDTA, Citrate or Heparin) or serum) and the standard were prepared in appropriate dilutions, added to the wells, and incubated for 30 min at room temperature (100 µL/well; diluted in dilution buffer DB107). After washing 4x with wash buffer WB21, an HRP-labelled monoclonal antibody recognizing bound C1-INH in the complexes was added and incubated for 30 min at room temperature (100 µL/well; diluted in DB107). Afterwards, wells were washed again, before 100 µL of TMB substrate was added to each well, leading to an enzymatic reaction. The reaction was stopped after 15 min by adding 100 µL of stop solution (Hycult Biotech), before the absorbance was measured using a spectrophotometer (450 nm, reference: 620 nm).

This protocol was used every time C1-INH complex levels were determined during assay development and functional as well as clinical validation of the assays.

The %CV was determined as a measure for variation between samples or conditions according to following equation (1):

$$\%CV = \frac{\text{standard deviation (SD)}}{\text{mean}} \times 100 \quad (1)$$

Equation (1): Coefficient of determination (%CV).

3.6 Validation of newly developed immunoassays

3.6.1 Recovery of C1-INH complexes in EDTA plasma

Recovery of C1-INH complexes in EDTA plasma was analysed by mixing plasma samples of three healthy individuals with known low, middle, and high C1s/C1-INH or MASP-1/C1-INH complex concentrations in following ratios (%): 100-0, 75-25, 50-50, 25-75, 0-100. After incubation for 30 min at room temperature, the concentration of C1-INH complexes was determined in the complex immunoassays as described before. Expected concentrations were plotted against the measured concentration and the recovery was calculated using following equation (2):

$$\text{recovery [\%]} = = \frac{\text{measured concentration of mixed sample}}{\text{expected concentration } [(\% \times \text{concentration sample A}) + (\% \times \text{concentration sample B})]} \times 100 \quad (2)$$

Equation (2): Recovery of C1-INH complexes in EDTA plasma.

Sufficient recovery was defined prior to the experiment as a value between 80 % - 120 %.

3.6.2 Test of assay specificity

Another test performed during assay development was the analysis of cross-reactivity of the immunoassays with either un-complexed complement proteins as samples or with sera of animal origin.

In the C1s/C1-INH complex assay, C1s purified and in recombinant form, as well as purified C1-INH were tested. In the MASP-1/C1-INH complex assay, recombinant MASP-1 as well as purified C1-INH were tested. In both cases, a serial dilution of the proteins was prepared in DB107, and the samples were measured in the C1-INH complex assays.

For determining cross-reactivity of the assays with different species, serum samples deriving from animals (mouse, rat, rabbit, guinea pig, bovine, sheep, horse, pig, wild boar, dog, orang utan, monkey, chicken, tiger, bear, fox, sea lion, and rhino) were diluted in DB107 and measured in the C1-INH complex immunoassays. Of note, animal samples were diluted 10x less compared to human samples.

In general, signals were considered positive if OD450 nm values were ≥ 0.2 after subtraction of the blank.

3.6.3 Inter- and intra-assay variation

To determine the variance between data points within an assay, intra-assay variation was determined by measuring three separate aliquots each of four different samples within a single testrun. The experiment was performed twice by two operators to determine inter-assay variation. %CVs were calculated between the different aliquots tested (intra-assay variation), as well as between the independent testruns from both operators (inter-assay variation).

For intra-assay variation, a coefficient of variation < 10 % indicates low variation, whereas for inter-assay variation, a %CV < 20 % indicates a low level of variation.

3.6.4 Stability testing of C1-INH complexes

Stability of the C1-INH complexes was tested in EDTA plasma as well as in Citrate plasma (benchtop stability) or in PBS/buffer (freeze-thaw stability).

For benchtop testing, aliquots of EDTA plasma or Citrate plasma were incubated either on ice or at room temperature for timespans ranging from 10 min to 16 h. After incubation, C1-INH complex concentrations of the samples were measured in one assay run as described before. A sample incubated for 10 min at the respective condition (either on ice or at room temperature) served as a reference.

Stability of C1-INH complexes during freeze-thawing was investigated by repeatedly freezing and thawing individual aliquots of the samples at -80 °C (up to 4 times). Again here, the C1-INH complex concentrations were determined using the complex ELISAs as described before. For freeze-thaw stability, an unthawed aliquot served as a control.

Stability was evaluated based on the samples recovery when compared to the controls (benchtop testing: 10 min sample, freeze-thaw testing: unthawed sample), while concentrations 80-120 % of the reference C1-INH complex levels were considered acceptable due to natural variation prior to the experiment.

3.7 Complement activation experiments

3.7.1 General complement activation using zymosan

To verify the use of C1-INH complexes as potential markers for early complement activation, zymosan was boiled for 1 h in PBS, before it was washed 4x using PBS. Afterwards, the zymosan was added to a final concentration of 10 mg/mL in VBS^{++} buffer and 2 % complement-preserved NHS. Negative controls contained EDTA (10 mM), while an additional control was included without the addition of zymosan (NHS) in order to determine the levels of auto-activation.

After mixing, tubes were incubated at 37 °C on a shaker (250 RPM), while samples were taken at T_0 (directly after mixing), as well as after 5, 10, 20, 30 min and 1, 2, 3 and 5 hours. In all approaches, EDTA was added directly after sampling to avoid further complement activation after incubation (final concentration: 10 mM). Samples were centrifuged to remove zymosan (2 min, 2400 xg), and subsequently kept at -80 °C until the measurement of C1-INH complex levels in an appropriate dilution as described before.

3.7.2 Specific activation of CP or LP

For investigation of *in vitro* conditions where only one of the two pathways is triggered, 2 % complement-preserved NHS was activated on WIESLAB® Complement System Screen plates (SVAR Life Science; WIESLAB® Complement System Classical Pathway 295 (COMPLCP310RUO) coated with IgM for specific CP activation, WIESLAB® Complement System MBL Pathway 296 (COMPLMP320RUO) coated with mannan for specific LP activation), using the provided CP and LP dilution buffers of the kits. After mixing, a sample (T_0) was collected as a control and stored at -80 °C until further usage. Then samples were activated for several different time intervals (5, 10, 20, 30 min, 1 h, 2 h, 3 h), before the samples/supernatants were collected and stored at -80 °C for C1-INH complex determinations as described before.

Directly after sample collection/removal, CP or LP activity was measured via determination of C9 neoepitope formation during activation in the wells in accordance with instructions provided by the manufacturer. Positive and negative controls provided by the kits were used to express percentage activities calculated based on the measured OD values.

3.8 Determination of additional complement and laboratory parameters

Additional complement and laboratory parameters were measured using assays available from commercial sources and following manufacturer's instructions. All assays used are summarized in Table 10 in chapter 3.1.5. Besides that, additional laboratory parameters (e.g. CRP, anti SARS-CoV-2 antibody levels) and disease outcomes (development of Long COVID/mortality) were extracted from clinical reports, if needed.

3.9 Determination of *MBL2* gene SNPs

Genotyping of the six common *MBL2* gene SNPs was performed by colleagues from Semmelweis University, Budapest, and from collaborators of the Addenbrooke's Hospital Cambridge, UK, as described previously (112), and extracted from hospital databases. The six SNPs included in the analysis are summarized in Table 1, while the grouping according to short genotypes is shown in Table 12.

Table 12: Short genotype groups of *MBL2* and associated MBL expression. Table taken with permission from supplementary material of Hurler *et al.* (112).

SHORT GENOTYPE	MBL EXPRESSION
YA/YA	MBL high/wildtype
YA/XA **XA/XA**	MBL intermediate
YA/0	MBL low
XA/0 **0/0**	MBL deficient

3.10 Binding of MBL to SARS-CoV-2 spike protein

To investigate binding of human MBL to SARS-CoV-2, 96-well plates were coated with recombinant SARS-CoV-2 spike protein (AcroBiosystems) in PBS at 4 °C overnight (2-fold serial dilution, start: 50 pmol/mL). Wells coated with 10 µg/mL mannan (Sigma Aldrich) in PBS served as a positive control. Afterwards, blocking was performed for 2 h at 37 °C with 200 µL of 2 % BSA in TBST-Ca^{2+}, before plates were washed 3x with TBST-Ca^{2+}. Then, 100 µL of 10 % serum of individuals with different *MBL2* genotypes in TBST-Ca^{2+}, 1000 ng/mL recombinant MBL (rMBL; positive control) in TBST-Ca^{2+},

or 5 % BSA in TBST-Ca^{2+} (negative control) were added to the wells and incubated for 1 h at 37 °C. After incubation, plates were washed again 3x with TBST-Ca^{2+}, before wells were incubated with 2 µg/mL anti MBL (Statens Serum Institut) in TBST-Ca^{2+} for 1 h at 37 °C. After three TBST-Ca^{2+} washing steps, 1:4000 diluted goat anti-mouse HRP-labelled antibody (Southern Biotech) in TBST-Ca^{2+} was incubated for 1 h at 37 °C, before plates were washed 3x again. TMB was added for 5 min at room temperature, before the reaction was stopped using stop solution (Hycult Biotech), and the absorbance was measured at 450 nm (reference: 620 nm) on a microplate reader. Binding of MBL to the spike protein was determined based on the measured OD450 values, while OD values of uncoated wells were subtracted from coated wells before analysis. If not stated otherwise, incubation steps were preformed with a volume of 100 µL/well.

3.11 Statistical analysis

Statistica 13.5 (Tibco Softwares Inc., Palo Alto, CA, USA) as well as Graphpad Prism 9 (GraphPad Inc., LaJolla, CA, USA) were used for statistical analysis and data visualization. Normal distribution was analysed with the D'Agostino & Pearson test, and concentrations are shown in mean ± SD if not indicated otherwise. Depending on the experiment, comparisons of concentrations in two different groups were either performed with the Mann-Whitney U or the one sample t test, while more than two groups were compared using a one-way ANOVA (Kruskal-Wallis test with Dunn's post-hoc test to correct for multiple comparisons). Influence of two different parameters was analysed by performing a two-way ANOVA and Tukey's multiple comparison test.

Categorical data is reported as numbers (n) with frequencies (%), and is investigated using the Fisher's exact test, thereby reporting odds ratios (ORs) and 95 % confidence intervals (CIs).

In all statistical tests, a p-value ≤ 0.05 was considered statistically significant (* $p < 0.05$, ** $p < 0.01$, *** $p < 0.001$, **** $p < 0.0001$). To maintain a 5 % false discovery rate, multiple testing was corrected using the Benjamini-Hochberg procedure.

4 RESULTS

4.1 Development and characterization of immunoassays measuring C1s/C1-INH and MASP-1/C1-INH complexes

Parts of the results concerning assay development, characterization and validation (chapters 4.1, 4.2, 4.3, and 4.4.1) were summarized in a manuscript that was published in Frontiers in Immunology (38). The published content of our study was reused with permission in adapted form in this thesis, under the terms of the Creative Commons Attribution License (CC BY 4.0).

Hurler L, Toonen EJM, Kajdácsi E, van Bree B, Brandwijk RJMGE, de Bruin W, Lyons PA, Bergamaschi L, Cambridge Institute of Therapeutic Immunology and Infectious Disease-National Institute of Health Research (CITIID-NIHR) COVID BioResource Collaboration, Sinkovits G, Cervenak L, Würzner R and Prohászka Z (2022). Distinction of early complement classical and lectin pathway activation via quantification of C1s/C1-INH and MASP-1/C1-INH complexes using novel ELISAs. Front. Immunol. 13:1039765. doi: 10.3389/fimmu.2022.1039765.

In this study, the thesis' author was the leading investigator under the supervision of Prof. Dr. Zoltán Prohászka, Dr. Erik J.M. Toonen and Prof. Dr. Reinhard Würzner. The author's contribution included methodology, validation, formal analysis, investigation, data curation, visualization, interpretation of data, writing original draft, writing: reviewing, and editing. The author performed, analyzed, and evaluated all experimental parts within this objective in consultation with the additional authors of the manuscript. Detailed contributions of other authors can be found in the published manuscript.

4.1.1 Monoclonal antibodies are specific for C1-INH complex components

Monoclonal antibodies directed against either recombinant C1s (CCP1-CCP2-SP fragment), recombinant MASP-1 (CCP1-CCP2-SP fragment), or affinity-purified C1-INH (derived from Berinert® concentrate) were developed *in-house* using hybridoma technology as described elsewhere (222, 236, 237). Several different antibodies were generated and tested, but here only results for the selected three monoclonals are shown.

No proteins with > 60 % similarity to the antigens used for antibody development were identified in *in silico* amino acid searches (data not shown).

In a direct ELISA, the murine antibodies did show highly specific signals for the respective proteins, while no cross-reactivity with additionally tested proteins were observed (Figure 8A+B; taken and adapted with permission from (38)). Besides that, all antibodies used for assay development were further investigated for their potential application in Western Blots. Whereas the C1-INH antibody did show inconclusive results when used as primary antibody in Western Blots (data not shown), and therefore needs further testing in the future, both the anti C1s antibody (Figure 8C) and the anti MASP-1 antibody (Figure 8D) showed high specificity as evidenced by Western Blotting. While anti C1s could detect the recombinant C1s CCP1-CCP2-SP fragment (Figure 8C, lane 2) with a band at 37 kDa, native C1s (80 kDa) in the NHS (lane 4) and the ZAS samples (lane 5) as well as the *in-house* C1s/C1-INH complex (about 150 kDa, lane 6), there were also traces of C1s/C1-INH complex detectable in the NHS and ZAS samples. The antibody did not show a signal for C1-INH (lane 3).

A similar pattern is seen when using the anti MASP-1 antibody for detection (Figure 8D). Again here, the antibody could identify the recombinant MASP-1 CCP1-CCP2-SP fragment (lane 2, 45 kDa) and native MASP-1 in NHS (lane 4) and ZAS (lane 5) at a size of around 80 kDa, there are further bands visible in the serum samples, potentially caused by complex formation with other interaction partners of MASP-1 (> 80 kDa). Also the *in-house* MASP-1/C1-INH complex (lane 6, 155 kDa) could be detected in the Western Blot, while again no signal was observed for the C1-INH (lane 3).

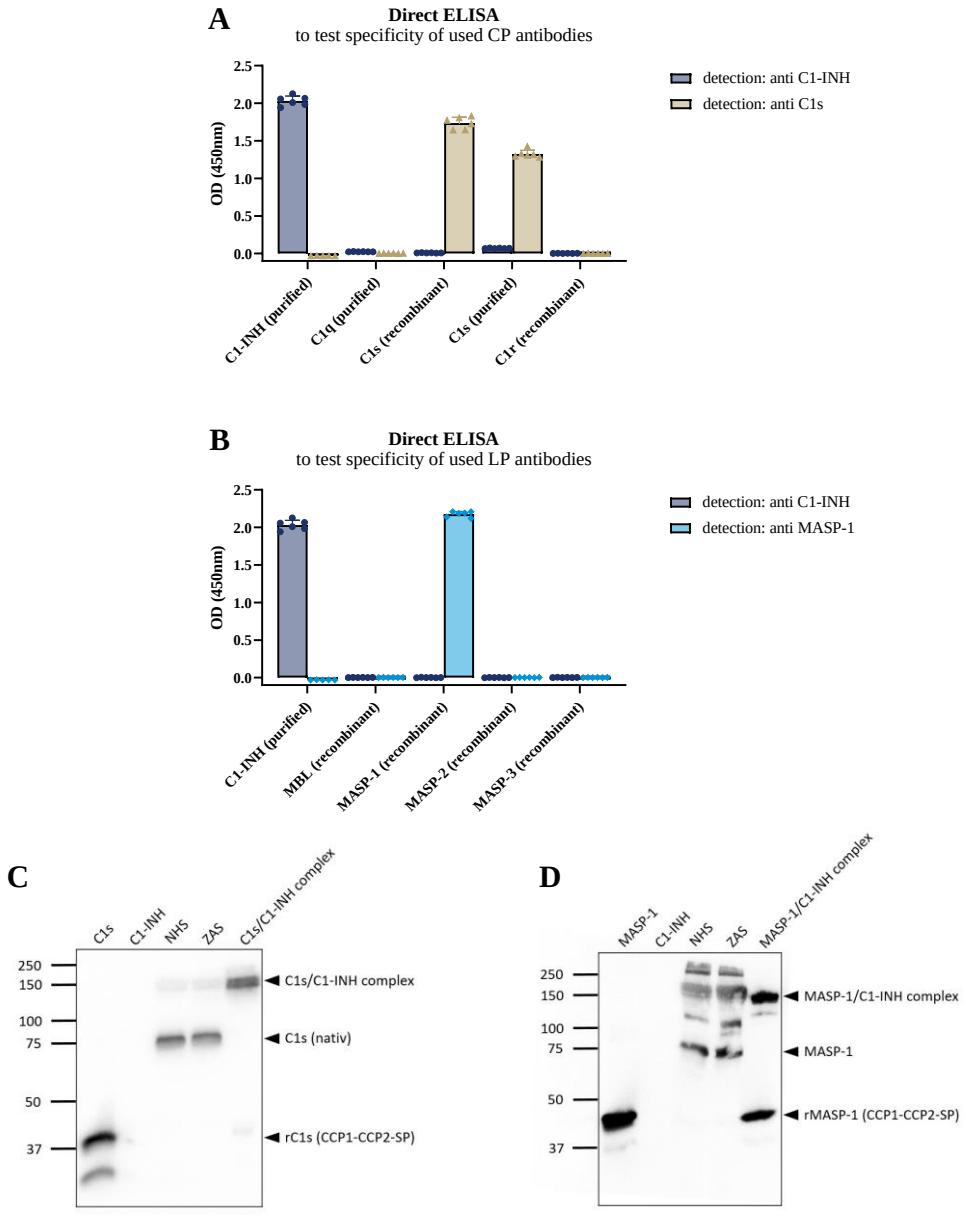

Figure 8: Test of anti C1-INH, anti C1s and anti MASP-1 in a direct ELISA as well as in Western Blots. (A+B) Test of classical and lectin pathway antibodies in a direct ELISA. Plates were coated with complement proteins of the respective pathways, and detection was performed using either anti C1-INH and anti C1s (A) or anti C1-INH and anti MASP-1 antibodies (B). Single conditions were tested in duplicates, while the experiment was performed in triplicates. (C+D) Test of selected antibodies targeting the serine proteases in Western Blot. Western Blots were performed with either 200 ng of protein/lane or 1:20 diluted serum samples (NHS or ZAS) under non-reducing conditions. Anti C1s (C) and anti MASP-1 (D) were used as primary antibodies, while detection was performed with goat anti-mouse Ig-HRP. Presented Blots show exemplary results for each antibody, while Western Blots were performed a total of four times each. Parts of the figure (panels A+B) taken and adapted with permission from Hurler *et al.* (38), under the terms of the Creative Commons Attribution License (CC BY), https://creativecommons.org/licenses/by/4.0/.

4.1.2 Development and technical validation of immunoassays detecting C1s/C1-INH and MASP-1/C1-INH complexes

After suitable monoclonal antibodies were selected, two novel immunoassay were developed, detecting levels of C1s/C1-INH (cat #HK399) and MASP-1/C1-INH (cat#HK3001) complex. Both assays are based on the principle of basic sandwich ELISAs, and several experiments have been performed in order to come up with a proper and reliable assay setup. Experiments during assay development and optimization included testing of various different monoclonal antibodies and antibody combinations as well as concentrations, buffer optimizations, and comparisons between different calibrators. Only experiments with the final assay setup will be presented and discussed within the scope of this thesis.

While the standard curve for the C1s/C1-INH complex assay ranges from 1.6-100.0 ng/mL (LloQ: 0.2 ng/mL, UloQ: 100.0 ng/mL; Figure 9A), the one for the MASP-1/C1-INH complex assay covers biomarker levels from 0.4-25.0 ng/mL (LloQ: 0.06 ng/mL, UloQ: 50 ng/mL; Figure 9B). As a regression model, non-linear regression (one-site binding, Hyperbola) was chosen, leading to a coefficient of determination between C1s/C1-INH complex or MASP-1/C1-INH complex concentrations and measured OD values of $R^2 = 0.9990$ and $R^2 = 0.9987$, respectively.

When mixing samples with high, medium and low concentrations in different ratios, the average recovery was > 90 % for both complexes (Figure 9C+D; taken and adapted with permission from Hurler *et al.* (38); individual concentrations and determined recovery values of the experiments are listed in the published manuscript (38)). The correlation between expected and measured concentrations were highly significant for C1s/C1-INH complex ($R = 1.000$, $p < 0.0001$; Figure 9C) and MASP-1/C1-INH complex ($R = 0.999$, $p < 0.0001$; Figure 9D).

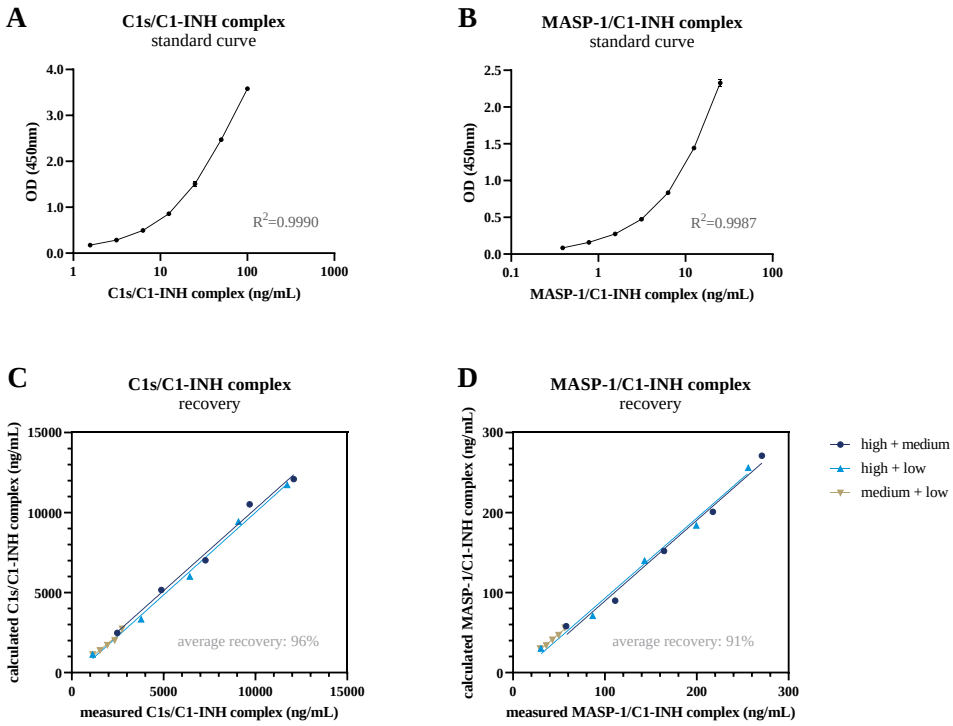

Figure 9: Standard curves of new immunoassays and recovery of C1-INH complexes in EDTA plasma. Representative standard curves of the new C1s/C1-INH complex assay (A), ranging from 1.6-100.0 ng/mL, and the MASP-1/C1-INH complex assay (B), ranging from 0.4-25 ng/mL. Non-linear regression (One-site binding, Hyperbola) was used to obtain the coefficient of determination (R^2). Recovery of C1s/C1-INH (C) and MASP-1/C1-INH complex (D) was investigated by mixing EDTA plasma samples of three individuals with high, medium and low C1-INH complex concentrations in different ratios. After 30 min of incubation, C1-INH complex levels were determined in the immunoassays and recovery was calculated according to the equation stated in the Material and Methods section. Figures taken and adapted with permission from Hurler *et al.* (38), under the terms of the Creative Commons Attribution License (CC BY), https://creativecommons.org/licenses/by/4.0/.

Both assays show low inter- and intra-assay variations (Table 13; taken with permission from Hurler *et al.* (38)), and can measure the particular C1-INH complexes in plasma (citrate, heparin or EDTA) and serum in a reliable way (Table 14; taken with permission from Hurler *et al.* (38)). Of note, C1-INH complex concentrations differ depending on the matrix used. Highest levels were measured in serum samples, and complex concentrations were lower in all kinds of plasma (citrate, heparin, EDTA) of the same individuals. Hence the dilution of the samples needs to be adjusted to the sample type used for the measurement, while serum samples should be diluted at least 200x (C1s/C1-INH complex) or 10x (MASP-1/C1-INH complex), and plasma samples not less than 100x (C1s/C1-INH complex) or 5x (MASP-1/C1-INH complex).

Table 13: Analysis of Intra- and Inter-assay variation of new C1-INH complex assays. Table taken with permission from Hurler *et al.* (38).

C1s/C1-INH complex		**sample 1**	**sample 2**	**sample 3**	**sample 4**
Intra-assay variation					
Operator 1	mean aliquot 1-3 (ng/mL)	1161	1967	1595	1285
	SD (ng/mL)	90	121	49	63
	CV (%)	7.8	6.2	3.1	4.9
Operator 2	mean aliquot 1-3 (ng/mL)	1245	2135	1868	1399
	SD (ng/mL)	47	166	99	43
	CV (%)	3.8	7.8	5.3	3.1
Inter-assay variation					
	mean operator 1 and 2 (ng/mL)	1203	2051	1731	1342
	SD (ng/mL)	79	159	165	79
	CV (%)	6.6	7.8	9.5	5.9

MASP-1/C1-INH complex		**sample 1**	**sample 2**	**sample 3**	**sample 4**
Intra-assay variation					
Operator 1	mean aliquot 1-3 (ng/mL)	273.2	115.5	57.3	35.5
	SD (ng/mL)	6.6	0.7	3.6	0.5
	CV (%)	2.4	0.6	6.2	1.5
Operator 2	mean aliquot 1-3 (ng/mL)	259.0	108.3	52.4	34.7
	SD (ng/mL)	8.1	2.4	1.2	0.6
	CV (%)	3.1	2.2	2.4	1.8
Inter-assay variation					
	mean operator 1 and 2 (ng/mL)	266.1	111.9	54.9	35.1
	SD (ng/mL)	10.2	4.3	3.6	0.7
	CV (%)	3.8	3.8	6.6	1.9

Table 14: Analysis of different matrices of single representative individuals in the C1-INH complex assays. Table taken with permission from Hurler *et al.* (38).

	C1s/C1-INH complex				MASP-1/C1-INH complex			
matrix	Citrate	Heparin	EDTA	Serum	Citrate	Heparin	EDTA	Serum
mean concentration (ng/mL)	2270	6215	2348	4612	37.5	16.6	26.5	121.7
SD (ng/mL)	81	279	93	251	1.8	0.8	1.6	10.6
CV (%)	3.6	4.5	4.0	5.4	4.7	4.7	5.9	8.7

The assays are very specific for the C1-INH complexes, while no signals are observed by the non-complexed components (Figure 10A+B; taken and adapted with permission from Hurler *et al.* (38)). Only the commercially available purified C1s (CompTech) did give a slight increase in C1s/C1-INH complex concentration (Figure 10A). Because of that, the C1s preparation was analysed using mass spectrometry at Medical University Innsbruck. Traces of C1-INH were found in the 50 most abundant proteins within the preparation (data not shown). Although the abundance of C1-INH was only 0.0001 % of the total protein amount, the affinity of C1s' and C1-INH is high, so there is the possibilty of C1s/C1-INH complex formation in the „purified C1s" preparation, which explains the weak signal seen in the complex assay.

Furthermore, cross-reactivity of the new immunoassays with animals was investigated to see if they can also be utilized for investigations of C1-INH complexes in species other than human.

C1s/C1-INH complexes could also be measured in murine samples, although results were not conclusive, as some of the five samples did not give positive signals, while others did (Figure 10C). Additionally, very high C1s/C1-INH complex levels were detected in the orang utan sample (9600 ng/mL), and the spider monkey sample also showed C1s/C1-INH complex concentrations higher than background (228 ng/mL).

In the MASP-1/C1-INH complex assay, only the orang utan (56 ng/mL) and the spider monkey (13 ng/mL) samples showed concentrations above background. All the other animals tested, including mice, did not show clear positive signals (Figure 10D).

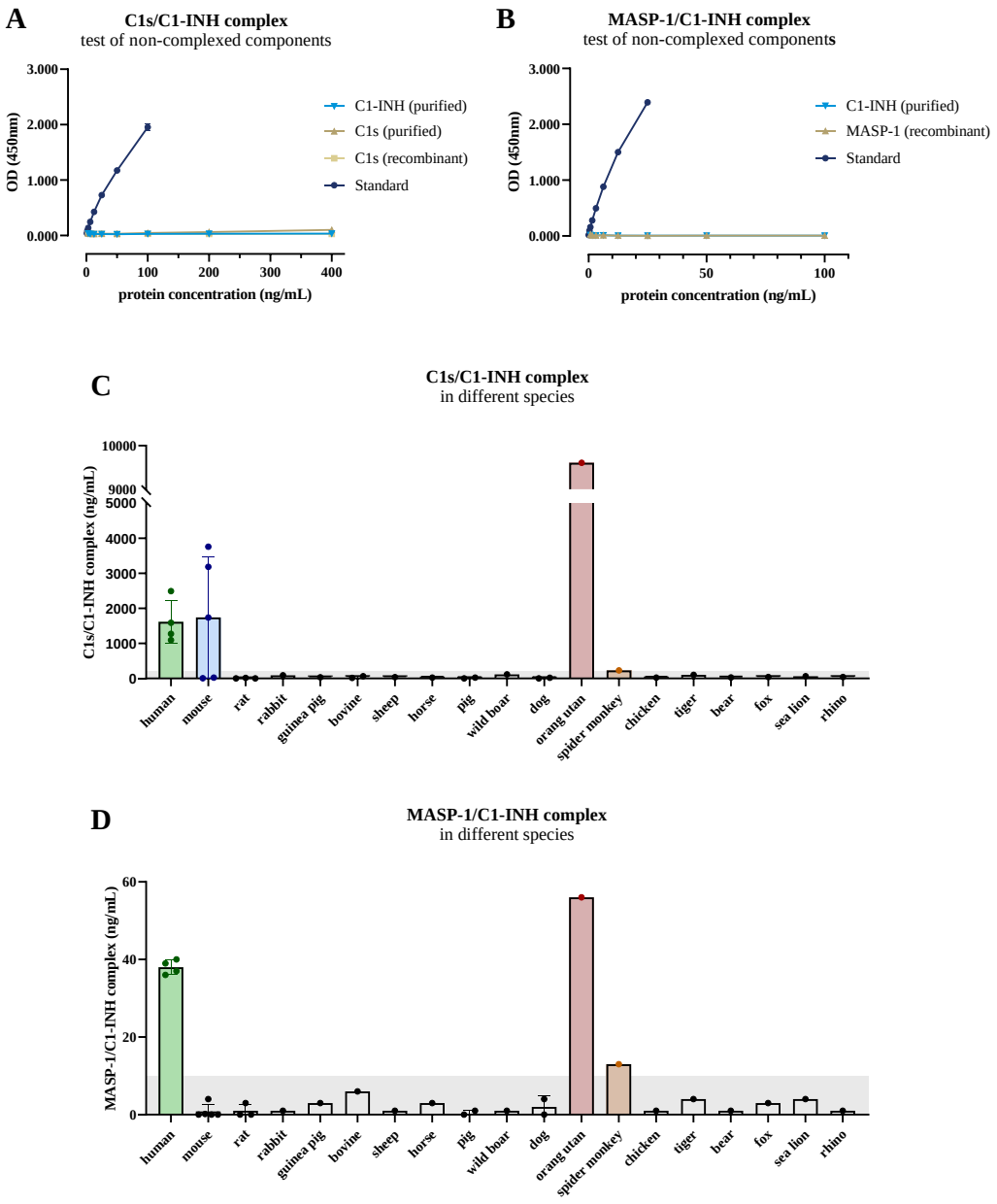

Figure 10: Cross-reactivity of the C1-INH complex assays with non-complexed components and with C1-INH complexes from different species. Purified C1-INH, serine proteases (C1s purified and C1s recombinant or MASP-1 recombinant) as well as the respective standards were tested in the C1s/C1-INH complex assay (A) and the MASP-1/C1-INH complex assay (B). Besides that, serum samples of different species were tested in the C1s/C1-INH (C) and the MASP-1/C1-INH complex assay (D). In addition to human samples (n = 5) as a control, animal samlples derived from mice (n = 5), rat (n = 3), rabbit, guinea pig, bovine (n = 2), sheep, horse, pig, wild boar, dog (n = 2), orang utan, spider monkey, chicken, tiger, bear, fox, sea lion, and rhino (n = 1 if not stated otherwise). Concentration ranges considered as background are marked in grey. Figures taken and adapted with permission from Hurler *et al.* (38), under the terms of the Creative Commons Attribution License (CC BY), https://creativecommons.org/licenses/by/4.0/.

Although many animals show MASP-1/C1-INH complex concentrations between 0 and 10 ng/mL, those values are most likely caused by background and can not certainly be considered as positive signals.

In summary, the C1-INH complex assays work in a reliable way and are very specific for human C1s/C1-INH and MASP-1/C1-INH complex without giving false-positive signals by the non-complexed human proteins.

4.1.3 Sample type and handling is important when investigating C1-INH complexes

Since proper sample handling is highly important when measuring complement activation products, stability of the C1-INH complexes was investigated at room temperature and on ice, as well as during multiple freeze-thaw cycles (Figure 11; taken and adapted with permission from Hurler *et al.* (38)).

In EDTA plasma, C1-INH complex levels are not significantly changing when keeping samples on ice for up to 16 h (Figure 11A+B). However, there is an increase in C1-INH complexes when samples are kept at room temperature for more than two hours, which is especially true for the C1s/C1-INH complex (16 h: $p = 0.0465$). Besides that, *de novo* complex formation does occur way faster in citrate plasma, where C1-INH levels of samples kept at room temperature increase to levels more than double the starting concentrations within 16 h, with significantly increased concentrations of both C1-INH complexes already after 1 h of incubation (Figure 11C+D). Incubation on ice does slow down additional complex formation, but again levels increase faster in citrate plasma than in EDTA plasma.Additionally, stability of C1-INH complexes in EDTA plasma and in purified form (C1s/C1-INH complex from CompTech or *in-house* MASP-1/C1-INH complex in buffer) was tested in multiple freeze-thaw cycles. Both complex levels in EDTA plasma do not markedly change when performing up to four freeze-thaw cycles, while the C1s/C1-INH complex in purified form seems to be prone to degradation when being repeatedly frozen and thawed (Figure 11E+F).

Overall, those findings emphasize the importance of appropriate sample handling, storage of samples in aliquots, the preferred use of EDTA plasma, and the recommendation of keeping samples on ice after thawing until the meausrement of C1-INH complexes.

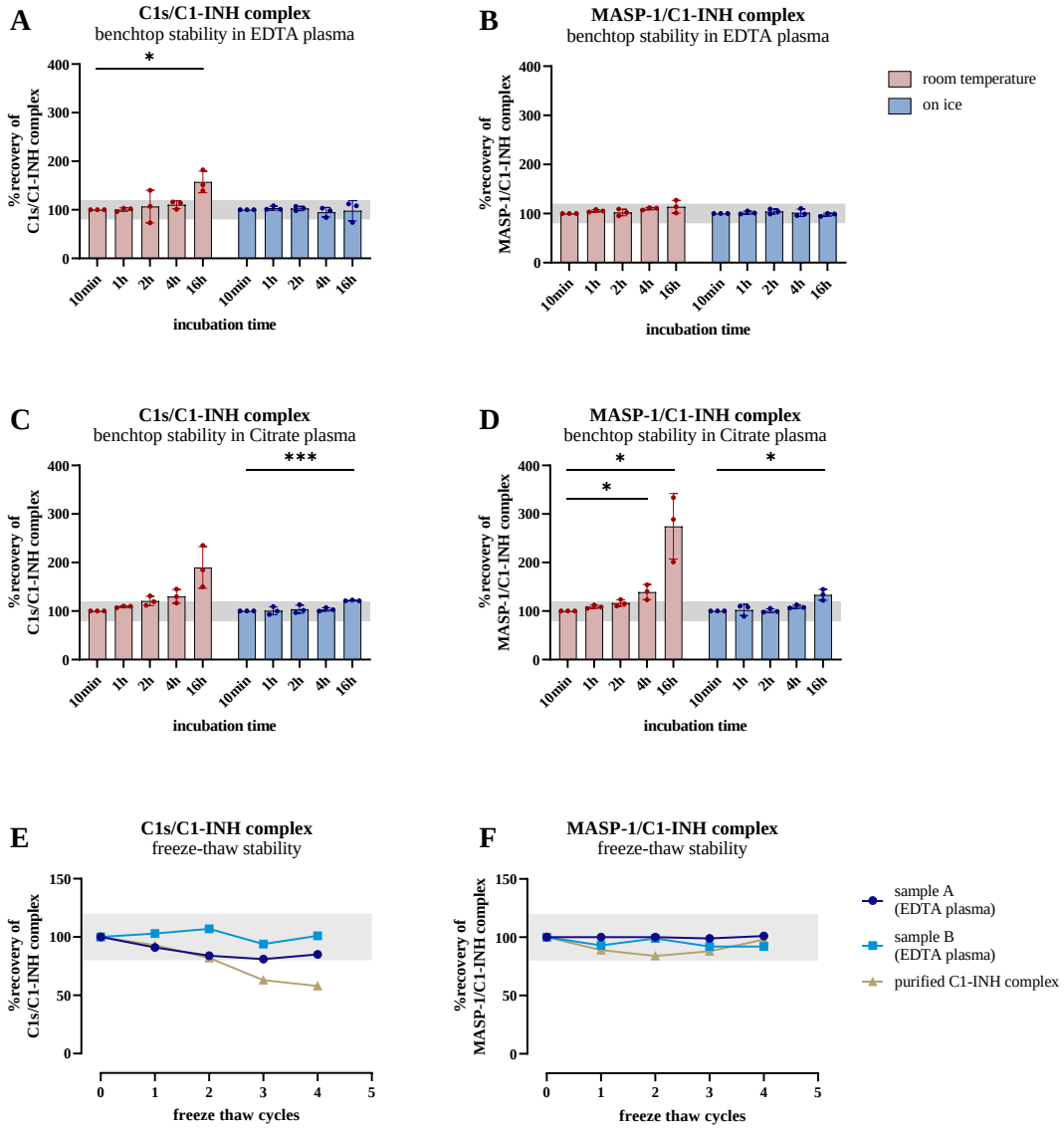

Figure 11: Stability testing of C1-INH complexes. Benchtop stability of C1s/C1-INH complex (A: EDTA plasma, C: Citrate plasma) and MASP-1/C1-INH complex (B: EDTA plasma, D: Citrate plasma) was tested by storing samples at room temperature (red graphs) or on ice (blue graphs) for time intervals ranging from 10 min to 16 h. Afterwards C1-INH complex levels were measured and recovery was caluclated based on the concentrations of the 10 min sample. Differences to the 10 min sample were analysed using the one sample t-test (* $p < 0.05$, *** $p < 0.001$). Freeze thaw stability was tested by exposing aliquots of either purified C1-INH complex (brown) or two independent EDTA plasma samples (dark and light blue) to up to 4 freeze-thaw cycles. Afterwards concentrations of C1s/C1-INH (E) and MASP-1/C1-INH complex (F) were measured and recovery was calculated based on the concentrations measured in the sample without freeze-thaw cycles. Figure taken and adapted with permission from Hurler *et al.* (38), under the terms of the Creative Commons Attribution License (CC BY), https://creativecommons.org/licenses/by/4.0/.

4.2 C1s/C1-INH and MASP-1/C1-INH complexes are suitable markers for early classical and early lectin pathway activation

To support the assumption that C1-INH complexes are suitable markers for the measurement of ongoing CP and LP activation, NHS was activated with zymosan and the levels of C1s/C1-INH and MASP-1/C1-INH complex were analysed over time.

As seen in Figure 12 (taken and adapted with permission from Hurler *et al.* (38)), both complex concentrations increased in a time-dependent manner upon activation of complement with zymosan, while no such increase was seen in negative controls treated with EDTA. Besides that, concentrations at T_0 (directly after mixing) were comparable in the different approaches, with average concentrations of 2829 ± 138 ng/mL for the C1s/C1-INH complex and 111.4 ± 3.5 ng/mL for the MASP-1/C1-INH complex before activation.

In the NHS+zymosan sample, C1s/C1-INH complex levels increased a total of 5.7-fold up to 16000 ng/mL within 5 hours, while even in the NHS sample without zymosan (NHS) concentrations of 14000 ng/mL C1s/C1-INH complex were reached within the same time, suggesting strong auto-activation of the classical pathway in the serum while performing the experiment (Figure 12A). Concentrations in the negative controls (samples containing EDTA) did not show a marked increase of the complex levels. When performing a two-way ANOVA, for the zymosan-treated sample the effect was statistically significant for the incubation time ($p < 0.0001$) as well as the treatment (NHS+zymosan vs. NHS: $p = 0.0399$, NHS+zymosan vs. NHS+zymosan+EDTA: $p < 0.0001$, NHS+zymosan vs. NHS+EDTA: $p < 0.0001$).

Zymosan activation of NHS also led to a very rapid increase of MASP-1/C1-INH, while the complex concentration doubled from 111 ng/mL to 224 ng/mL within only one hour of incubation ($p < 0.0001$, Figure 12B). Afterwards a plateau is reached and MASP-1/C1-INH complex concentrations do not further increase anymore, even when activation is continued for up to 5 h. Contrary to the C1s/C1-INH complex, no increase in MASP-1/C1-INH complex could be observed in NHS only, while again no additional complex formation was observed in the negative controls treated with EDTA (NHS+zymosan vs. all other treatments tested: $p < 0.0001$).

Additionally, experiments only activating one of the two pathways were also performed, and formation of C1-INH complexes was monitored in accordance with the activation experiments utilizing zymosan for CP and LP triggering.

Again here, baseline levels (T_0) of C1-INH complexes were comparable in the different approaches, with 1897 ± 120 ng/mL C1s/C1-INH complex and 58.0 ± 2.3 ng/mL MASP-1/C1-INH complex. Of note, a different NHS pool was used for the CP/LP specific activation and the zymosan activation experiments due to the performance of experiments in different laboratories.

Using IgM coating to specifically activate the classical pathway, C1s/C1-INH complex levels increased significantly ($p = 0.0101$) within 5 min in line with the CP activity, measured by the C9 neoepitope formation in the wells of the same samples. After at least 10 min of incubation, C1s/C1-INH complex levels were highly increased compared to the baseline levels ($p < 0.0001$), reaching as high as 16000 ng/mL, while there was a slight increase in MASP-1/C1-INH complex levels observed within the first 30 min of incubation, too (Figure 12C+D). When comparing those changes to MASP-1/C1-INH complex formation caused by specific lectin pathway activation through mannan coating, the effect seen during CP activation is negligible.

Using mannan coating, a highly significant increase in MASP-1/C1-INH complex levels (≤60 min activation: $p = 0.0140$; > 60 min activation: $p < 0.0001$), again to more than double the initial concentration, is seen (Figure 12D), although *de novo* complex formation takes longer compared to the zymosan activation (Figure 12B). Similarly, LP activity, again measured by formation of the C9 neoantigen, did increase in a time-dependent manner, while C1s/C1-INH complex levels stayed at baseline for up to 2 h (Figure 12C). Afterwards, new formation of C1s/C1-INH complex could be detected ($p = 0.0456$), caused by auto-activation of the CP as seen before.

While C1s/C1-INH complex levels perfectly correlated with CP activity ($r = 0.9870$, $p < 0.0001$; Figure 12E), there is also a strong positive correlation between MASP-1/C1-INH complex formation and LP activity ($r = 0.7336$, $p = 0.0002$; Figure 12F), although not as prominent as seen for the CP marker.

Overall, those *in vitro* findings confirm the hypothesis that C1s/C1-INH and MASP-1/C1-INH complexes are specific markers for early CP and early LP activation, respectively.

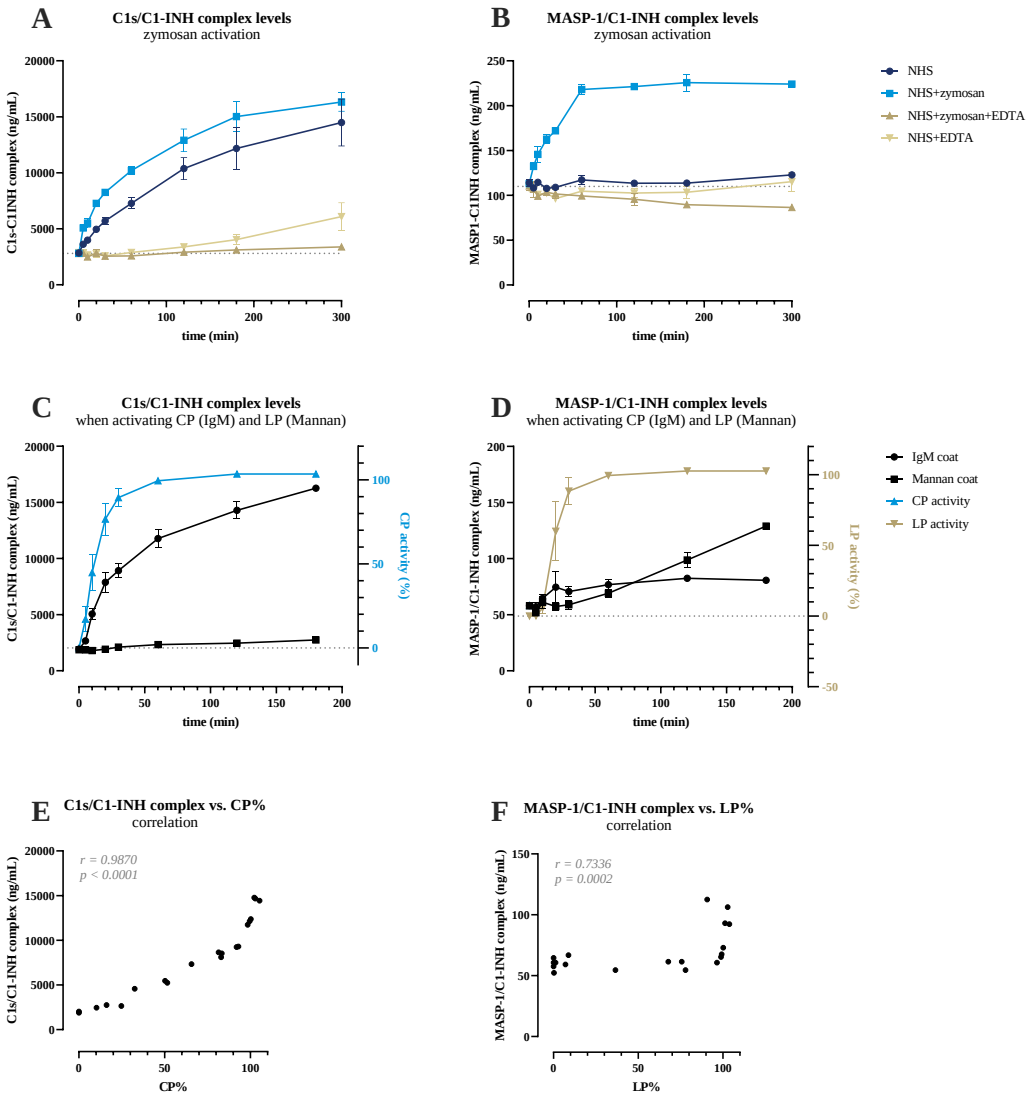

Figure 12: Validation of C1-INH complexes as markers for classical and lectin pathway activation. Complement in NHS was either activated with zymosan, IgM or Mannan and levlels of C1s/C1-INH complex (A: zymosan, C: IgM and Mannan) and MASP-1/C1-INH complex (B: zymosan, D: IgM and Mannan) were determined in the complex assays. Besides that, CP and LP activity, measured by the formation of the Terminal complement complex (TCC/C5b-9) was further determined in the experiments specifically activating the respective pathways (C: CP, D: LP). Auto-activation was determined in NHS without additions, while EDTA served as a negative control (A+B). Influence of activation agents or incubation time was analysed with a two-way ANOVA with Tukey's multiple comparisons test. Besides that, C1s/C1-INH complex levels were plotted against measured CP activity (E) and MASP-1/C1-INH complex levels were plotted against LP activity (F). Correlations between pathway activities and the respective C1-INH complexes was determined using the Spearman Rank correlation. Figure panels A-D taken and adapted with permission from Hurler *et al.* (38), under the terms of the Creative Commons Attribution License (CC BY), https://creativecommons.org/licenses/by/4.0/.

4.3 Analysis of C1-INH complexes in healthy individuals

To establish reference values for both C1-INH complexes, C1s/C1-INH and MASP-1/C1-INH complex levels were measured in EDTA plasma of 96 healthy adult individuals utilizing the newly developed immunoassays (distribution of gender and age is visualized in Figure 13).

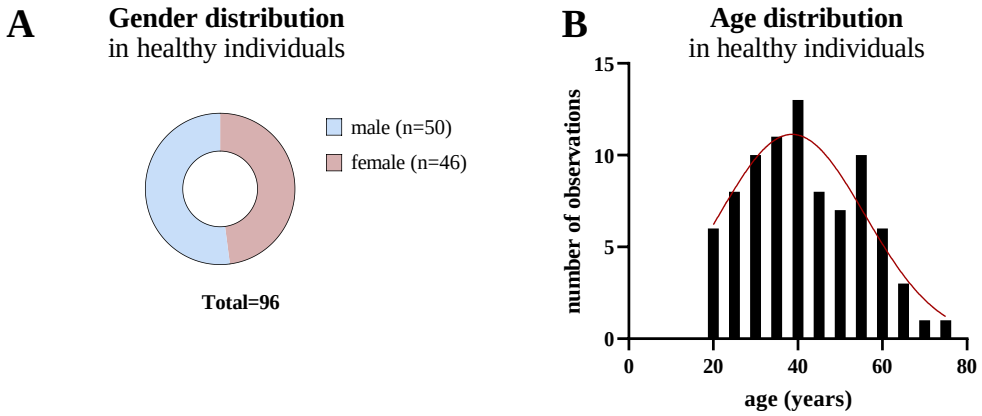

Figure 13: Gender and age distribution of healthy individuals used for reference determination for the C1-INH complex assays. C1-INH complex levels were measured in EDTA plasma of 96 healthy individuals, while gender (A) and age (B) distribution are visualized here. 50/96 healthy individuals were male and 46/96 female, while the mean age was 41.5 ± 13.1 years.

In EDTA plasma, physiological concentrations of 1846 ± 1060 ng/mL C1s/C1-INH complex (mean ± 2SD) and median 36.9 (13.18 - 87.89) ng/mL MASP-1/C1-INH complex [median (2.5 percentile range – 97.5 percentile range)] were observed (Figure 14, modified with permission from Hurler *et al.* (38)).

To define first reference ranges, different approaches were used, since physiological C1s/C1-INH complex levels were normally distributed (Figure 14A; D'Agostino & Pearson test: $p = 0.0974$), whereas MASP-1/C1-INH complex concentrations showed a right-skewed distribution and did not pass the normality test (Figure 14B; D'Agostino & Pearson test: $p < 0.0001$). None of the complexes differed significantly between males ($n = 50$) and females ($n = 46$) (Figure 14C+D; Mann-Whitney: $p = 0.1588$ for C1s/C1-INH complex; $p = 0.9674$ for MASP-1/C1-INH complex), while C1-INH complex concentrations also did not correlate with age when looking at healthy adult donors (Figure 14E+F; C1s/C1-INH complex: $r = 0.0306$, $p = 0.7832$; MASP-1/C1-INH complex: $r = -0.0150$, $p = 0.8926$).

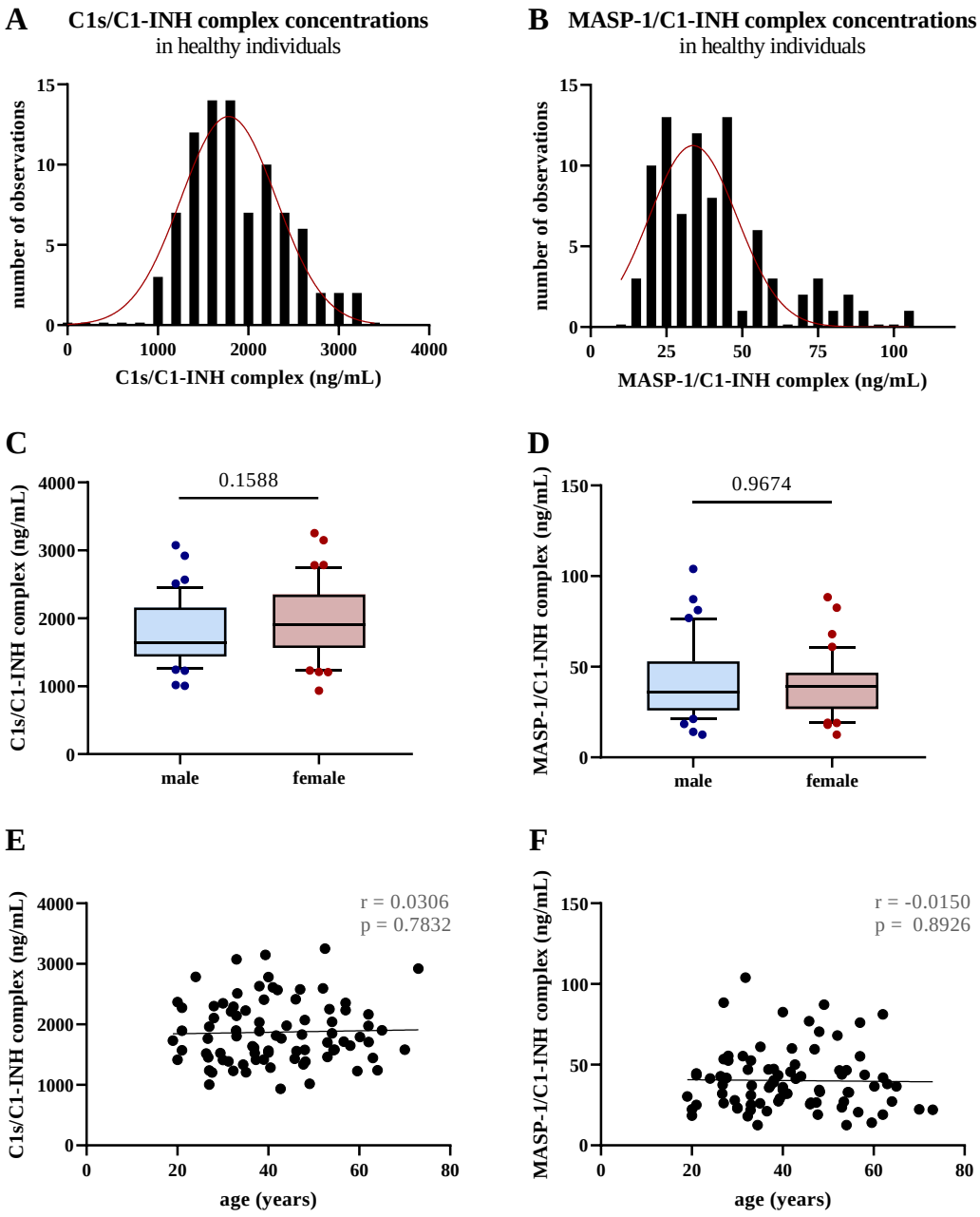

Figure 14: Levels of C1-INH complexes in healthy adults. C1-INH complex levels were measured in 96 healthy adult individuals, while distribution of C1s/C1-INH complex (A) and MASP-1/C1-INH complex levels (B) are illustrated in histograms, while normal distribution was checked with the D'Agostino & Person test. Measured concentrations were furthermore stratified according to gender (C: C1s/C1-INH complex, D: MASP-1/C1-INH complex), and differences between males and females were analysed using the Mann-Whitney test. Besides that, C1-INH complex levels were also checked for their correlation with age (E: C1s/C1-INH complex, F: MASP-1/C1-INH complex). Figure modified with permission from Hurler *et al.* (38), under the terms of the Creative Commons Attribution License (CC BY), https://creativecommons.org/licenses/by/4.0/.

4.4 Investigation of complement activation including C1-INH complexes in COVID-19

Parts of the here described results focusing on lectin pathway activation (chapters 4.4.2, 4.4.3, and 4.4.4), were summarized in a manuscript that was published in Frontiers in Immunology (112). The published content of our study was reused in adapted form in this thesis, under the terms of the Creative Commons Attribution License (CC BY 4.0).

Hurler L, Szilágyi Á, Mescia F, Bergamaschi L, Mező B, Sinkovits G, Réti M, Müller V, Iványi Z, Gál J, Gopcsa L, Reményi P, Szathmáry B, Lakatos B, Szlávik J, Bobek I, Prohászka ZZ, Förhécz Z, Csuka D, Kajdácsi E, Cervenak L, Kiszel P, Masszi T, Vályi-Nagy I, Würzner R, Cambridge Institute of Therapeutic Immunology and Infectious Disease-National Institute of Health Research (CITIID-NIHR) COVID BioResource Collaboration, Lyons PA, Toonen EJM, and Prohászka Z (2023). Complement lectin pathway activation is associated with COVID-19 disease severity, independent of *MBL2* genotype subgroups. Front. Immunol. 14:1162171. doi: 10.3389/fimmu.2023.1162171.

In this study, the thesis' author was the leading investigator under the supervision of Prof. Dr. Zoltán Prohászka and Dr. Erik J.M. Toonen. The author's contribution included methodology, validation, formal analysis, investigation, data curation, visualization, interpretation of data, writing original draft, writing: reviewing, and editing. The author performed, analyzed, and evaluated all experimental parts within this objective in consultation with the additional authors of the manuscript, while genotyping of the *MBL2* gene was performed by colleagues in the respective institutions. Detailed contributions of other authors can be found in the published manuscript.

Two COVID-19 cohorts originating from Budapest (BUD) (173) and Cambridge (CAM) (232), were included in the analysis. An overview of the cohorts is listed in Table 15 (taken with permission from Hurler *et al.* (112)).

Table 15: Baseline characteristics of COVID-19 cohorts and healthy controls included in the analysis. Table taken with permission from Hurler *et al.* (112).

Variables	COVID Cambridge (CAM)	COVID Budapest (BUD)	Healthy controls (CAM)	Healthy controls (BUD)
total, n	215	128	47	339
Male sex, n (%)	118 (54.9)	71 (55.5)	26 (55.3)	154 (45.4)
Mean age ± SD	52.9 ± 17.8	60.5 ± 16.5	42.3 ± 15.0	42.1 ± 12.8
Delay between first symptom and sampling, days median (IQR)	11 (6-31)	9 (5-20)	-	-
MODERATE cases	**n (% of total cases)**	**n (% of total cases)**		
not requiring hospitalization (MILD/CONV[§])	56 (26.0)	26 (20.3) [§]	-	-
hospitalized, but not requiring O_2 or ventilation (HOSP)	47 (21.9)	27 (21.1)	-	-
SEVERE cases				
hospitalized, requiring O_2 (HOSP+O_2)	40 (18.6)	33 (25.8)	-	-
Intensive care unit (ICU)	72 (33.5)	42 (32.8)	-	-
Laboratory findings, median (IQR)				
C-reactive protein [ref <10 mg/L]	25.5 (3.1-122.3)	29.4 (3.7–107.6)	1.8 (1.2-2.4)	2.1 (1.1-4.2)
Interleukin 6 [ref 2–4.4 pg/mL]	2.3 (0.5-11.2)	24.2 (7.1–67.9)	0.2 (0.2-0.2)	NA
TCC/C5b-9 [ref <1000 mAU/mL]	3804 (2913-6144)	-	2104 (1753-2527)	-
sC5b-9 [ref 110-252 ng/mL]	-	265 (185-380)	-	198 (148-298)
Disease outcome				
Long COVID*, n (%)	32 (53.3)	NA	-	-
COVID-19 related death/mortality, n (%)	19 (8.8)	25 (19.5)	-	-

[§] Sampling in all 26 patients with only mild COVID-19 from the Budapest cohort (BUD) was done in the convalescent phase, hence biomarker measurements were excluded from merged analysis showing levels in acute COVID-19, but individuals were included in genetic analysis. Results with biomarker levels of those 26 patients are termed CONV.

* In total, 60 COVID-19 patients from the Cambridge cohort (CAM) were administered to a questionnaire asking about persisting symptoms (Long COVID). In the Budapest cohort (BUD) no questionnaires were performed/sent out to the patients.

The ratio between males and females was similar in both cohorts (Fisher's exact: $p > 0.9999$), while patients were significantly older in the Hungarian cohort (52.9 ± 17.8 years vs. 60.5 ± 16.5 years, Mann-Whitney: $p < 0.0001$). Besides that, healthy controls were significantly younger in both cohorts (Mann-Whitney: CAM: $p = 0.0014$, BUD: $p < 0.0001$).

The Cambridge (CAM) COVID-19 cohort consisted of 215 patients with approved SARS-CoV-2 infection, while 47 healthy adults served as the controls (HC). The Hungarian (BUD) COVID-19 cohort included 128 SARS-CoV-2 patients. Additionally, 339 historical healthy individuals were enrolled in Hungary for genetic analysis. The COVID-19 patients were stratified according to disease severity, while the 'moderate' (MOD) patients group consisted of individuals not requiring hospital admission (MILD/CONV) and patients requiring hospitalization, but no O_2 (HOSP). The 'severe' (SEV) patient group contained hospitalized patients which needed O_2 (HOSP+O_2) and patients admitted to the intensive care unit (ICU). An overview of the severity stratification for different analyses is depictured in Figure 15 (taken and adapted with permission from Hurler *et al.* (112)).

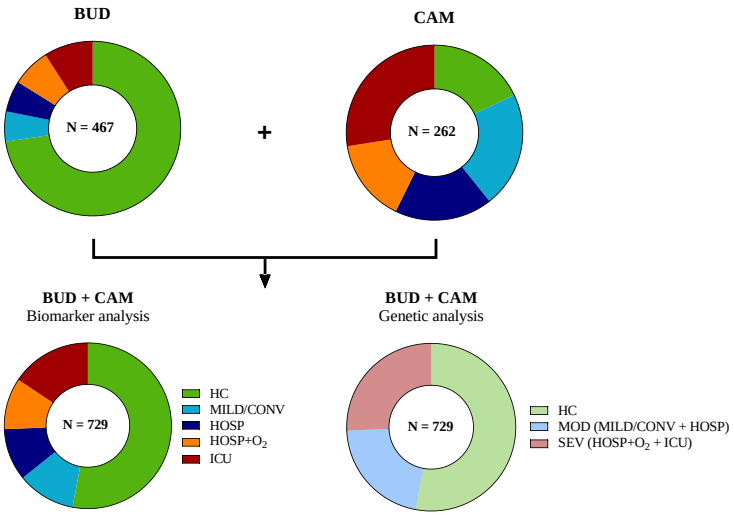

Figure 15: Distribution of cases and controls in the two cohorts (BUD and CAM) included in biomarker and genetic analysis. For biomarker analysis, individuals were stratified according to five severity groups (HC, MILD/CONV, HOSP, HOSP+O_2, ICU), while the MILD/CONV and HOSP groups were merged into the moderate (MOD), and the HOSP+O_2 and ICU groups into the severe (SEV) group for genetic analysis. Figure taken and adapted with permission from Hurler *et al.* (112), under the terms of the Creative Commons Attribution License (CC BY), https://creativecommons.org/licenses/by/4.0/.

4.4.1 C1-INH complex levels are increased in COVID-19

COVID-19 cohorts were chosen for a first proof-of-concept study when measuring C1-INH complex levels in disease *in vivo*, since the potential involvement of the CP and LP in the pathomechanism of SARS-CoV-2 infections was shown by several studies (163, 169, 170, 238).

First measurements in a total of 414 SARS-CoV-2 infected patients, deriving from the CAM and the BUD cohorts, showed increased levels of both C1-INH complexes, with mean concentrations of 2407 ± 1283 ng/mL C1s/C1-INH complex (Mann-Whitney: $p < 0.0001$; Figure 16A) and 51.5 (33.5-76.1) ng/mL MASP-1/C1-INH complex (Mann-Whitney: $p < 0.0001$; Figure 16B) in COVID-19 patients, when compared to healthy individuals (n = 96; Figure taken and adapted with permission from Hurler *et al.* (38)).

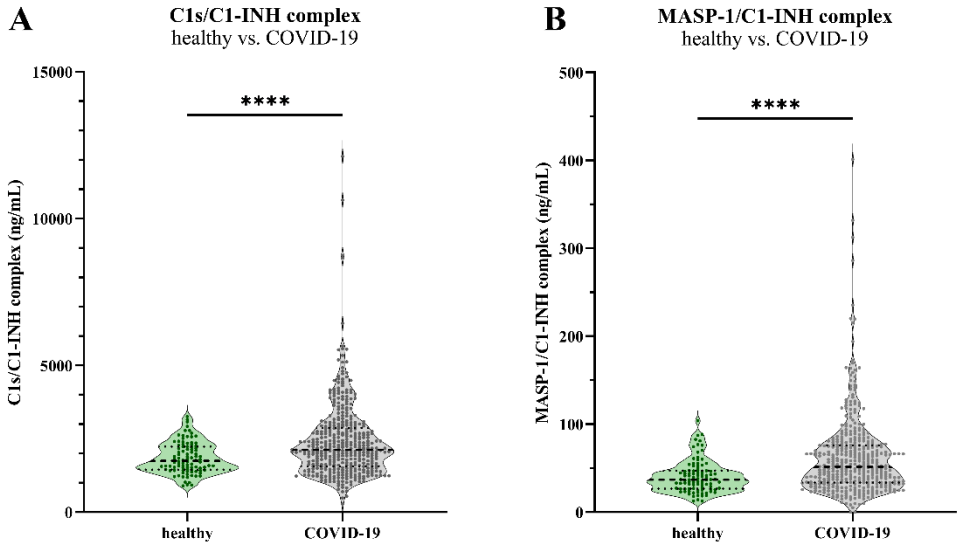

Figure 16: C1-INH complex levels in healthy individuals and COVID-19 patients. C1s/C1-INH complex (A) and MASP-1/C1-INH complex levels (B) were measured in COVID-19 patients (n = 414) and healthy controls (n = 96). P values for the pair-wise group comparisons (healthy vs. COVID-19) were calculated by the Mann-Whitney test, and significance is indicated by asterisks (**** $p < 0.0001$). Figure modified with permission from Hurler *et al.* (38), under the terms of the Creative Commons Attribution License (CC BY), https://creativecommons.org/licenses/by/4.0/.

In COVID-19 cases, C1s/C1-INH complex levels showed strong positive correlation with MASP-1/C1-INH complex concentrations in the Cambridge cohort (Figure 17A), while there was also moderate positive correlation between the two markers as well as between C1s/C1-INH complex and the CP/LP common marker C4d in the Budapest cohort (Figure 17B). Besides, C1s/C1-INH complex concentrations moderately correlated with

common complement activation markers C3a and C5b-9, as well as with C1-INH levels and CRP concentrations in both COVID-19 cohorts.

Also MASP-1/C1-INH complex levels showed moderate positive correlation with CP/LP common marker C4d in COVID-19 cases (Figure 17B), while in both cohorts weak positive correlations were also observed between MASP-1/C1-INH complex concentrations and levels of C3a, C5b-9, and C1-INH.

In healthy controls, significant correlations could only be observed between the two C1-INH complexes and C1-INH concentrations (Figure 17A+B), and between C1s/C1-INH and MASP-1/C1-INH complexes in the Budapest control cohort (Figure 17B).

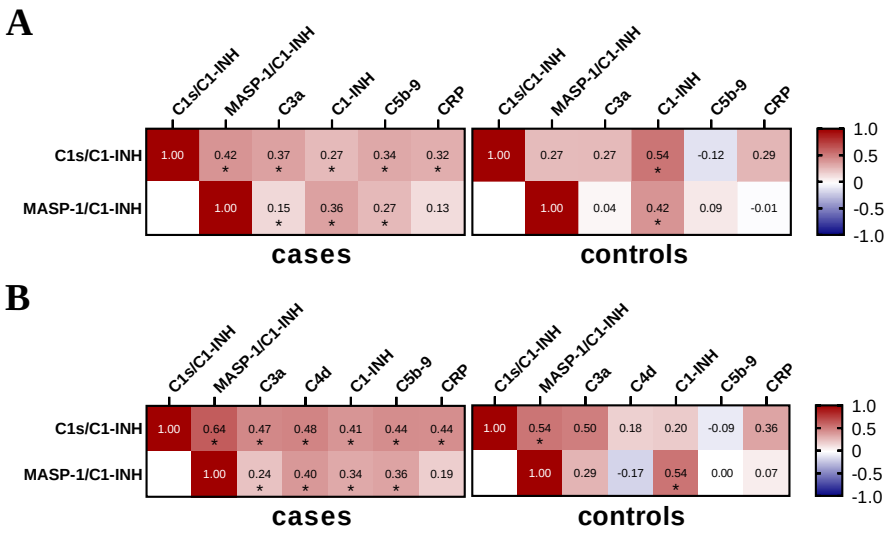

Figure 17: Correlation between C1-INH complex levels and additional complement and laboratory parameters in COVID-19 cases and controls. Heatmap of correlation matrix of C1s/C1-INH and MASP-1/C1-INH complex levels and additional complement as well as inflammatory parameters of the Cambridge cohort (A) and the Budapest cohort (B). Correlations in COVID-19 cases are presented in the left panel each, while correlations in healthy controls are shown on the right. The strength of each correlation, as calculated by the Spearman rank correlation, is indicated via color-coding. Significant correlations are marked by asterisks after 5% false discovery rate correction using the Benjamini-Hochberg method.

Since both complexes were increased in COVID-19 patients, and C1-INH complex levels also correlated with additional complement activation markers in COVID-19 patients, more in-depth studies regarding the role of classical and lectin pathway activation, as well as long-term changes of C1-INH complex levels in severe SARS-CoV-2 infections, were conducted, as summarized in the following chapters.

4.4.2 The lectin pathway is activated in acute COVID-19, and LP activation is associated with disease severity

Both, the early lectin pathway marker MASP-1/C1-INH complex (Figure 18A), as well as the CP and LP common marker C4d (Figure 18B) showed significantly different concentrations between several COVID-19 severity groups and healthy controls (Kruskal-Wallis: MASP-1/C1-INH complex: $p = 0.0011$; C4d: $p < 0.0001$), with higher levels in more severe groups (HOSP, HOSP+O_2 and ICU) (Figure 18; taken and adapted with permission from Hurler *et al.* (112)). Those findings indicate that lectin pathway is activated after a SARS-CoV-2 infection, and that LP activation is associated with COVID-19 disease severity.

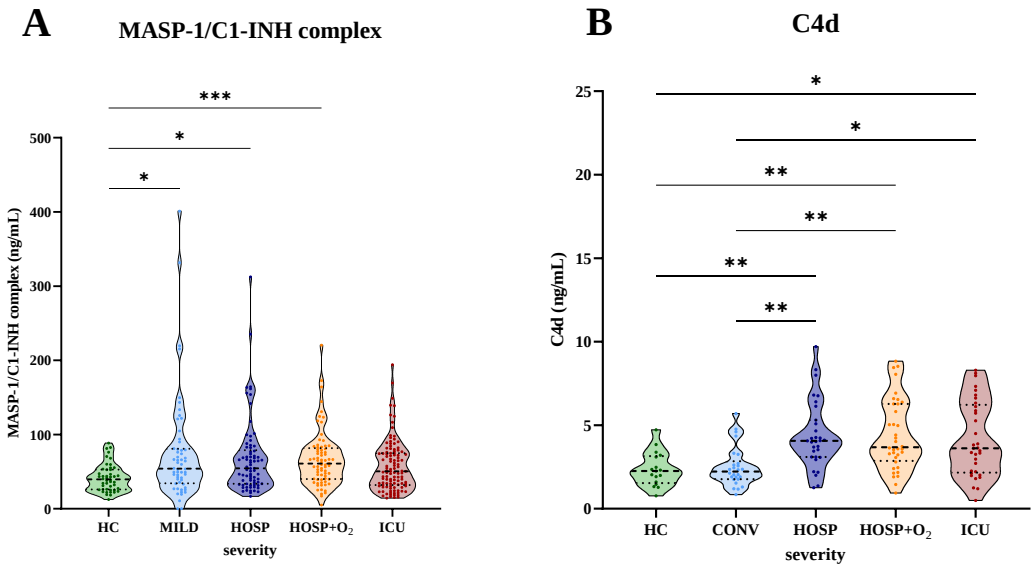

Figure 18: Lectin pathway activation markers in COVID-19 patients and healthy controls. Levels of lectin pathway activation markers MASP-1/C1-INH complex (A) and C4d (B) were measured in EDTA plasma of COVID-19 patients and healthy controls and stratified according to disease severity. Differences between different severity groups were analysed using the Kruskal-Wallis test with Dunn's multiple comparison test. Asterisks indicate significance (* $p < 0.05$, ** $p < 0.01$, *** $p < 0.001$), while non-significant results are not shown. Abbreviations: HC, Healthy controls; MILD, mild patients not requiring hospitalization; CONV, mild patients not requiring hospitalization and sampled in the convalescent stage; HOSP, Hospitalized patients not requiring ventilation; HOSP+O2, Hospitalized patients requiring ventilation; ICU, Intensive care unit patients. Figure taken and adapted with permission from Hurler *et al.* (112), under the terms of the Creative Commons Attribution License (CC BY), https://creativecommons.org/licenses/by/4.0/.

4.4.3 *MBL2* genetic variants do not strongly associate with COVID-19 susceptibility or outcome

To investigate the role of the lectin pathway in COVID-19, genotyping of the *MBL2* gene, the key pattern recognition molecule of the LP, was performed in COVID-19 patients as well as in additionally enrolled healthy controls. While information of all six common polymorphisms was available, data was analysed either looking at the short haplotype combinations (only the promoter polymorphism -221 X/Y (rs7096206) and the exonic SNPs A or 0 (indicating missense variants B, C and D)), the variants of allele A in exon 1 of *MBL2* (combinations of A, B, C, and D), or according to the long haplotype combinations (including all six common polymorphisms). No clinically meaningful differences in the distribution of the short genotypes (Table 16), the wildtype and variants of allele A in exon 1 (Table 17), or the long haplotype combinations in *MBL2* (Table 18) between COVID-19 cases and controls could be observed (Tables taken with permission from Hurler *et al.* (112)). Besides that, analysis were also performed according to the severity status (moderate COVID-19 vs. severe COVID-19) as well as separately for the two cohorts, but no significant differences were noted in the frequency of specific *MBL2* genetic variants (data not shown, for details see Supplementary Material in Hurler *et al.* (112)).

When stratifying MBL levels (CAM cohort; Figure 19A) and Lectin pathway activity (BUD cohort; Figure 19B) according to *MBL2* genotypes as well as COVID-19 severity, it is obvious that both parameters mainly depend on the *MBL2* genetics.

However, different patterns in MBL protein levels are visible when investigating MBL high and intermediate (YA/YA and YA/XA+XA/XA) and MBL low and deficient (YA/0 and XA/0+0/0) genetic groups. While MBL high and intermediate groups show increased MBL concentrations in moderate and severe COVID-19 cases, MBL low and deficient groups show higher MBL levels in healthy controls compared to the cases. This trend is also seen when looking at the lectin pathway activity (Figure 19B), although not statistically significant for most comparisons.

Table 16: Distribution of short *MBL2* haplotype combinations in healthy controls and COVID-19 cases. Table taken with permission from Hurler *et al.* (112).

	controls (n = 377)		cases (n = 314)		Odds ratio (95 % CI)	p-value[a]
	n	%	n	%		
YA/YA	102	27.1 %	83	26.4 %	0.969 (0.695-1.362)	0.864
YA/XA	93	24.7 %	87	27.7 %	1.170 (0.838-1.640)	0.385
YA/0	97	25.7 %	69	22.0 %	0.813 (0.574-1.157)	0.283
XA/XA	17	4.5 %	13	4.1 %	0.915 (0.453-1.853)	0.853
XA/0	44	11.7 %	41	13.1 %	1.137 (0.713-1.801)	0.642
0/0	24	6.4 %	21	6.7 %	1.054 (0.578-1.889)	0.878

[a] p-values reported as non-corrected for multiple testing. Threshold for significance after Benjamini-Hochberg correction for multiple testing: p = 0.0083.

Table 17: Distribution of *MBL2* exonic wildtype and variant alleles in healthy controls and COVID-19 cases. Table taken with permission from Hurler *et al.* (112).

	controls (n = 377)		cases (n = 315)		Odds ratio (95 % CI)	p-value[a]
	n	%	n	%		
Wildtype						
A/A	**212**	**56.2 %**	**183**	**58.1 %**	**1.032 (0.761-1.386)**	**0.878**
Heterozygous						
A/B	86	22.8 %	73	23.2 %	1.021 (0.720-1.464)	0.928
A/C	7	1.9 %	5	1.6 %	0.853 (0.304-2.442)	1.000
A/D	48	12.7 %	33	10.5 %	0.802 (0.504-1.296)	0.406
Total A/0	**141**	**37.4 %**	**111**	**35.2 %**	**0.911 (0.671-1.247)**	**0.579**
Homozygous variant						
B/B	9	2.4 %	8	2.5 %	1.066 (0.416-2.610)	1.000
B/C	2	0.5 %	1	0.3 %	0.597 (0.041-5.160)	1.000
B/D	9	2.4 %	8	2.5 %	1.066 (0.416-2.610)	1.000
C/C	1	0.3 %	1	0.3 %	1.197 (0.063-22.810)	1.000
C/D	1	0.3 %	0	0.0 %	0.000 (0.000-10.770)	1.000
D/D	2	0.5 %	3	1.0 %	1.803 (0.366-10.210)	0.664
Total 0/0	**24**	**6.4 %**	**21**	**6.7 %**	**1.051 (0.576-1.883)**	**0.878**

[a] p-values reported as non-corrected for multiple testing. Threshold for significance after Benjamini-Hochberg correction for multiple testing: p = 0.0042.

Table 18: Distribution of long *MBL2* haplotype combinations in healthy controls and COVID-19 cases. Table taken with permission from Hurler *et al.* (112).

	controls (n = 373)		cases (n = 314)		Odds ratio (95 % CI)	p-value[a]
	n	%	n	%		
HYPA/LXPA	41	11.0 %	45	14.3 %	1.355 (0.859-2.153)	0.204
LXPA/LYQA	44	11.8 %	31	9.9 %	0.819 (0.504-1.327)	0.462
HYPA/LYQA	46	12.3 %	28	8.9 %	0.696 (0.429-1.141)	0.174
HYPA/LYPB	36	9.7 %	32	10.2 %	1.062 (0.640-1.740)	0.898
HYPA/HYPA	32	8.6 %	34	10.8 %	1.294 (0.777-2.169)	0.363
LXPA/LYPB	26	7.0 %	23	7.3 %	1.055 (0.579-1.882)	0.883
LYQA/LYPB	22	5.9 %	12	3.8 %	0.634 (0.318-1.275)	0.223
LXPA/LXPA	17	4.6 %	13	4.1 %	0.904 (0.448-1.833)	0.853
HYPA/HYPD	17	4.6 %	10	3.2 %	0.689 (0.324-1.512)	0.432
LXPA/HYPD	12	3.2 %	14	4.5 %	1.404 (0.669-3.082)	0.427
LYQA/LYQA	12	3.2 %	11	3.5 %	1.092 (0.496-2.559)	0.835
LXPA/LYPA	8	2.1 %	11	3.5 %	1.656 (0.682-4.019)	0.352
LYPB/LYPB	9	2.4 %	8	2.5 %	1.057 (0.413-2.590)	> 0.999
HYPD/LYPB	8	2.1 %	7	2.2 %	1.037 (0.394-2.876)	> 0.999
LYQA/HYPD	13	3.5 %	2	0.6 %	0.178 (0.040-0.678)	0.016
HYPA/LYPA	6	1.6 %	5	1.6 %	0.990 (0.343-3.361)	> 0.999
LYPA/LYPB	2	0.5 %	6	1.9 %	3.614 (0.869-17.700)	0.151
LYPA/LYQA	3	0.8 %	4	1.3 %	1.591 (0.424-6.352)	0.708
LXPA/LYQC	4	1.1 %	3	1.0 %	0.890 (0.223-3.337)	> 0.999
HYPD/HYPD	2	0.5 %	3	1.0 %	1.789 (0.363-10.130)	0.665
LYQA/LYQC	2	0.5 %	2	0.6 %	1.189 (0.185-7.627)	> 0.999
LYQA/LYPD	0	0.0 %	3	1.0 %	Infinity (1.032-infinitiy)	0.095
LYPB/LYQC	2	0.5 %	1	0.3 %	0.593 (0.041-5.121)	> 0.999
HYPD/LYPA	1	0.3 %	1	0.3 %	1.188 (0.062-22.640)	> 0.999
LXPA/LYPD	1	0.3 %	1	0.3 %	1.188 (0.062-22.640)	> 0.999
LYPA/LYPD	1	0.3 %	1	0.3 %	1.188 (0.062-22.640)	> 0.999
LYPB/LYPD	1	0.3 %	1	0.3 %	1.188 (0.062-22.640)	> 0.999
LYQC/LYQC	1	0.3 %	1	0.3 %	1.188 (0.062-22.640)	> 0.999
HYPA/LYPD	2	0.5 %	0	0.0 %	0.000 (0.000-2.567)	0.503
LYPA/LYPA	0	0.0 %	1	0.3 %	Infinity (0.132-infinity)	0.457
HYPA/LYQC	1	0.3 %	0	0.0 %	0.000 (0.000-10.690)	> 0.999
HYPD/LYQC	1	0.3 %	0	0.0 %	0.000 (0.000-10.690)	> 0.999

[a] p-values reported as non-corrected for multiple testing. Threshold for significance after Benjamini-Hochberg correction for multiple testing: p = 0.0016.

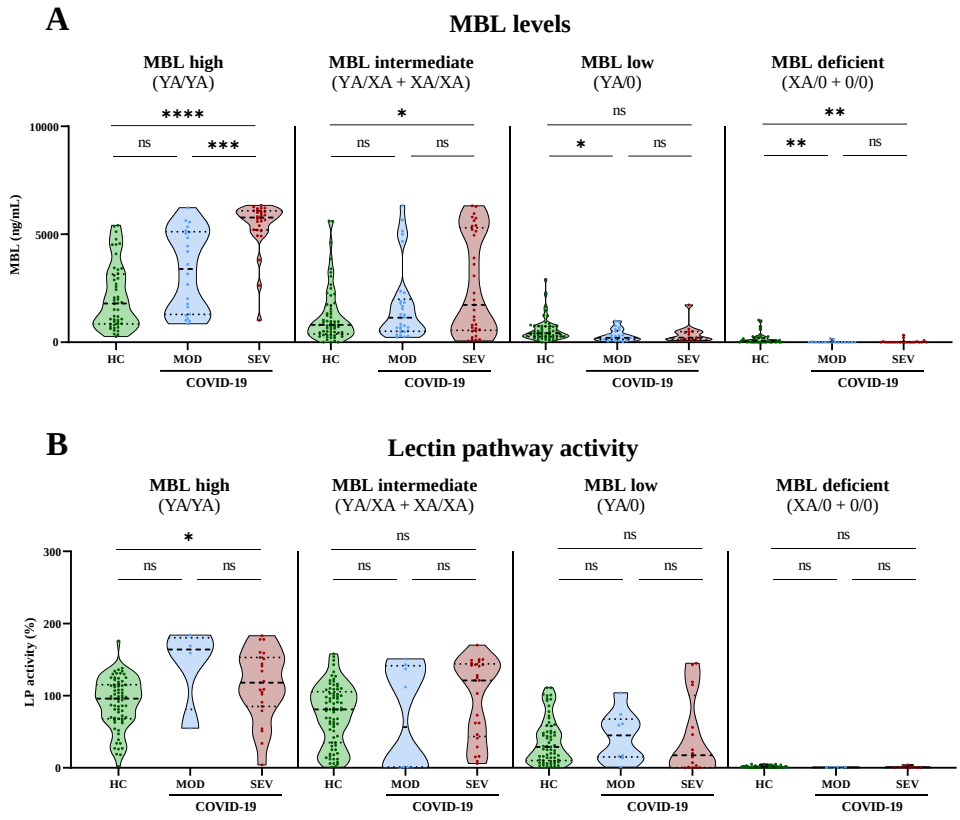

Figure 19: Levels of MBL and lectin pathway activity stratified according to *MBL2* genetic groups and COVID-19 severity. Levels of MBL (A) and Lectin pathway activity (B) in healthy controls (HC) and moderate (MOD) as well as severe (SEV) COVID-19 cases were stratified according to the short *MBL2* genotypes (MBL high: YA/YA, MBL intermediate: YA/XA+XA/XA, MBL low: YA/0, MBL deficient: XA/0+0/0). Differences between groups were analysed with ANOVA with Dunn's multiple comparison post-hoc test. Asterisks indicate significance: * $p < 0.05$, ** $p < 0.01$, *** $p < 0.001$, **** $p < 0.0001$. Abbreviations: HC, Healthy controls; MOD, moderate COVID-19 patients; SEV, severe COVID-19 patients. Figure taken and adapted with permission from Hurler *et al.* (112), under the terms of the Creative Commons Attribution License (CC BY), https://creativecommons.org/licenses/by/4.0/.

Those findings imply that SARS-CoV-2 infections might have an effect on MBL levels and hence increase the protein concentrations in MBL high and intermediate groups (YA/YA and YA/XA+XA/XA).

Stratification according to *MBL2* genetic groups as well as disease severity was also done for lectin pathway activation markers MASP-1/C1-INH complex and CP/LP joint activation fragment C4d, but differences were only observed between different COVID-19 severity groups (data not shown, for details see Hurler *et al.* (112)), suggesting that increased lectin pathway activation products only moderately reflect increased MBL levels and lectin pathway activity in COVID-19.

4.4.4 MBL does bind to SARS-CoV-2 spike protein, while binding is dependent on MBL protein levels

Since the lectin pathway can be activated by SARS-CoV-2 directly, binding of MBL to SARS-CoV-2 spike protein was investigated using recombinant MBL (rMBL) and serum samples from healthy individuals with different *MBL2* genotypes. As illustrated in Figure 20 (taken and adapted with permission from Hurler *et al.* (112)), rMBL as well as serum-derived MBL could bind to the viral protein in a concentration-dependent way. The highest binding was observed using recombinant MBL. Looking at the sera samples tested, highest OD signals were observed in sera from *MBL2* high-expressing/wildtype (YA/YA) healthy donors, followed by MBL intermediate (YA/XA+XA/XA) and MBL low (YA/0) groups. Neglecting signals were observed in MBL deficient (XA/0+0/0) sera, with OD values similar to BSA, which served as a negative control. There were no differences in the binding signals between binding to the SARS-CoV-2 S-protein and binding to mannan (data not shown).

The results suggest that binding of MBL to SARS-CoV-2 spike protein is solely dependent on the average MBL concentration ($\bar{x}$) present in sera, and binding behaviour does not differ between different genetic groups.

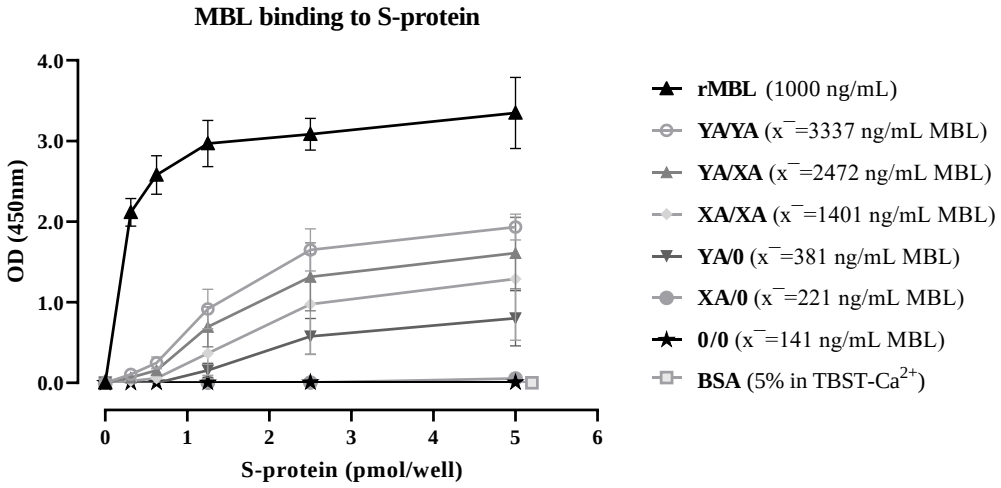

Figure 20: Binding of MBL to SARS-CoV-2 spike protein. Plates were coated with SARS-CoV-2 spike protein, and incubated with either recombinant MBL (rMBL; 1000 ng/mL), serum from patients with different *MBL2* genotypes (10 %) or BSA (5 %) in TBST-Ca^{2+}, before binding of MBL was detected. Genotype groups were as follows: YA/YA (n = 5), YA/XA (n = 3), XA/XA (n = 3), YA/0 (n = 4), XA/0 (n = 2) and 0/0 (n = 3). Mean±SD of two independent experiments are shown. Abbreviations: $\bar{x}$, average concentration; BSA, bovine serum albumin; TBST-Ca^{2+}, Tris-HCl buffer containing calcium. Figure taken and adapted with permission from Hurler *et al.* (112)), under the terms of the Creative Commons Attribution License (CC BY), https://creativecommons.org/licenses/by/4.0/.

4.4.5 Associations between Lectin pathway and disease outcome

The investigated proteins and *MBL2* genotypes were also tested for their potential to predict either the development of Long COVID (Figure 21; taken with permission from Hurler *et al*. (112)), defined as persisting symptoms 6-12 months after SARS-CoV-2 infection (based on questionnaires administered to the patients of the CAM cohort), or COVID-19 related mortality (Figure 22; taken with permission from Hurler *et al*. (112)), as outcome of the SARS-CoV-2 infection.

As illustrated in Figure 21, the development of Long COVID 6-12 months past infection was not associated with either MBL (Figure 21A), MASP-1/C1-INH complex (Figure 21B) or C5b-9 levels (Figure 21C). Besides that, there was also no association with either the *MBL2* A allele (Figure 21D) or the *MBL2* short genotype groups (Figure 21E), suggesting that lectin pathway activation does not have any significant role in the development of Long COVID.

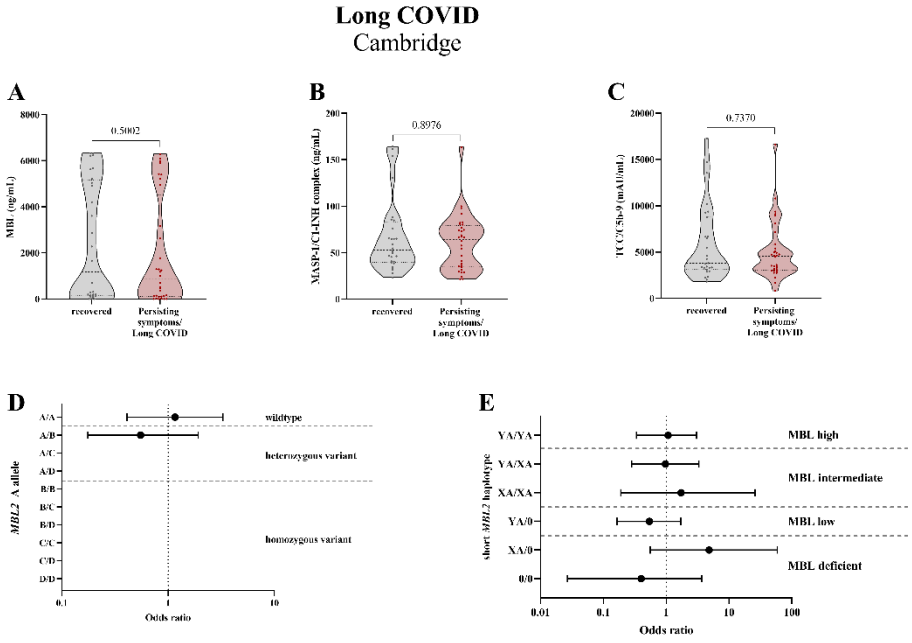

Figure 21: Relationship between complement markers, *MBL2* genotype and the development of Long COVID in COVID-19 patients. Levels of complement markers MBL (A), MASP-1/C1-INH complex (B) and TCC/C5b-9 (C) were stratified according to the development of Long COVID (recovered vs. persisting symptoms/Long COVID). The Mann-Whitney test was performed to analyse differences between the two groups. Forest plots displaying Odds ratios (ORs) with 95 % confidence intervals (CIs) for the development of Long COVID, stratified according to the *MBL2* A allele distribution (D) as well as according to the short *MBL2* genotypes (E). Odds ratios of 0 or infinite are not indicated on the forest plots. Figure taken and adapted with permission from supplementary material of Hurler *et al.* (112), under the terms of the Creative Commons Attribution License (CC BY), https://creativecommons.org/licenses/by/4.0/.

In contrast, a different picture is seen when looking at mortality as an outcome of COVID-19 (Figure 22). Mortality data was available from both cohorts, and whereas 8.8 % of the Cambridge COVID-19 patients died (19/215 cases), the Hungarian cohort showed a higher incidence of non-survivors (19.5 %; 25/128 cases; Fisher's exact: p = 0.007). Levels of MASP-1/C1-INH complex (Figure 22B+G) and lectin pathway activity (Figure 22F) did not vary between survivors and non-survivors, while initial C5b-9 levels were significantly increased in patients later on deceasing from COVID-19 (p=0.0004, Figure 22C; p = 0.0186, Figure 22H), whereas MBL levels were significantly lower in the deceased group (p = 0.0062, Figure 22A). This can also be seen when looking at the *MBL2* A allele (Figure 22D) and short *MBL2* genotype groups (Figure 22E) of the CAM cohort. While individuals with the *MBL2* wildtype allele (A/A) were at a ~70 % lower risk of dying from the SARS-CoV-2 infection (OR 0.3192 (95 % CI 0.1172-0.8664), p = 0.0261), patients with the homozygous variant B/B were over 8-times more likely to die from COVID-19 (OR 8.750 (95 % CI 1.442-44.470), p = 0.0499) (Figure 22D), when compared to individuals not homozygous variant for B/B. Nevertheless, those associations between genetic variations of the *MBL2* gene and the risk of a COVID-19 related death did not pass correction for multiple tesing (significance threshold using Benjamini-Hochberg correction: p = 0.0050). This trend towards lower ORs in MBL high- and intermediate-expressing groups (YA/YA, YA/XA) and increased risk of COVID-19 related mortality in low-expressing (YA/0) and MBL-deficient (XA/0+0/0) groups is also evident when looking at the short *MBL2* genotype groups (Figure 22E). However, those findings could not be replicated in the BUD cohort (Figure 22I+J).

Outcome analysis were also performed according to the *MBL2* long haplotype combinations, but no significant results were obtained (data not shown).

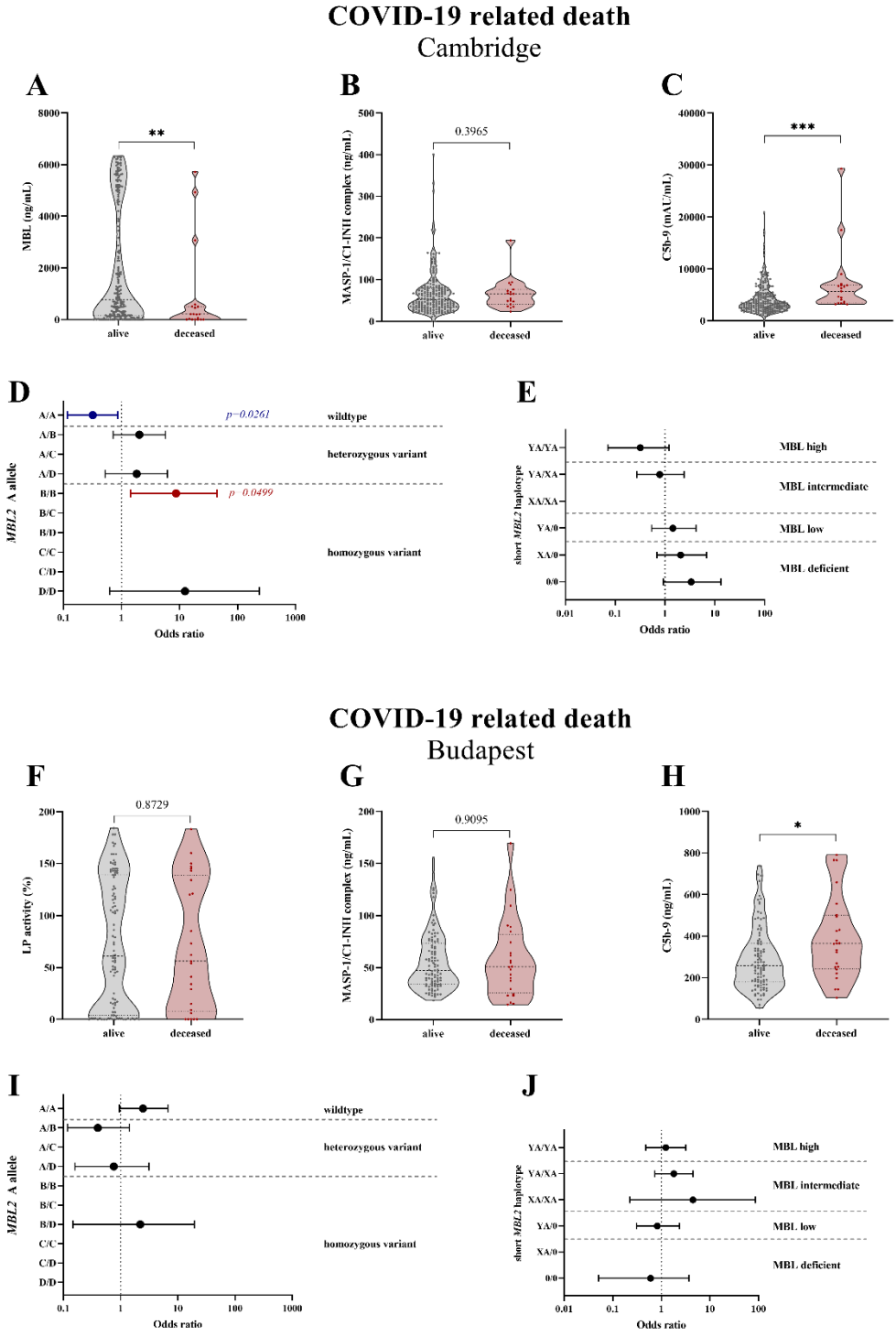

Figure 22: Relationship between complement markers, *MBL2* genotype and COVID-19 related mortality. Levels of complement markers MBL (A), MASP-1/C1-INH complex (B) and C5b-9 (C) in the Cambridge cohort, as well as Lectin pathway activity (F), MASP-1/C1-INH complex (G) and C5b-9 (H) in the Budapest cohort were stratified according to survival (alive vs. deceased). The Mann-Whitney test was performed to analyse differences between the two groups, while asterisks indicate significance (* $p < 0.05$, ** $p < 0.01$, *** $p < 0.001$). For non-significant differences, p-values are indicated. Forest plot displaying Odds ratios (ORs) with 95 % confidence intervals (CIs) for COVID-19 related death in individuals,

stratified according to the *MBL2* A allele distribution (D: Cambridge, I: Budapest) as well as according to the short *MBL2* genotypes (E: Cambridge, J: Budapest). Odds ratios of 0 or infinite are not indicated on the forest plots. P-values reported are non-corrected for multiple-testing. Significance thresholds using Benjamini-Hochberg correction for multiple testing are p = 0.0050 for the *MBL2* A allele, and p = 0.0083 for the short *MBL2* haplotype combinations. Figure taken and adapted with permission from Hurler *et al.* (112), under the terms of the Creative Commons Attribution License (CC BY), https://creativecommons.org/licenses/by/4.0/.

4.4.6 Classical pathway activation is associated with COVID-19 disease severity, and C1s/C1-INH complex levels are associated with CP activators

As seen in Figure 16, not only the lectin pathway but also the classical pathway is activated in acute COVID-19.

C1s/C1-INH complex levels gradually increased with increasing severity of the SARS-CoV-2 infection (Figure 23A, Kruskal-Wallis test: $p < 0.0001$), with levels of 2022 ± 487 ng/mL in healthy controls, 1904 ± 911 ng/mL in the MILD group, 2373 ± 1183 ng/mL in the HOSP, and 2595 ± 1173 ng/mL in the HOSP+O_2 group. Highest C1s/C1-INH complex levels of 2848 ± 1576 ng/mL were observed in the ICU group.

Associations between C1s/C1-INH complex levels and several classical pathway activators was investigated by stratification of measured C1-INH complex concentrations according to anti SARS-CoV-2 antibody status (negative vs. positive; cut-off based on the highest value observed in healthy controls) or according to CRP and PTX3 levels (quartiles). C1s/C1-INH complex levels did not significantly differ between individuals positive or negative for anti spike IgG ($p = 0.1815$; Figure 23B), but were significantly higher in anti nucleocapsid IgG positive patients ($p = 0.0112$; Figure 23C). Besides that, C1s/C1-INH complex concentrations were significantly higher in patients with high CRP (Figure 23D; Kurskal-Wallis test: $p < 0.0001$) and high PTX3 (Figure 23E; Kruskal-Wallis test: $p = 0.0055$) levels.

In summary, those findings indicate that classical pathway is activated upon SARS-CoV-2 infection, while the activation rate is associated with COVID-19 disease severity. In addition, there seems to be an association between classical pathway activation and the anti SARS-CoV-2 antibody response as well as with acute phase proteins CRP and PTX3, while C1s/C1-INH complex levels increase in accordance with increasing acute phase protein concentrations.

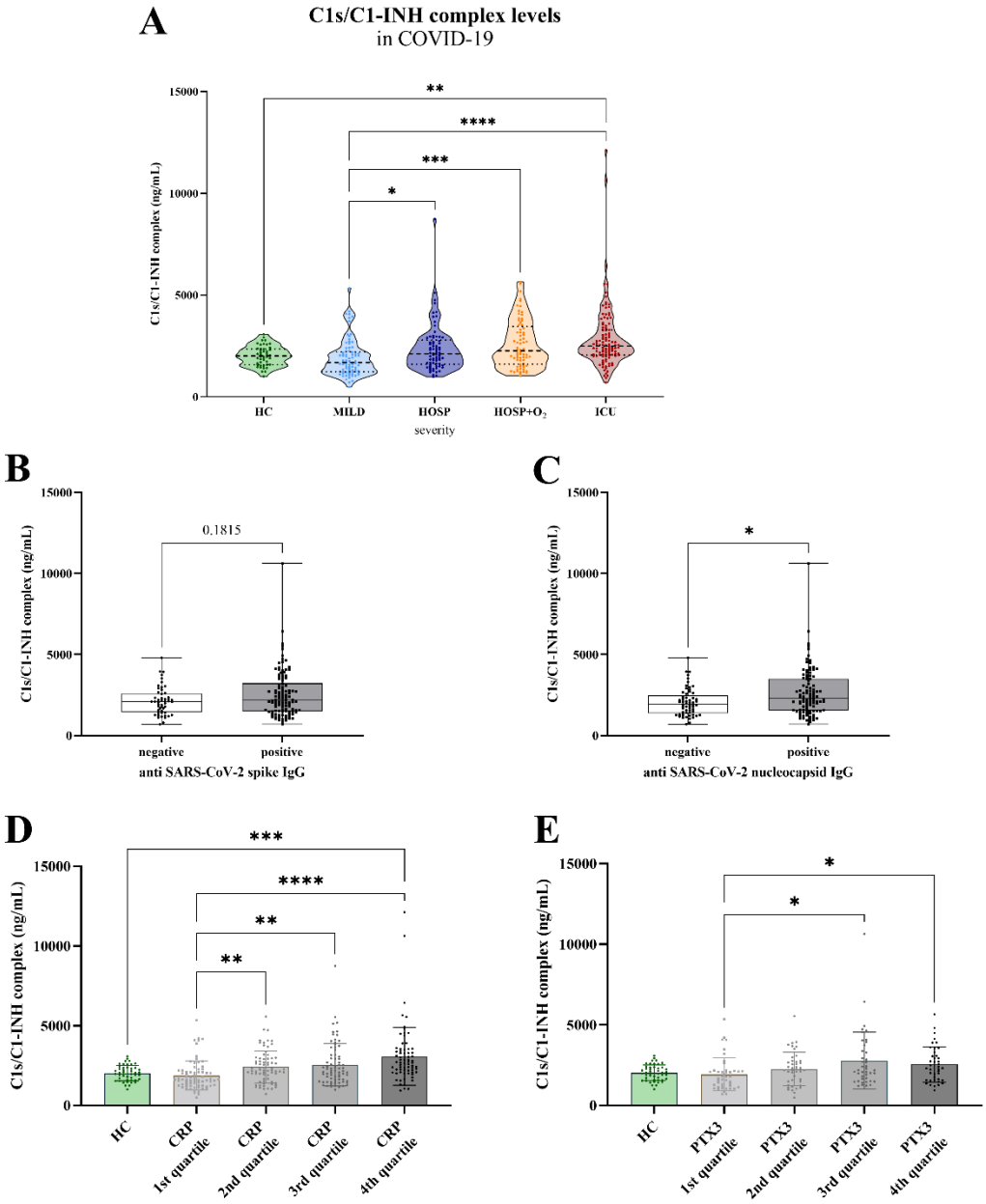

Figure 23: Classical pathway activation in COVID-19 patients and healthy controls. Levels of classical pathway activation marker C1s/C1-INH complex (A) was measured in EDTA plasma of COVID-19 patients and healthy controls and stratified according to disease severity. Differences between different severity groups were analysed using the Kruskal-Wallis test with Dunn's multiple comparison test or the Mann-Whitney test. Levels of C1s/C1-INH complex were further stratified according to the status (negative vs. positive) of anti SARS-CoV-2 spike IgG (B), anti nucleocapsid IgG (C), CRP quartiles (D) and PTX3 quartiles (E). Asterisks indicate significance (* $p < 0.05$, ** $p < 0.01$, *** $p < 0.001$, **** $p < 0.0001$), while non-significant results are not shown. Abbreviations: HC, Healthy controls; HOSP, Hospitalized patients not requiring ventilation; HOSP+O_2, Hospitalized patients requiring ventilation; ICU, Intensive care unit patients.

4.4.7 C1-INH complex levels in long-term samples of hospitalized COVID-19 patients change in the presence of co-infections

Follow-up samples of 12 severely infected COVID-19 patients, treated at the Department of Internal Medicine in the Hospital St. Vinzenz, Zams, were collected as part of a prospective, longitudinal study investigating complement activation and systemic inflammation in COVID-19 (233). While all patients required hospitalization and ventilation, ten out of 12 patients were male (83.3 %), and the mean age of the patients was 79.2 ± 5.1 years. Seven patients deceased from their severe SARS-CoV-2 infection (58.3 %), while seven individuals presented co-infections next to COVID-19 (*Candida spp.*: n = 4, *Escherichia coli*: n = 2, *Aspergillus spp.*: n = 2). Investigated co-infections were determined in tracheal fluid samples of the patients, as described previously (233).

After C5a and TCC serum levels were shown to be significantly increased in severe COVID-19 cases with and without co-infections in the cohort (233), the samples were analysed for their C1-INH complex levels, under supervision of Prof. Dr. Reinhard Würzner at Medical University Innsbruck, Austria.

Measurements revealed that there are no significant differences in C1-INH complex levels between survivors and non-survivors (Figure 24A+B; C1s/C1-INH: $p = 0.2287$, MASP-1/C1-INH: $p = 0.1717$). However, MASP-1/C1-INH complex levels were increased ($p = 0.0251$) in patients with additional *Candida* infection, especially during the first few days of hospitalization, while C1s/C1-INH complex concentrations did not differ significantly from individuals without *Candida* co-infection ($p = 0.9144$) (Figure 24C+D). In contrast, both C1-INH complexes were increased when hospitalized COVID-19 patients had a co-infection with *E.coli* ($p < 0.0001$ for both C1-INH complexes) (Figure 24E+F), whereas they were decreased if SARS-CoV-2 infected individuals suffered additionally from an *Aspergillus* infection (C1s/C1-INH: $p < 0.0001$, MASP-1/C1-INH: $p = 0.0001$) (Figure 24G+H). In none of the groups investigated there were significant changes of either the C1s/C1-INH or the MASP-1/C1-INH complex levels within the 30 days of follow-up (time), while there was also no interaction between the groups and time observed.

Those findings indicate that even C1-INH complex levels might already be increased due to a SARS-CoV-2 infection, co-infections with either *Candida spp.*, *E. coli* or

Aspergillus spp. can further influence C1s/C1-INH and MASP-1/C1-INH complex levels.

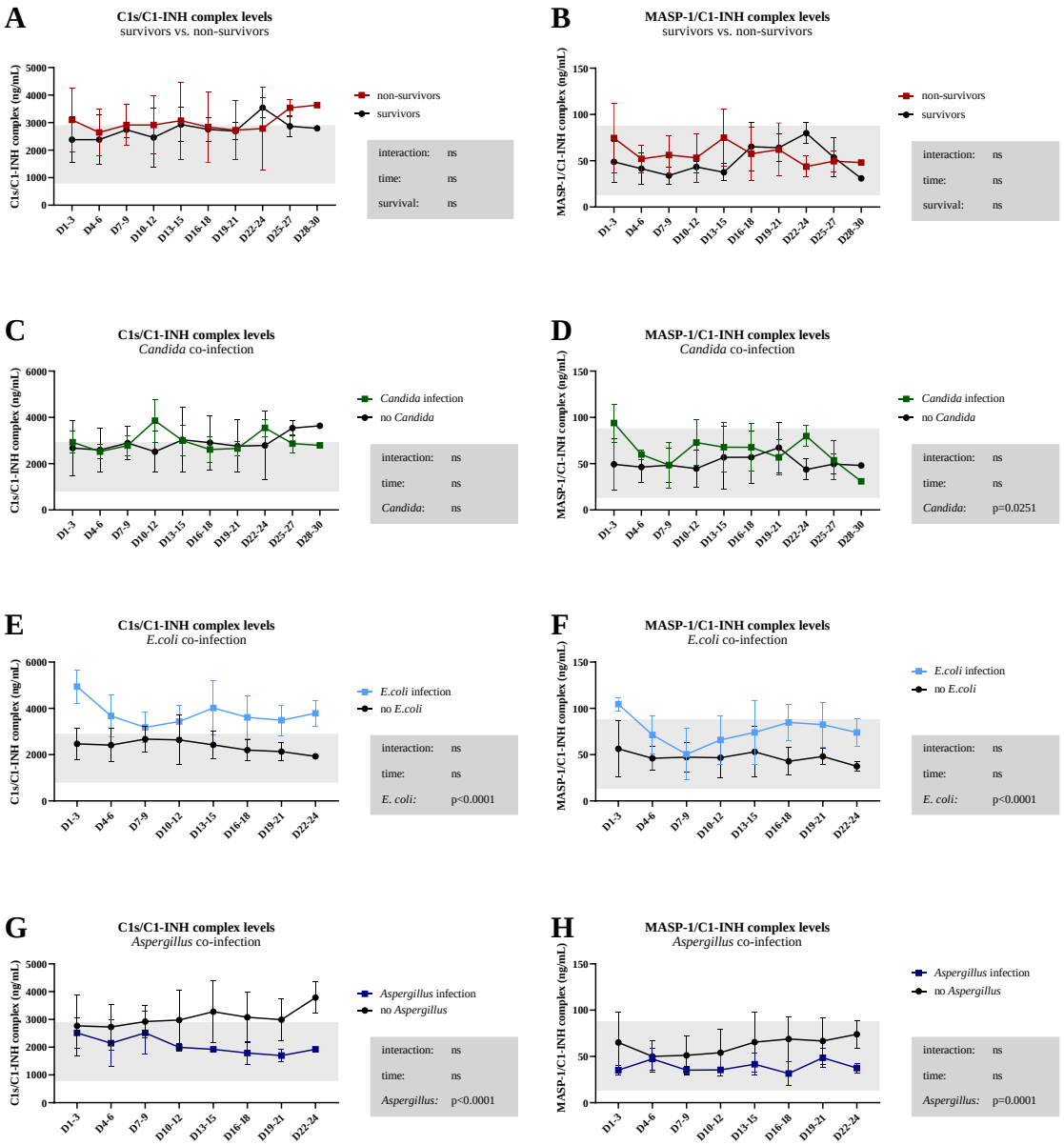

Figure 24: Long-term follow-up of C1-INH complex levels in severe COVID-19 patients. Levels of C1s/C1-INH and MASP-1/C1-INH complex levels were measured in severe COVID-19 patients at different time points up to 30 days past start of hospitalization (D1-D30). Measurements were grouped according to the days after hospitalization start, and results were stratified according to survival (A: C1s/C1-INH, B: MASP-1/C1-INH complex) and co-infections with either *Candida* (C: C1s/C1-INH, D: MASP-1/C1-INH complex), *E.coli* (E: C1s/C1-INH, F: MASP-1/C1-INH complex) or *Aspergillus* (G: C1s/C1-INH, H: MASP-1/C1-INH complex) and analysed using a two-way ANOVA. Earlier determined ranges of C1-INH complex concentrations measured in healthy controls are indicated in grey.

4.5 Early complement activation in Sepsis

Early classical and lectin pathway activation was also investigated in a cohort of Sepsis patients, sampled as part of a prospective cohort study dealing with blood stream infections (234, 239), under supervision of Prof. Dr. Reinhard Würzner at Medical University Innsbruck, Austria.

The cohort consisted of 70 Sepsis patients, treated from October 2019 to July 2021 at the Department of Internal Medicine and at the Department of Operative Medicine of Medical University Innsbruck, as well as 25 healthy controls. Of note, due to limited sample volumes, not all samples included in previous analysis (234, 239) were available for the here shown study. The mean age of the 70 patients included in the present analysis was 65.2 ± 18.5 years, while the controls were significantly younger (Mann-Whitney: $p < 0.0001$), with a mean age of 34.7 ± 12.0 years. Besides that, the diseased cohort was predominated by male patients (n = 47/70, 67.1 %), while the control cohort consisted of more women (n = 15/25, 60.0 %). A total of 11 sepsis patients (15.7 %) died within the first four weeks after sampling. Besides that, a positive blood culture was observed in 7 sepsis patients (10.0 %), while 14 patients suffered from COVID-19 (20.0 %). In an earlier study, significantly increased plasma TCC levels were detected in all sepsis patients when compared to healthy controls (234), indicating activation of the complement system. Based on those findings, the cohort was chosen for an additional external study utilizing the newly developed C1-INH complex immunoassays.

When looking at early complement activation, levels of both C1-INH complexes were significantly increased in sepsis patients vs. HC, with 3493 ± 2176 vs. 1163 ± 508 ng/mL C1s/C1-INH complex (Mann-Whitney: $p < 0.0001$; Figure 25A), and 65.5 ± 49.5 vs. 31.0 ± 17.1 ng/mL MASP-1/C1-INH complex (Mann-Whitney: $p < 0.0001$; Figure 25B). Besides that, C1s/C1-INH and MASP-1/C1-INH complex levels showed a moderate positive correlation in healthy controls ($r = 0.4606$, $p = 0.0102$), and a strong positive correlation in Sepsis patients ($r = 0.6574$, $p < 0.0001$; Figure 25C).

In contrast, the levels were not significantly different between survivors and non-survivors (Mann-Whitney: $p = 0.7798$ for C1s/C1-INH complex, $p = 0.0501$ for MASP-1/C1-INH complex; Figure 25D+E), although there is a trend towards higher MASP-1/C1-INH complex levels in survivors. C1-INH complex levels did not correlate significantly in non-survivors, while a strong positive correlation between C1s/C1-INH

and MASP-1/C1-INH complex levels was observed in Sepsis survivors (r = 0.7054, p < 0.0001; Figure 25F).

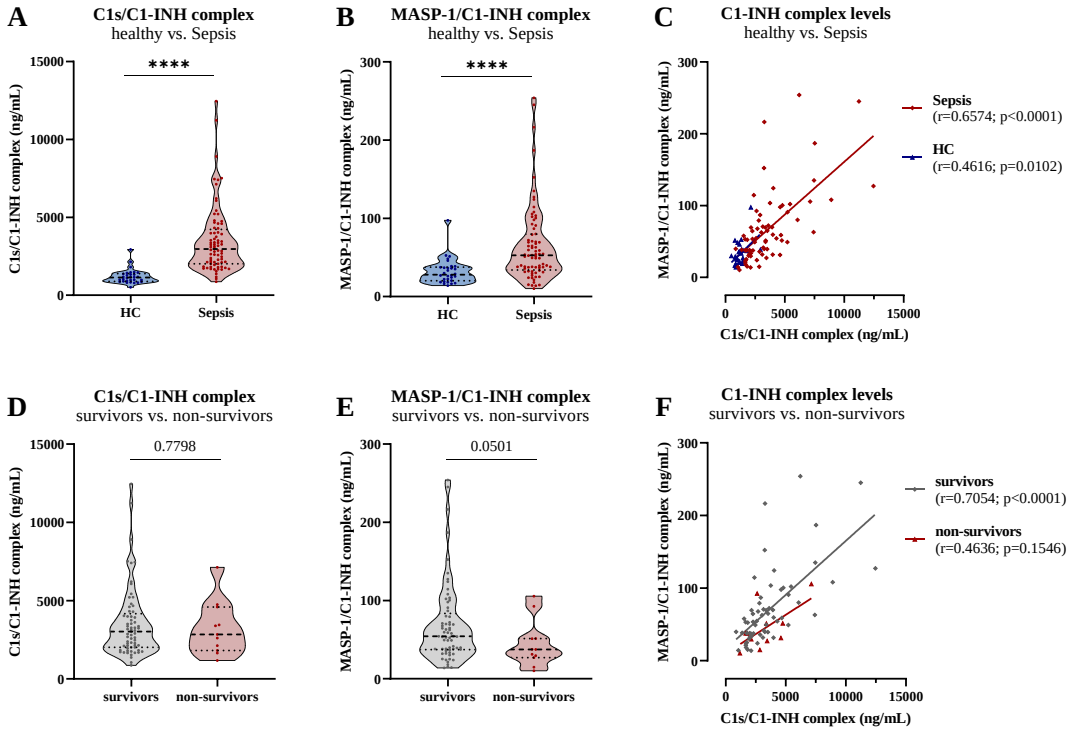

Figure 25: C1-INH complex levels in sepsis and association with outcome. C1s/C1-INH complex (A) and MASP-1/C1-INH complex levels (B) were measured in healthy controls (HC) and Sepsis patients. Correlations between C1s/C1-INH and MASP-1/C1-INH complex levels in HC and Sepsis patients were determined using the Separman rank correlation (C). Besides that, C1-INH complex levels in Sepsis patients were further stratified according to the survival outcome (D: C1s/C1-INH complex, E: MASP-1/C1-INH complex). Correlations between C1s/C1-INH and MASP-1/C1-INH complex levels in survivors and non-survivors were determined using the Separman rank correlation (F). Differences between two groups were analysed using the Mann-Whitney test, with asterisks indicating significance (**** p < 0.0001), and p-values given for non-significant differences.

When stratifying the patients according to the presence of either bloodculture infection (Figure 26A+B) or COVID-19 infection (Figure 26C+D), C1-INH complex levels show different patterns between the different groups.

C1s/C1-INH complex levels were significantly lower in healthy controls when compared to bloodculture positive (p = 0.0002) or negative (p < 0.0001) sepsis patients, while the difference between bloodculture positive and negative sepsis patients was not significant (Figure 26A). In contrast, MASP-1/C1-INH complex levels were significantly different between bloodculture positive and negative sepsis patients (p = 0.0456), with higher

levels in bloodculture negative patients (Figure 26B). Besides that, levels also differed significantly between healthy controls and bloodculture negative patients (p = 0.0001), with higher levels in the patients.

Furthermore, both C1-INH complexes did not differ significantly in sepsis patients with and without COVID-19 infection (p = 1.000 for both complexes; Figure 26C+D).

All in all, those findings indicate that both, the classical and the lectin pathway, are activated in Sepsis patients, while the level of activation can differ depending on the underlying infection.

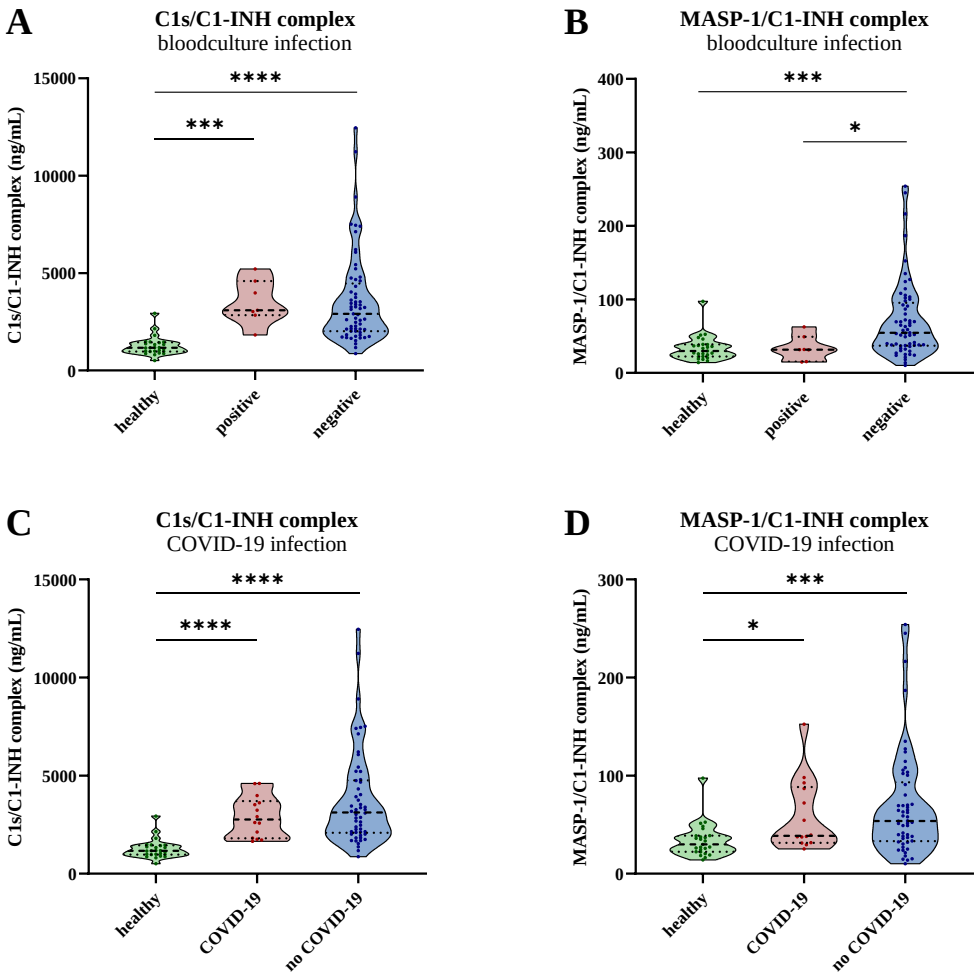

Figure 26: C1s/C1-INH and MASP-1/C1-INH complex levels in healthy controls and Sepsis patients, additionally stratified according to the presence of a bloodstream or COVID-19 infection. C1-INH complex levels were measured in a total of 25 HC and 81 sepsis samples, and results were stratified according to the presence of a bloodculture infection (A: C1s/C1-INH, B: MASP-1/C1-INH complex) or a COVID-19 infection (C: C1s/C1-INH, D: MASP-1/C1-INH complex). Differences between groups were analysed using the Kruskal-Wallis test, and signficant differences are indicated with asterisks (* $p < 0.05$, *** $p < 0.001$, **** $p < 0.0001$), while non-significant differences are not indicated.

5 DISCUSSION

5.1 Development and characterization of immunoassays measuring C1s/C1-INH and MASP-1/C1-INH complexes

Although the complement system is an essential component of the immune system, complement overactivation and dysregulation plays a major role in many different conditions and diseases (31, 240). To get a better understanding about those diseases, it is of utmost importance to reveal which pathways are activated most. Since there were no validated tools to investigate early classical and early lectin pathway activation so far, we proposed C1s/C1-INH and MASP-1/C1-INH complexes as suitable markers to distinguish between the two pathways. Although C1/C1-INH complexes were used as a measure of classical pathway activation in several studies before (221-225, 241-244), MASP-1/C1-INH complexes were only measured in two published studies, while they were not directly declared as a marker for lectin pathway activation (222, 226). In the scope of this PhD project, two novel immunoassays, measuring C1s/C1-INH complex as a marker for early classical pathway activation, and MASP-1/C1-INH complex as a marker for early lectin pathway activation, were developed and validated.

The new immunoassays measure C1-INH complex levels in a robust and reliable manner. The antibodies used for assay development are specific for the complex components and do not cross-react with other proteins of the respective complement pathways. Besides that, the anti C1s and anti MASP-1 monoclonals can also be used in Western Blot applications. Although very specific signals for C1-INH are observed with the anti C1-INH monoclonal in the direct ELISA, the antibody did not show conclusive results in Western Blot applications (n=4), suggesting that a discontinuous epitope might be recognized, which is destroyed when performing an SDS-PAGE. Besides that, inconclusive results might also be explained by different protocols, equipment and reagents used while performing the experiments in different laboratories. While applicability of the anti C1-INH monoclonal will be tested further in the future, the main purpose was to use the antibody in immunoassay applications, where it is working as expected in detecting purified C1-INH as well as the C1-INH complexes.

With regard to cross-reactivity with species other than human, both complex ELISAs could also detect C1-INH complexes in serum from orang utan and spider monkey. This is not surprising, considering the close relationship of apes/monkeys to humans and the

similarity of most parts of the DNA (245). Cross-reactivity results seen in murine samples are not 100 % conclusive and should be re-tested in additional samples in the future, while signals observed in other species are most likely only background.

Intra- and inter-assay variation in the new immunoassays is low and recovery of C1-INH complexes in EDTA plasma > 90 %, supporting the robustness of the sandwich ELISAs. Measurement of complement components in a reliable way can be challenging, since often large variation is present between different laboratories due to a lack of standardized reagents, assays and experimental procedures (246-248). Besides that, especially levels of complement activation products might vary depending on sample type and handling, so proper sample selection and handling is essential for reliable measurements (249, 250). As shown here, the C1-INH complexes can be measured in Citrate plasma, Heparin plasma, EDTA plasma or serum, while concentrations differ slightly depending on the matrix, therefore requiring adaption of dilution factors appropriate for the sample type used. Nevertheless, heparin plasma should be avoided, because heparin was shown to interact with several complement proteins and regulators, such as the C1 complex, C1-INH, as well as MASP-1 and -2 (123, 251-254), which might give erroneous results when measuring C1-INH complexes in the presence of heparin. While heparin can artificially enhance C1s/C1-INH complex formation by increasing the rate of inhibition of active C1s by C1-INH (255), MASP-1/C1-INH complex levels might be essentially influenced by affinity changes between MASP-1 and its several interaction partners. As an example, MASP-1 is more likely to form complexes with antithrombin when heparin is present (256), which might explain lower levels of MASP-1/C1-INH complex found in the here performed measurements using heparin plasma.

EDTA plasma should be the preferred sample type when investigating complement activation products, since EDTA can block complement function via chelating Mg^{2+} and Ca^{2+}, both required to stabilize the pattern-recognition complexes (257-259). In our experiments, an EDTA concentration of 10 mM could minimize *in vitro* complement activation. Even when supplementing EDTA, additional activation of the complement system and hence *de novo* formation of C1-INH complexes can occur *ex vivo*, especially when samples are not kept on ice. In an extensive review about complement analysis, Brandwijk and colleagues suggested anticoagulation with additional EDTA

(≥20 mM EDTA instead of 10 mM used in common EDTA collection tubes) in order to measure complement activation products more reliably (260).

In accordance with our findings, Yang *et al.* could show rather stable levels of complement activation products for 4 h at room temperature or 16 h on ice (261). In their study, they also highlighted the impact of multiple freeze-thaw cycles on complement fragments. Some activation products, such as C4d, are quite sensitive and concentrations can increase rapidly due to artificial complement activation upon repeated freezing and thawing (261). While C1s/C1-INH and MASP-1/C1-INH complex concentrations in EDTA plasma did not differ significantly for up to four freeze-thaw cycles in our experiments, the purified complexes are prone to degradation, highlighting the importance of small aliquots for purified complexes.

In summary, two well performing immunoassays were developed, which allow the specific measurement of C1s/C1-INH and MASP-1/C1-INH complexes in human plasma and serum. To obtain most reliable results, EDTA plasma is the recommended sample type when investigating C1-INH complexes. Samples should be stored at -80 °C, and kept on ice after thawing before the measurement for not longer than 1 h, in order to avoid artificial complex formation and erroneous results.

5.2 Functional validation of C1-INH complexes as markers for early classical and early lectin pathway activation

Although C1/C1-INH complexes have been used extensively for measuring complement activation before (221-225, 242, 244, 262), same does not hold true for MASP-1/C1-INH complexes. The potential of the C1-INH complexes to function as markers for CP and LP activation was therefore investigated in several activation experiments.

Zymosan A, a *Saccharomyces cerevisiae* derived cell wall carbohydrate polymer, can activate all three pathways of complement and was therefore chosen for initial activation experiments (263-265). While the classical pathway is activated through naturally occuring antibodies against the yeast in human circulation (265), thereby also enhancing alternative pathway activation (265), AP activation can furthermore occur through an zymosan-induced increase in alternative C3 convertase formation and stability (263). In addition, the lectin pathway can be activated directly through the carbohydrate-rich surface structure of the cell wall components (264).

Both C1-INH complexes showed a time-dependent increase in their concentration when incubating complement-preserved serum (NHS) with zymosan, supporting their usability as activation markers. While no MASP-1/C1-INH complex increase was observed in the NHS sample without zymosan, C1s/C1-INH complex concentrations were also strongly increasing over time without the addition of an activator, indicating auto-activation due to naturally occuring immune complexes in the circulation or Ig aggregation *ex vivo* while performing the experiment (266, 267). Those findings again stress out the importance of sample handling and the selection of the appropriate sample type when investigating C1-INH complex levels, as also shown in the stability experiments.

In additional experiments, *de novo* formation of C1-INH complexes in human serum upon specific activation of the classical (IgM) and lectin (mannan) pathway was in accordance with CP and LP activity, measured by the C9 neoepitope formation in the wells, as also done in functional complement ELISAs (207, 208). Furthermore, the C1-INH complex levels also correlated strongly with the corresponding pathway activities, further confirming the specificity of C1s/C1-INH and MASP-1/C1-INH complexes for CP and LP activation, respectively.

In contrast to measurements of CP and LP activity using functional ELISAs (207, 208) or hemolytic assays (201), the new C1-INH complex assays do not require complement-preserved serum and allow determination of classical or lectin pathway activation at the time of sampling. Besides that, a further advantage of C1s/C1-INH and MASP-1/C1-INH complex determinations in respect to traditional hemolytic assays is that no fresh animal blood cells are required for experiments, thereby increasing standardization and facilitating comparison between different measurements.

5.3 Analysis of C1-INH complexes in healthy individuals

After the potential usage of C1-INH complexes as markers for early classical and early lectin pathway activation was confirmed, the new immunoassays were utilized to determine a first reference range in healthy adult donors. For C1s/C1-INH complexes, concentrations were found to be normally distributed in a range of 1846 ± 1060 ng/mL (mean ± 2SD), which is in line with concentrations in literature using *in-house* assays. Concentrations reported by others were 1.0 ± 0.2 mg/L C1s/C1-INH complex in plasma or 2.1 ± 0.8 mg/L in serum of nine healthy adults (268) or 25.04 (13.9-36.9) nM in EDTA

plasma of six healthy individuals (222). Several other studies utilizing C1/C1-INH complexes as a measure of classical pathway activation reported the C1-INH complex levels as arbitrary units or ratios only (241-244, 262, 269-272), not allowing comparison of our findings in healthy individuals to those published results.

In contrast, MASP-1/C1-INH complex levels showed a right-skewed distribution in healthy individuals, indicating the potential influence of other factors, such as genetics as an example (273). Besides that, both MASP-1 and C1-INH are known to also be key players in other biological systems like the coagulation or the kallikrein system (129, 274), which might have an influence on MASP-1/C1-INH complex concentrations. While C1-INH is the only known blocking molecule of C1s, MASP-1 has several other inhibitors besides C1-INH, such as factor XIII (FXIII), fibrinogen, prothrombin, high molecular weight kininogen (HMWK) and protease activated receptors (PARs) (275), which potentially further explain the non-normal distribution of MASP-1/C1-INH complex levels seen in healthy individuals. Due to the multi-functional roles of MASP-1 in several biological systems, measurement of MASP-1/C1-INH complexes might not only give information about lectin pathway activation, but might also shed light on other cascades, such as the coagulation or the kinin-system, as well as the activation state of endothelial cells (274). As an example, functions of MASP-1 in the coagulation system include activation of prothrombin, fibrinogen and FXIII, as well as stabilization of clot formation (276). Because of that, it will be of utmost importance to not only look at MASP-1/C1-INH complex levels separately, but to also include measurements of general complement activation products such as C3 split products, C5b-9/TCC levels, or C4d as a common CP/LP activation marker. This way, it can be said with higher confidence if elevated MASP-1/C1-INH complex levels are indeed caused by an over-activated lectin pathway, or if other biological systems might lead to an increase in MASP-1/C1-INH complex levels.

Since measured MASP-1/C1-INH complex concentrations in healthy individuals were not normally distributed, the reference range was defined as the 2.5 - 97.5 percentile range, leading to physiological concentrations of 36.9 (13.18 - 87.89) ng/mL MASP-1/C1-INH complex. The only study reporting MASP-1/C1-INH complex levels in EDTA plasma of healthy individuals so far found levels of 0.38 (0.24-0.50) nM (222), while in

a second study the levels were expressed as percentages in comparison to a pathological group (226), not allowing comparison to our result.

Although some complement protein levels are reported to differ significantly between males and females, and to change with age in human adults (277), same does not apply for the here described C1-INH complexes. Those findings are in line with a study from Bergseth *et al*. in 2013, where no significantly different levels were observed between males and females in several complement activation products, including C1rs/C1-INH complex, C4bc and TCC (278). In addition, also other lectin pathway protein levels were shown to be independent of age in healthy adults (279).

In summary, a first reference range was determined for both C1-INH complexes, while in future investigations it is most likely not necessary to correct for either gender or age. However, only around 100 healthy individuals were investigated in the scope of this work, and additional studies in other cohorts are necessary to see if the determined physiological ranges are widely applicable in the general population.

5.4 Investigation of complement activation in COVID-19

So far, the SARS-CoV-2 pandemic has caused over 6.8 million deaths worldwide (153). Although there is increasing evidence of complement playing a role in the pathogenesis of the disease, the exact mechanisms are still not 100 % clear. Further knowledge about complement activation, and more precisely the involvement of the different pathways during SARS-CoV-2 infections, does not only give indications about the disease course, but could also be of great importance when it comes to specifically targeting complement during the disease progression.

Early studies targeting complement activation on the levels of either C3 or C5 did indeed show promising results (280-283). Just recently, the anti C5a antibody Vilobelimab was shown to be beneficial in critically ill COVID-19 patients (284, 285). Besides that, also Narsoplimab, a monoclonal antibody targeting MASP-2 and hence interfering at the level of lectin pathway activation, was shown to reduce the risk of COVID-19 related thrombosis and endothelial cell damage (286). However, none of the trials met end point criteria in their clinical studies (287, 288). Since complement activation in COVID-19 seems to be very heterogenous (238), in-depth knowledge about complement profiles of the treated individuals might have led to more successful clinical trials.

As scope of this project, early classical and lectin pathway activation in COVID-19 patients was investigated, focusing on the lectin pathway and its key pattern recognition molecule MBL. We could show that both, the classical and the lectin pathway are activated after onset of the disease, with higher C1-INH complex levels in more severe cases. Those findings provided a first proof for the usability of C1s/C1-INH and MASP-1/C1-INH complexes *in vivo* and support the application of the new immunoassays to unreveal CP and LP activation also in other complement-mediated diseases. However, lectin pathway activation seems to only play a minor role in the disease course, since no great associations between the six common *MBL2* single nucleotide polymorphisms and susceptibility to SARS-CoV-2 or disease outcome were found, although the virus seems to have an effect on MBL levels in COVID-19 patients. While complement overactivation and consumption of C3 in COVID-19 was associated with mortality (173), the SARS-CoV-2 spike protein was shown to directly activate the alternative pathway (289). Besides that, deposition of complement complexes in tissue, in combination with continuous alternative pathway amplification, was shown to be an important component of severe disease courses in COVID-19 (290). In cluster analysis by Defendi *et al.*, the main pathways activated during COVID-19 infection were found to be the alternative pathway as well as the lectin pathway (238). MASP-2, C4d, C5b-9 and MBL deposition was reported in lung tissue from SARS-CoV-2 infected patients, pointing towards lectin pathway involvement already very early after the pandemic started (169, 170). Based on those findings, extensive research started regarding the role of lectin pathway activation in COVID-19. MASP-2 deposition was also found in kidneys of patients deceased from COVID-19, while Niederreiter and colleagues further showed deposition of alternative pathway proteins FD and C3d, C5b-9 and again MASP-2, proposing pronounced complement activation via the LP and AP (171). Significant correlations between MASP-2 and complement activation product C5b-9, as well as inflammatory marker CRP, were found in COVID-19 (291), while the SARS-CoV-2 nucleocapsid protein was shown to bind to MASP-2, followed by lectin pathway activation *in vitro* and *in vivo* (292). In line with those findings, increased MASP-1/C1-INH complex, as well as C4d levels in more severe SARS-CoV-2 infections, as seen in our measurements, further provide evidence that lectin pathway activation is involved in the pathomechanism of COVID-19.

During the SARS-CoV outbreak twenty years ago, MBL was shown to not only activate complement on the virus via the lectin pathway, but to also inhibit the infectivity of SARS-CoV by binding to the virus (293). The study further provided first evidence that MBL contributes to the first line defence of coronavirus infections and that susceptibility might be influenced by the *MBL2* genotype (293). While several subsequent studies could confirm a higher frequency of individuals bearing MBL low or deficient genotypes (B allele) in SARS patients than in healthy controls (294-296), those findings could not be replicated in a all studies (297). Contradictory results were also observed in the present SARS-CoV-2 pandemic. While there are again inconsistent results in literature (298), many investigators showed associations between disease severity or outcome and *MBL2* genetic variants (162, 299, 300). Especially the *MBL2* B allele at codon 54 seems to be associated with a higher risk for a more severe disease course, such as the development of pneumonia, or the need for hospitalization, in COVID-19 (301, 302). Together with the findings of Stravalaci *et al.*, showing that MBL is able to recognize the spike protein and therefore inhibiting viral entry into host cells (162), a protective role for MBL is suggested during SARS-CoV-2 infections.

This might also be strengthened by our findings, where higher MBL levels were observed in survivors when compared to deceased COVID-19 patients (CAM cohort). Also when looking at the genetic background, a decreased risk of COVID-19 related mortality was associated with the wildtype/MBL high A alleles. Besides that, also the short *MBL2* haplotype groups showed a trend towards a protective role for MBL in the risk of a COVID-19 related death. On the other hand, those findings could not be replicated in the BUD cohort, and associations of genetic variants with disease severity and mortality did not pass multiple testing correction in our analysis. Nevertheless, they are in line with previous findings (301, 302) and should be re-investigated and potentially confirmed in larger cohorts in the future.

Interestingly, we could further show that MBL protein levels seem to be increased in MBL high (YA/YA) and MBL intermediate (YA/XA and XA/XA) COVID-19 patients within the individual genetic groups, while same does not hold true for MBL low (YA/0) and MBL deficient (XA/0 and 0/0) patients. Those findings suggest that MBL acts as an acute phase protein and MBL expression is influenced by SARS-CoV-2. Already in 1988 it was proposed that MBL can act as an acute phase protein in the course of

infections (303). Increased MBL levels were shown during acute phase reactions in severe infections as well as in sepsis patients (107, 304, 305). Those enhanced levels, as also seen in our COVID-19 cohort, might be caused by increased IL-6 levels. While significantly increased IL-6 levels were previously reported in severe COVID-19 cases in both of our here described cohorts (173, 232), *in vitro* studies showed an increase in MBL expression by IL-6 (306), potentially explaining our findings of higher MBL levels in SARS-CoV-2 infected patients. In summary, a strong *MBL2* promoter is driving high MBL levels in response to the SARS-CoV-2 infection, resulting in LP activation, clearance of the virus, decrease of the viral load and limitation of pneumonia. Hence a good LP response might prevent from a COVID-19 related death, as seen in higher MBL levels and the A/A genotype in survivors.

However, the alternative and lectin pathway are no the only ones associated with COVID-19. Messner *et al.* reported upregulation of several complement proteins, mainly associated with the classical pathway (*C1S, C1R*), the alternative pathway (*CFB*), as well as AP complement regulators (*CFH, CFI*) (307). Similar findings were made by Satyam *et al.*, where deposition of classical pathway components C1q and C4d, alternative pathway regulator Factor H, common complement activation products C3d and C5b-9, as well as IgM and IgG was shown in lungs of patients infected with SARS-CoV-2 (164). Additionally, CH_{50} activity was shown to be greatly reduced in COVID-19 patients, indicating increased classical pathway activity and hence complement consumption (308).

In our analysis, classical pathway activation could be verified by increased C1s/C1-INH complex levels in more severe COVID-19 cases. Concentrations of the newly validated marker for classical pathway activation were also associated with the presence of anti SARS-CoV-2 IgG, and levels of CRP and PTX3. Very early after an infection, increased C1s/C1-INH complex levels might be caused by acute phase proteins like CRP or PTX3 (83), whereas later on in the disease course, the C1-INH complex formation could be triggered by circulating anti SARS-CoV-2 antibodies in complex with the virus or viral proteins such as the spike or the nucleocapsid protein (163, 164).

As also seen in literature, co-infections are quite common in SARS-CoV-2 infected patients (309, 310). We hence performed analysis of follow-up samples from 12 hospitalized patients, stratified according to survival as well as three common fungal and

bacterial co-infections: *Candida* spp. (n = 4), *Escherichia coli* (n = 2) and *Aspergillus* spp. (n = 2).

While C1-INH complex levels did not differ significantly between survivors and non-survivors, all co-infections resulted in changes of (at least one of) the C1-INH complexes. The pathogens investigated here can activate all three complement pathways via the generally known mechanisms, as summarized in the introduction.

In patients with *Candida* co-infections, levels of MASP-1/C1-INH complex were higher, which is especially true during the early days after hospitalization was started. This was expected, since around 40 % of *Candida* cell wall consist of mannan (311), which is able to activate the LP and hence increase MASP-1/C1-INH complex levels, as also shown in the activation experiments here. Although all three complement pathways can be triggered by *Candida* spp., it is somewhat surprising that there is no significant difference in C1s/C1-INH complex levels between hospitalized patients with and without additional *Candida* infection. Not only can the CP be activated through circulating anti-*Candida* antibodies, but Serum Amyloid P (SAP), an acute phase protein able to activate the classical pathway (312), was also shown to deposit on the yeast cells (313). Potentially, the *Candida* infection was mainly locally, and hence did not have a great effect on circulating C1s/C1-INH complex levels. Additionally, C1s' and/or C1-INH levels might also be exhausted due to the concurrent SARS-CoV-2 infection, so that an additional increase in C1s/C1-INH complex levels is not possible anymore.

In contrast, both, C1s/C1-INH as well as MASP-1/C1-INH complex levels were higher in COVID-19 patients with *E.coli* co-infection compared to patients without. This might be explained by additional activation of the two pathways via the common triggers, or by immune-complex independent CP activation through direct interactions between C1q and the acute-phase protein CRP or *E. coli* (314).

Aspergillus is able to activate the classical as well as lectin pathway via PTX bound to the surface, while the lectin pathway can further be activated through sugar moieties on the surface of the pathogen (315, 316). One thus would expect increased C1s/C1-INH as well as MASP-1/C1-INH complex levels. However, the opposite is the case in the performed measurements: both C1-INH complexes were lower in patients with *Aspergillus* co-infection. A potential explanation is that complement activation might occur mainly through a C2 bypass mechanism, resulting in alternative pathway

activation (317). In addition, Rambach *et al.* showed the potential of *Aspergillus* to secrete complement-degrading proteases, which could have an effect on C1-INH complex levels or suppress complement activation (318).

Although follow-up samples of only 12 hospitalized COVID-19 patients with and without co-infection were analysed and therefore no firm conclusions can be drawn, the findings suggest that determination of C1-INH complexes might give an indication about the presence of bacterial or fungal co-infections, as seen by further altered C1s/C1-INH or MASP-1/C1-INH complex levels. Next to investigation of C1-INH complex levels in bigger cohorts, in future studies it would also be of interest to analyse the CP and LP activation products in patients only suffering from either a bacterial or a fungal infection, to see if similar patterns are obtained.

5.5 Early complement activation in Sepsis and other diseases

5.5.1 Complement activation in Sepsis

While complement activation plays an important role in the clearance of invading pathogens, which is essential during sepsis, over-activation of the complement system might also lead to collateral tissue damage (319).

Regarding general complement components, C3 deficiency was shown to be associated with sepsis-induced mortality (320) as well as higher susceptibility to infection, while C3 and C5 activation fragments were highly increased in sepsis patients and individuals suffering from septic shock (184, 321), and C3a was associated with fatal outcome (179). Besides that, C5a inhibition was shown to be beneficial for survial during sepsis (322).

In a clinical study by León *et al.*, significantly decreased C3 and C4 levels as well as CP activity were found in patients struggling with a septic shock, indicating a potential role of classical pathway involvement in the pathomechanism of septic shock (323). In a more recent study, Huson *et al.* reported increased levels of C4 activation products and thus C4 consumption (324). In addition, C4a and C3a levels were shown to correlate with clinical outcome (179), further pointing towards the activation of the classical and/or lectin pathway. Since several SNPs able to influence LP proteins and activation are known, potential relationships between sepsis and LP-associated SNPs were investigated by Bronkhorst *et al.* (325). The study showed a higher incidence in the development of sepsis and septic shock in severely injured patients with SNPs in the *MBL2* exon 1, the *FCN2* or the *MASP2* gene, indicating a beneficial role of lectin pathway activation during the disease course of sepsis (325).

Measurements of C1-INH complex levels showed highly increased C1s/C1-INH and MASP-1/C1-INH complex concentrations in septic patients, indicating strong activation of the classical and the lectin pathway, respectively. There further seems to be no difference in C1-INH complex levels in the presence of bloodstream infections, while MASP-1/C1-INH complex levels are slightly lower in bloodculture positive patients. However, the difference might not be clinically meaningful and just be a finding by chance. Another explanation is that LP pattern recognition molecules might be consumed by the pathogens by binding, opsonization and removal by scavanger receptors, before LP activation is possible, or that the patients are already in a disease state where lectin pathway activation does not play a significant role anymore due to overwhelming AP

activation. In addition, there was also no difference in C1-INH complex levels between COVID-19 negative and COVID-19 positive sepsis patients, similarly as reported recently in the same cohort for inflammatory mediators by Eichhorn *et al.* (239).

Increased C1/C1-INH complex levels were also shown in sepsis in a study from 1987, where Hack and colleagues investigated complement activation products in 48 patients (179). In their study, they showed a tendency towards increased concentrations of C1/C1-INH complex in patients deceasing from sepsis (179), which we could not replicate in our measurements. Here, we can see a trend towards higher C1-INH complex levels in sepsis survivors, which further strengthens the suggestion that during early stages of severe infections the complement system has a protective role for the host due to its pro-inflammatory and antimicrobial properties. In later stages of sepsis, anaphylatoxin C5a triggers cytokin release, followed by exacerbating inflammation and complement activation, potentially leading to the destruction of host tissue and the development of septic shock (188).

5.5.2 C1-INH complexes in other diseases

Although the new complex immunoassays could only be tested in COVID-19 and sepsis patients within the scope of this thesis, there are several other disease areas where C1-INH complex levels have been investigated so far, utilizing *in-house* assays.

In hereditary angioedema (HAE), levels of C1rs/C1-INH complex were significantly increased in patients (32.8 U/mL) compared to controls (3.4 U/mL; $p < 0.0001$), suggesting that C1rs/C1-INH complex might be a suitable marker to predict disease severity (262). When there is no functional C1-INH present, acting as the only regulator of the classical pathway, C1 activation occurs spontaneously, leading to uncontrolled cleavage of C4 and C2 (326). Therefore, highly increased C1rs/C1-INH complex levels indicate that all C1-INH present in the circulation is bound to C1s in HAE patients. In another study, Nielsen *et al.* also showed increased C1rs/C1-INH complex concentrations in HAE patients, while concentrations were further enhanced during physical stress, as long as the patients were untreated (221). Those changes could not be observed in levels of complexes formed between C1-INH and other serine proteases, such as FXII and kallikrein. Based on their results, the authors concluded that complement is more activated in untreated HAE patients following exercise (221).

MASP-1/C1-INH complex levels were also altered in HAE patients. While Hansen *et al.* showed significantly lower MASP-1/C1-INH complex levels in HAE patients when compared to healthy controls, without further classifying the HAE cases (226), others reported increased MASP-1/C1-INH complex concentrations in type II HAE patients (222). Kajdacsi *et al.* further showed increased C1s/C1-INH complex levels in HAE patients, with highest amounts in type II HAE (222).

Besides that, slightly increased C1rs/C1-INH complex levels were also observed in Congestive Heart Failure (CHF) patients (241). Additionally, high CIC levels in infective endocarditis (IE) also led to an increase in C1rs/C1-INH complex concentration, suggesting that classical pathway activation is involved in extracardiac manifestation development and worsening of IE (244). C1/C1-INH complex levels, next to TCC concentrations, were also significantly increased in untreated autoimmune thyroid disease (242), HIV (225), active as well as inactive Systemic lupus erythematosus (SLE) (224, 243), and Rheumatoid arthritis (RA) (224).

In a further study of us, utilizing the new C1-INH complex assays next to several other complement markers and activation products, we could demonstrate highly increased activation marker levels of the classical (C1s/C1-INH complex and C4d), the alternative (Bb) and the terminal pathway (sC5b-9) in multisystem inflammatory syndrome in children (MIS-C) patients during the acute stage of the disease (327). In contrast, MASP-1/C1-INH complex levels were not found to be increased in the patients, indicating no profound role of lectin pathway involvement in the development of MIS-C. Besides that, we could show that activation of the classical pathway was largely independent of the anti-SARS-CoV-2 humoral immune response, while activation marker levels went back to normal after treatment with IVIG (327).

5.6 Future applications for C1-INH complex assays

When looking at all those studies investigating (mainly C1/)C1-INH complexes, it is evident that changes in complex levels cover a wide range of diseases. For future studies, it will be very interesting to include the new C1-INH complex assays also for other diseases or conditions where the classical and/or the lectin pathway are known to be activated, or where therapeutics targeting CP and LP serine proteases are in use or in clinical studies, as summarized in Figure 27.

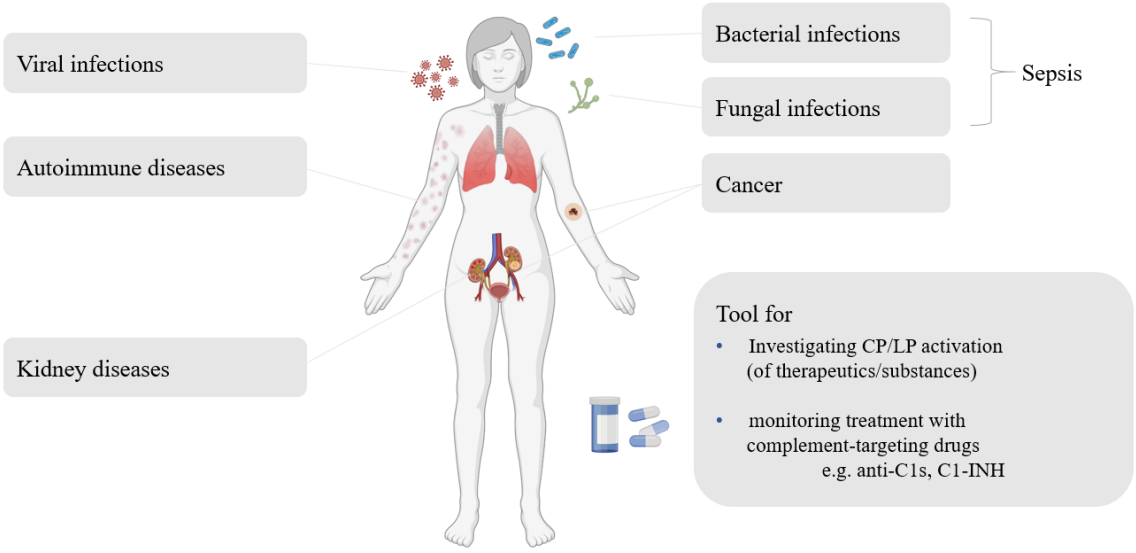

Figure 27: Summary of future disease areas and applications for C1-INH complex assays. Figure created with BioRender.com.

As an example, just recently a monoclonal antibody targeting C1s (Sutimlimab) was developed by Sanofi. Blocking of C1s was shown to be effective in the treatment of cold agglutinin disease (CAD), resulting in approval of the anti-C1s antibody in CAD by the FDA in February 2022 (328-331). Additionally, the antibody was also applied in clinical studies investigating patients with Chronic Immune Thrombocytopenia (ITP) (NCT03275454; (332)), complement-mediated conditions (NCT02502903) such as antibody-mediated allograft rejection (333, 334) and bullous pemphigoid, an autoimmune disease affecting the skin (335). Periodontal Ehlers Danlos syndrome (pEDS), a disease associated with mutations in C1s and aberrant CP activation (336), would also be an interesting disease candidate for C1s/C1-INH complex investigations in the future.

In addition, investigation of both C1-INH complexes next to each other in conditions associated with altering levels of C4d, a marker for common CP and LP activation, might shed further light on the involvement of early complement activation and maybe even allows to distinguish which pathway is activated most. As an example, C4d was shown to be of prognostic value in several kinds of cancer (48, 337, 338), whereas complement involvement in cancer is still a rather new field. In this respect, determination of C1-INH complex levels in cancer patients might expose the contribution of classical and lectin pathway activation to cancer progression.

Besides that, Narsoplimab, a human monoclonal antibody targeting MASP-2 and therefore early lectin pathway activation, was developed by Omeros Corporation and is currently in clinical trials for thrombotic microangiopathies (TMAs) like aHUS (NCT03205995) and TTP (NCT02222545), as well as nephropathies such as IgA Nephropathy (Berger's Disease), C3 glomerulopathy and lupus nephritis (NCT02682407; (339, 340)). Those clinical trials highlight the potential of lectin pathway blockade, and additional LP targeting drugs (e.g. also targeting MASP-1) might arise in the future. MASP-1/C1-INH complex levels might therefore also allow to monitor lectin pathway inhibition.

A deeper knowledge about early classical and early lectin pathway activation might further help in the field of infectious diseases and personalized medicine, allowing to specifically target one of the two pathways via serine protease inhibition early after the onset of abberant complement activation.

6 CONCLUSION AND OUTLOOK

In summary, two well-performing sandwich immunoassays, measuring C1s/C1-INH complex and MASP-1/C1-INH complex in a reliable way, were developed and are in the meantime commercialized by Hycult Biotech (C1s/C1-INH complex: cat# HK399, MASP-1/C1-INH complex: cat# HK3001).

It was shown that both complex levels increase over time when the respective complement pathways are activated *in vitro*, making them suitable markers to measure ongoing activation of the classical pathway (C1s/C1-INH complex) as well as of the lectin pathway (MASP-1/C1-INH complex).

A first reference range for healthy adults was set for both C1-INH complexes, and studies in patients suffering from COVID-19, where the classical and lectin pathway are known to be activated, showed increased C1-INH complex levels, confirming the potential of the complexes as complement activation markers also *in vivo*. Besides that, connections between LP activation and *MBL2* polymorphisms were investigated in COVID-19, and the impact of bacterial and fungal co-infections on C1-INH complex levels was analysed. Additionally, both C1-INH complex concentrations were also signficantly increased in Sepsis patients, pointing towards an advantage of investigating C1s/C1-INH and MASP-1/C1-INH complex levels to unreveal complement activation and involvement of the respective pathways also in other human diseases.

In future studies, C1-INH complex measurements will be especially interesting in conditions where complement is activated, but the exact mechanism of activation is not yet clear. Besides that, the immuoassays are also a helpful tool to determine if specific substrates, such as therapeutics or pathogens, are activating either the classical or the lectin pathway, through the measurement of *de novo* formation of C1-INH complexes. In addition, serum deficient of different complement components should be investigated for complex formation, and the influence of other biological systems (such as the coagulation or the kinin-kallikrein system), or excess amounts of CP or LP proteins on C1s/C1-INH and MASP-1/C1-INH complex levels should be thoroughly investigated.

7 REFERENCES

1. Parkin J, Cohen B. An overview of the immune system. Lancet. 2001;357(9270):1777-89.

2. Clark R, Kupper T. Old meets new: the interaction between innate and adaptive immunity. J Invest Dermatol. 2005;125(4):629-37.

3. Beutler B. Innate immunity: an overview. Mol Immunol. 2004;40(12):845-59.

4. Moens E, Veldhoen M. Epithelial barrier biology: good fences make good neighbours. Immunology. 2012;135(1):1-8.

5. Ganz T, Lehrer RI. Antimicrobial peptides of vertebrates. Curr Opin Immunol. 1998;10(1):41-4.

6. Abraham SN, Arock M. Mast cells and basophils in innate immunity. Semin Immunol. 1998;10(5):373-81.

7. Janeway CA, Jr. Approaching the asymptote? Evolution and revolution in immunology. Cold Spring Harb Symp Quant Biol. 1989;54 Pt 1:1-13.

8. Medzhitov R. Toll-like receptors and innate immunity. Nat Rev Immunol. 2001;1(2):135-45.

9. Kawai T, Akira S. The role of pattern-recognition receptors in innate immunity: update on Toll-like receptors. Nat Immunol. 2010;11(5):373-84.

10. Rabinovitch M. Professional and non-professional phagocytes: an introduction. Trends Cell Biol. 1995;5(3):85-7.

11. Lancaster CE, Ho CY, Hipolito VEB, Botelho RJ, Terebiznik MR. Phagocytosis: what's on the menu? (1). Biochem Cell Biol. 2019;97(1):21-9.

12. Medina E. Neutrophil extracellular traps: a strategic tactic to defeat pathogens with potential consequences for the host. J Innate Immun. 2009;1(3):176-80.

13. Schroder K, Hertzog PJ, Ravasi T, Hume DA. Interferon-gamma: an overview of signals, mechanisms and functions. J Leukoc Biol. 2004;75(2):163-89.

14. Agnello V, Winchester RJ, Kunkel HG. Precipitin reactions of the C1q component of complement with aggregated gamma-globulin and immune complexes in gel diffusion. Immunology. 1970;19(6):909-19.

15. Banchereau J, Steinman RM. Dendritic cells and the control of immunity. Nature. 1998;392(6673):245-52.

16. Medzhitov R, Janeway CA, Jr. Innate immunity: impact on the adaptive immune response. Curr Opin Immunol. 1997;9(1):4-9.

17. Bonilla FA, Oettgen HC. Adaptive immunity. J Allergy Clin Immunol. 2010;125(2 Suppl 2):S33-40.

18. Théry C, Amigorena S. The cell biology of antigen presentation in dendritic cells. Curr Opin Immunol. 2001;13(1):45-51.

19. Randolph GJ, Jakubzick C, Qu C. Antigen presentation by monocytes and monocyte-derived cells. Curr Opin Immunol. 2008;20(1):52-60.

20. Horny HP, Wehrmann M, Griesser H, Tiemann M, Bültmann B, Kaiserling E. Investigation of bone marrow lymphocyte subsets in normal, reactive, and neoplastic states using paraffin-embedded biopsy specimens. Am J Clin Pathol. 1993;99(2):142-9.

21. Nutt SL, Hodgkin PD, Tarlinton DM, Corcoran LM. The generation of antibody-secreting plasma cells. Nat Rev Immunol. 2015;15(3):160-71.

22. Barry M, Bleackley RC. Cytotoxic T lymphocytes: all roads lead to death. Nat Rev Immunol. 2002;2(6):401-9.

23. Abbas AK, Murphy KM, Sher A. Functional diversity of helper T lymphocytes. Nature. 1996;383(6603):787-93.

24. Josefowicz SZ, Lu LF, Rudensky AY. Regulatory T cells: mechanisms of differentiation and function. Annu Rev Immunol. 2012;30:531-64.

25. Vitetta ES, Berton MT, Burger C, Kepron M, Lee WT, Yin XM. Memory B and T cells. Annu Rev Immunol. 1991;9:193-217.

26. Alper CA, Johnson AM, Birtch AG, Moore FD. Human C'3: evidence for the liver as the primary site of synthesis. Science. 1969;163(3864):286-8.

27. Morris KM, Aden DP, Knowles BB, Colten HR. Complement biosynthesis by the human hepatoma-derived cell line HepG2. J Clin Invest. 1982;70(4):906-13.

28. Walport MJ. Complement. First of two parts. N Engl J Med. 2001;344(14):1058-66.

29. Walport MJ. Complement. Second of two parts. N Engl J Med. 2001;344(15):1140-4.

30. Merle NS, Church SE, Fremeaux-Bacchi V, Roumenina LT. Complement System Part I - Molecular Mechanisms of Activation and Regulation. Front Immunol. 2015;6:262. doi: 10.3389/fimmu.2015.00262 [eCollection 2015].

31. Merle NS, Noe R, Halbwachs-Mecarelli L, Fremeaux-Bacchi V, Roumenina LT. Complement System Part II: Role in Immunity. Front Immunol. 2015;6:257. doi: 10.3389/fimmu.2015.00257 [eCollection 2015].

32. Cooper NR. The classical complement pathway: activation and regulation of the first complement component. Adv Immunol. 1985;37:151-216.

33. Berends ET, Gorham RD, Jr., Ruyken M, Soppe JA, Orhan H, Aerts PC, et al. Molecular insights into the surface-specific arrangement of complement C5 convertase enzymes. BMC Biol. 2015;13:93. doi: 10.1186/s12915-015-0203-8 [Epub 2015 Nov 9].

34. Müller-Eberhard HJ. The membrane attack complex of complement. Annu Rev Immunol. 1986;4:503-28.

35. Müller-Eberhard HJ. The killer molecule of complement. J Invest Dermatol. 1985;85(1 Suppl):47s-52s.

36. Ehrlich P MJ. Ueber Haemolysine: Zweite Mittheilung. Berl Klin Wschr. 1899;36:481-6.

37. Medzhitov R, Janeway CA, Jr. Decoding the patterns of self and nonself by the innate immune system. Science. 2002;296(5566):298-300.

38. Hurler L, Toonen EJM, Kajdácsi E, van Bree B, Brandwijk RJMGE, de Bruin W, et al. Distinction of early complement classical and lectin pathway activation via quantification of C1s/C1-INH and MASP-1/C1-INH complexes using novel ELISAs. Front. Immunol. 13:1039765. doi: 10.3389/fimmu.2022.1039765 [eCollection 2022].

39. Ehrengruber MU, Geiser T, Deranleau DA. Activation of human neutrophils by C3a and C5A. Comparison of the effects on shape changes, chemotaxis, secretion, and respiratory burst. FEBS Lett. 1994;346(2-3):181-4.

40. Hartmann K, Henz BM, Krüger-Krasagakes S, Köhl J, Burger R, Guhl S, et al. C3a and C5a stimulate chemotaxis of human mast cells. Blood. 1997;89(8):2863-70.

41. Nataf S, Davoust N, Ames RS, Barnum SR. Human T cells express the C5a receptor and are chemoattracted to C5a. J Immunol. 1999;162(7):4018-23.

42. Ottonello L, Corcione A, Tortolina G, Airoldi I, Albesiano E, Favre A, et al. rC5a directs the in vitro migration of human memory and naive tonsillar B lymphocytes: implications for B cell trafficking in secondary lymphoid tissues. J Immunol. 1999;162(11):6510-7.

43. Markiewski MM, DeAngelis RA, Strey CW, Foukas PG, Gerard C, Gerard N, et al. The regulation of liver cell survival by complement. J Immunol. 2009;182(9):5412-8.

44. Rutkowski MJ, Sughrue ME, Kane AJ, Ahn BJ, Fang S, Parsa AT. The complement cascade as a mediator of tissue growth and regeneration. Inflamm Res. 2010;59(11):897-905.

45. Richani K, Soto E, Romero R, Espinoza J, Chaiworapongsa T, Nien JK, et al. Normal pregnancy is characterized by systemic activation of the complement system. J Matern Fetal Neonatal Med. 2005;17(4):239-45.

46. Naito AT, Sumida T, Nomura S, Liu ML, Higo T, Nakagawa A, et al. Complement C1q activates canonical Wnt signaling and promotes aging-related phenotypes. Cell. 2012;149(6):1298-313.

47. Schartz ND, Tenner AJ. The good, the bad, and the opportunities of the complement system in neurodegenerative disease. J Neuroinflammation. 2020;17(1):354. doi: 10.1186/s12974-020-02024-8 [Epub 2020 Nov 25].

48. Daugan MV, Revel M, Russick J, Dragon-Durey MA, Gaboriaud C, Robe-Rybkine T, et al. Complement C1s and C4d as Prognostic Biomarkers in Renal Cancer: Emergence of Noncanonical Functions of C1s. Cancer Immunol Res. 2021;9(8):891-908.

49. Viiklepp K, Nissinen L, Ojalill M, Riihilä P, Kallajoki M, Meri S, et al. C1r Upregulates Production of Matrix Metalloproteinase-13 and Promotes Invasion of Cutaneous Squamous Cell Carcinoma. J Invest Dermatol. 2022;142(5):1478-88.

50. Pillemer L, Blum L, Lepow IH, Ross OA, Todd EW, Wardlaw AC. The properdin system and immunity. I. Demonstration and isolation of a new serum protein, properdin, and its role in immune phenomena. Science. 1954;120(3112):279-85.

51. Lachmann PJ, Nicol P. Reaction mechanism of the alternative pathway of complement fixation. Lancet. 1973;1(7801):465-7.

52. Pangburn MK, Müller-Eberhard HJ. Relation of putative thioester bond in C3 to activation of the alternative pathway and the binding of C3b to biological targets of complement. J Exp Med. 1980;152(4):1102-14.

53. Pangburn MK, Schreiber RD, Müller-Eberhard HJ. Formation of the initial C3 convertase of the alternative complement pathway. Acquisition of C3b-like activities by spontaneous hydrolysis of the putative thioester in native C3. J Exp Med. 1981;154(3):856-67.

54. Fearon DT, Austen KF, Ruddy S. Formation of a hemolytically active cellular intermediate by the interaction between properdin factors B and D and the activated third component of complement. J Exp Med. 1973;138(6):1305-13.

55. Sahu A, Kozel TR, Pangburn MK. Specificity of the thioester-containing reactive site of human C3 and its significance to complement activation. Biochem J. 1994;302(Pt 2):429-36.

56. Law SK, Dodds AW. The internal thioester and the covalent binding properties of the complement proteins C3 and C4. Protein Sci. 1997;6(2):263-74.

57. Bexborn F, Andersson PO, Chen H, Nilsson B, Ekdahl KN. The tick-over theory revisited: formation and regulation of the soluble alternative complement C3 convertase ($C3(H_2O)Bb$). Mol Immunol. 2008;45(8):2370-9.

58. Cortes C, Ohtola JA, Saggu G, Ferreira VP. Local release of properdin in the cellular microenvironment: role in pattern recognition and amplification of the alternative pathway of complement. Front Immunol. 2012;3:412. doi: 10.3389/fimmu.2012.00412 [eCollection 2012].

59. Mathern DR, Heeger PS. Molecules Great and Small: The Complement System. Clin J Am Soc Nephrol. 2015;10(9):1636-50.

60. Lachmann PJ. The amplification loop of the complement pathways. Adv Immunol. 2009;104:115-49.

61. Pangburn MK, Müller-Eberhard HJ. The C3 convertase of the alternative pathway of human complement. Enzymic properties of the bimolecular proteinase. Biochem J. 1986;235(3):723-30.

62. Schmidt CQ, Lambris JD, Ricklin D. Protection of host cells by complement regulators. Immunol Rev. 2016;274(1):152-71.

63. Nicholson-Weller A, Burge J, Fearon DT, Weller PF, Austen KF. Isolation of a human erythrocyte membrane glycoprotein with decay-accelerating activity for C3 convertases of the complement system. J Immunol. 1982;129(1):184-9.

64. Brodbeck WG, Kuttner-Kondo L, Mold C, Medof ME. Structure/function studies of human decay-accelerating factor. Immunology. 2000;101(1):104-11.

65. Cole JL, Housley GA, Jr., Dykman TR, MacDermott RP, Atkinson JP. Identification of an additional class of C3-binding membrane proteins of human peripheral blood leukocytes and cell lines. Proc Natl Acad Sci U S A. 1985;82(3):859-63.

66. Seya T, Turner JR, Atkinson JP. Purification and characterization of a membrane protein (gp45-70) that is a cofactor for cleavage of C3b and C4b. J Exp Med. 1986;163(4):837-55.

67. Medof ME, Iida K, Mold C, Nussenzweig V. Unique role of the complement receptor CR1 in the degradation of C3b associated with immune complexes. J Exp Med. 1982;156(6):1739-54.

68. Holguin MH, Fredrick LR, Bernshaw NJ, Wilcox LA, Parker CJ. Isolation and characterization of a membrane protein from normal human erythrocytes that inhibits reactive lysis of the erythrocytes of paroxysmal nocturnal hemoglobinuria. J Clin Invest. 1989;84(1):7-17.

69. Sims PJ, Rollins SA, Wiedmer T. Regulatory control of complement on blood platelets. Modulation of platelet procoagulant responses by a membrane inhibitor of the C5b-9 complex. J Biol Chem. 1989;264(32):19228-35.

70. Isenman DE. Conformational changes accompanying proteolytic cleavage of human complement protein C3b by the regulatory enzyme factor I and its cofactor H. Spectroscopic and enzymological studies. J Biol Chem. 1983;258(7):4238-44.

71. Blaum BS, Hannan JP, Herbert AP, Kavanagh D, Uhrín D, Stehle T. Structural basis for sialic acid-mediated self-recognition by complement factor H. Nat Chem Biol. 2015;11(1):77-82.

72. Fearon DT. Regulation by membrane sialic acid of beta1H-dependent decay-dissociation of amplification C3 convertase of the alternative complement pathway. Proc Natl Acad Sci U S A. 1978;75(4):1971-5.

73. Fujita T, Gigli I, Nussenzweig V. Human C4-binding protein. II. Role in proteolysis of C4b by C3b-inactivator. J Exp Med. 1978;148(4):1044-51.

74. Fujita T, Tamura N. Interaction of C4-binding protein with cell-bound C4b. A quantitative analysis of binding and the role of C4-binding protein in proteolysis of cell-bound C4b. J Exp Med. 1983;157(4):1239-51.

75. Bhakdi S, Tranum-Jensen J. Terminal membrane C5b-9 complex of human complement: transition from an amphiphilic to a hydrophilic state through binding of the S protein from serum. J Cell Biol. 1982;94(3):755-9.

76. Murphy BF, Kirszbaum L, Walker ID, d'Apice AJ. SP-40,40, a newly identified normal human serum protein found in the SC5b-9 complex of complement and in the immune deposits in glomerulonephritis. J Clin Invest. 1988;81(6):1858-64.

77. Hughes-Jones NC, Gardner B. The reaction between the complement subcomponent C1q, IgG complexes and polyionic molecules. Immunology. 1978;34(3):459-63.

78. Bindon CI, Hale G, Brüggemann M, Waldmann H. Human monoclonal IgG isotypes differ in complement activating function at the level of C4 as well as C1q. J Exp Med. 1988;168(1):127-42.

79. McGrath FD, Brouwer MC, Arlaud GJ, Daha MR, Hack CE, Roos A. Evidence that complement protein C1q interacts with C-reactive protein through its globular head region. J Immunol. 2006;176(5):2950-7.

80. Roy N, Ohtani K, Hidaka Y, Amano Y, Matsuda Y, Mori K, et al. Three pentraxins C-reactive protein, serum amyloid p component and pentraxin 3 mediate complement activation using Collectin CL-P1. Biochim Biophys Acta Gen Subj. 2017;1861(2):1-14.

81. Volanakis JE, Narkates AJ. Interaction of C-reactive protein with artificial phosphatidylcholine bilayers and complement. J Immunol. 1981;126(5):1820-5.

82. Bristow CL, Boackle RJ. Evidence for the binding of human serum amyloid P component to Clq and Fab gamma. Mol Immunol. 1986;23(10):1045-52.

83. Bottazzi B, Vouret-Craviari V, Bastone A, De Gioia L, Matteucci C, Peri G, et al. Multimer formation and ligand recognition by the long pentraxin PTX3. Similarities and differences with the short pentraxins C-reactive protein and serum amyloid P component. J Biol Chem. 1997;272(52):32817-23.

84. Roumenina LT, Popov KT, Bureeva SV, Kojouharova M, Gadjeva M, Rabheru S, et al. Interaction of the globular domain of human C1q with Salmonella typhimurium lipopolysaccharide. Biochim Biophys Acta. 2008;1784(9):1271-6.

85. Thielens NM, Tacnet-Delorme P, Arlaud GJ. Interaction of C1q and mannan-binding lectin with viruses. Immunobiology. 2002;205(4-5):563-74.

86. Navratil JS, Watkins SC, Wisnieski JJ, Ahearn JM. The globular heads of C1q specifically recognize surface blebs of apoptotic vascular endothelial cells. J Immunol. 2001;166(5):3231-9.

87. Nauta AJ, Trouw LA, Daha MR, Tijsma O, Nieuwland R, Schwaeble WJ, et al. Direct binding of C1q to apoptotic cells and cell blebs induces complement activation. Eur J Immunol. 2002;32(6):1726-36.

88. Kaul M, Loos M. Expression of membrane C1q in human monocyte-derived macrophages is developmentally regulated and enhanced by interferon-gamma. FEBS Lett. 2001;500(1-2):91-8.

89. Vegh Z, Goyarts EC, Rozengarten K, Mazumder A, Ghebrehiwet B. Maturation-dependent expression of C1q-binding proteins on the cell surface of human monocyte-derived dendritic cells. Int Immunopharmacol. 2003;3(3):345-57.

90. Reid KB, Porter RR. Subunit composition and structure of subcomponent C1q of the first component of human complement. Biochem J. 1976;155(1):19-23.

91. Brier S, Pflieger D, Le Mignon M, Bally I, Gaboriaud C, Arlaud GJ, et al. Mapping surface accessibility of the C1r/C1s tetramer by chemical modification and mass spectrometry provides new insights into assembly of the human C1 complex. J Biol Chem. 2010;285(42):32251-63.

92. Ziccardi RJ, Cooper NR. Activation of C1r by proteolytic cleavage. J Immunol. 1976;116(2):504-9.

93. Golan MD, Burger R, Loos M. Conformational changes in C1q after binding to immune complexes: detection of neoantigens with monoclonal antibodies. J Immunol. 1982;129(2):445-7.

94. Ikeda K, Sannoh T, Kawasaki N, Kawasaki T, Yamashina I. Serum lectin with known structure activates complement through the classical pathway. J Biol Chem. 1987;262(16):7451-4.

95. Kjaer TR, Thiel S, Andersen GR. Toward a structure-based comprehension of the lectin pathway of complement. Mol Immunol. 2013;56(3):222-31.

96. Hansen SW, Ohtani K, Roy N, Wakamiya N. The collectins CL-L1, CL-K1 and CL-P1, and their roles in complement and innate immunity. Immunobiology. 2016;221(10):1058-67.

97. Matsushita M, Fujita T. The role of ficolins in innate immunity. Immunobiology. 2002;205(4-5):490-7.

98. Degn SE, Thiel S, Nielsen O, Hansen AG, Steffensen R, Jensenius JC. MAp19, the alternative splice product of the MASP2 gene. J Immunol Methods. 2011;373(1-2):89-101.

99. Degn SE, Jensen L, Gál P, Dobó J, Holmvad SH, Jensenius JC, et al. Biological variations of MASP-3 and MAp44, two splice products of the MASP1 gene involved in regulation of the complement system. J Immunol Methods. 2010;361(1-2):37-50.

100. Skjoedt MO, Hummelshoj T, Palarasah Y, Honore C, Koch C, Skjodt K, et al. A novel mannose-binding lectin/ficolin-associated protein is highly expressed in heart and skeletal muscle tissues and inhibits complement activation. J Biol Chem. 2010;285(11):8234-43.

101. Gál P, Harmat V, Kocsis A, Bián T, Barna L, Ambrus G, et al. A true autoactivating enzyme. Structural insight into mannose-binding lectin-associated serine protease-2 activations. J Biol Chem. 2005;280(39):33435-44.

102. Rossi V, Cseh S, Bally I, Thielens NM, Jensenius JC, Arlaud GJ. Substrate specificities of recombinant mannan-binding lectin-associated serine proteases-1 and -2. J Biol Chem. 2001;276(44):40880-7.

103. Takahashi M, Iwaki D, Kanno K, Ishida Y, Xiong J, Matsushita M, et al. Mannose-binding lectin (MBL)-associated serine protease (MASP)-1 contributes to activation of the lectin complement pathway. J Immunol. 2008;180(9):6132-8.

104. Héja D, Kocsis A, Dobó J, Szilágyi K, Szász R, Závodszky P, et al. Revised mechanism of complement lectin-pathway activation revealing the role of serine protease MASP-1 as the exclusive activator of MASP-2. Proc Natl Acad Sci U S A. 2012;109(26):10498-503.

105. Iwaki D, Kanno K, Takahashi M, Endo Y, Matsushita M, Fujita T. The role of mannose-binding lectin-associated serine protease-3 in activation of the alternative complement pathway. J Immunol. 2011;187(7):3751-8.

106. Iwaki D, Kanno K, Takahashi M, Endo Y, Lynch NJ, Schwaeble WJ, et al. Small mannose-binding lectin-associated protein plays a regulatory role in the lectin complement pathway. J Immunol. 2006;177(12):8626-32.

107. Dean MM, Minchinton RM, Heatley S, Eisen DP. Mannose binding lectin acute phase activity in patients with severe infection. J Clin Immunol. 2005;25(4):346-52.

108. Turner MW. Mannose-binding lectin: the pluripotent molecule of the innate immune system. Immunol Today. 1996;17(11):532-40.

109. Garred P, Larsen F, Seyfarth J, Fujita R, Madsen HO. Mannose-binding lectin and its genetic variants. Genes Immun. 2006;7(2):85-94.

110. Garred P, Genster N, Pilely K, Bayarri-Olmos R, Rosbjerg A, Ma YJ, et al. A journey through the lectin pathway of complement-MBL and beyond. Immunol Rev. 2016;274(1):74-97.

111. Garred P, Larsen F, Madsen HO, Koch C. Mannose-binding lectin deficiency--revisited. Mol Immunol. 2003;40(2-4):73-84.

112. Hurler L, Szilágyi Á, Mescia F, Bergamaschi L, Mező B, Sinkovits G, et al. Complement lectin pathway activation is associated with COVID-19 disease severity, independent of MBL2 genotype subgroups. Front. Immunol. 14:1162171. doi: 10.3389/fimmu.2023.1162171 [eCollection 2023].

113. Sumiya M, Super M, Tabona P, Levinsky RJ, Arai T, Turner MW, et al. Molecular basis of opsonic defect in immunodeficient children. Lancet. 1991;337(8757):1569-70.

114. Madsen HO, Garred P, Kurtzhals JA, Lamm LU, Ryder LP, Thiel S, et al. A new frequent allele is the missing link in the structural polymorphism of the human mannan-binding protein. Immunogenetics. 1994;40(1):37-44.

115. Lipscombe RJ, Sumiya M, Hill AV, Lau YL, Levinsky RJ, Summerfield JA, et al. High frequencies in African and non-African populations of independent mutations in the mannose binding protein gene. Hum Mol Genet. 1992;1(9):709-15.

116. Eisen DP, Dean MM, Boermeester MA, Fidler KJ, Gordon AC, Kronborg G, et al. Low serum mannose-binding lectin level increases the risk of death due to pneumococcal infection. Clin Infect Dis. 2008;47(4):510-6.

117. Eisen DP, Dean MM, Thomas P, Marshall P, Gerns N, Heatley S, et al. Low mannose-binding lectin function is associated with sepsis in adult patients. FEMS Immunol Med Microbiol. 2006;48(2):274-82.

118. Kalia N, Singh J, Kaur M. The ambiguous role of mannose-binding lectin (MBL) in human immunity. Open Med (Wars). 2021;16(1):299-310. doi: 10.1515/med-2021-0239 [eCollection 2021].

119. Bork P, Beckmann G. The CUB domain. A widespread module in developmentally regulated proteins. J Mol Biol. 1993;231(2):539-45.

120. Campbell ID, Bork, P. Epidermal growth factor like modules. Curr Opin Struct Biol. 1993;3(3):385-92.

121. Reid KB, Bentley DR, Campbell RD, Chung LP, Sim RB, Kristensen T, et al. Complement system proteins which interact with C3b or C4b A superfamily of structurally related proteins. Immunol Today. 1986;7(7-8):230-4.

122. Forneris F, Wu J, Gros P. The modular serine proteases of the complement cascade. Curr Opin Struct Biol. 2012;22(3):333-41.

123. Rossi V, Bally I, Ancelet S, Xu Y, Frémeaux-Bacchi V, Vivès RR, et al. Functional characterization of the recombinant human C1 inhibitor serpin domain: insights into heparin binding. J Immunol. 2010;184(9):4982-9.

124. Stavenhagen K, Kayili HM, Holst S, Koeleman CAM, Engel R, Wouters D, et al. N- and O-glycosylation Analysis of Human C1-inhibitor Reveals Extensive Mucin-type O-Glycosylation. Mol Cell Proteomics. 2018;17(6):1225-38.

125. Bock SC, Skriver K, Nielsen E, Thøgersen HC, Wiman B, Donaldson VH, et al. Human C1 inhibitor: primary structure, cDNA cloning, and chromosomal localization. Biochemistry. 1986;25(15):4292-301.

126. Perkins SJ, Smith KF, Amatayakul S, Ashford D, Rademacher TW, Dwek RA, et al. Two-domain structure of the native and reactive centre cleaved forms of C1 inhibitor of human complement by neutron scattering. J Mol Biol. 1990;214(3):751-63.

127. Bos IG, Hack CE, Abrahams JP. Structural and functional aspects of C1-inhibitor. Immunobiology. 2002;205(4-5):518-33.

128. Bos IG, Lubbers YT, Roem D, Abrahams JP, Hack CE, Eldering E. The functional integrity of the serpin domain of C1-inhibitor depends on the unique N-terminal domain, as revealed by a pathological mutant. J Biol Chem. 2003;278(32):29463-70.

129. Zeerleder S. C1-inhibitor: more than a serine protease inhibitor. Semin Thromb Hemost. 2011;37(4):362-74.

130. Sim RB, Reboul A, Arlaud GJ, Villiers CL, Colomb MG. Interaction of 125I-labelled complement subcomponents C-1r and C-1s with protease inhibitors in plasma. FEBS Lett. 1979;97(1):111-5.

131. Ziccardi RJ. Activation of the early components of the classical complement pathway under physiologic conditions. J Immunol. 1981;126(5):1769-73.

132. Petersen SV, Thiel S, Jensen L, Vorup-Jensen T, Koch C, Jensenius JC. Control of the classical and the MBL pathway of complement activation. Mol Immunol. 2000;37(14):803-11.

133. Kerr FK, Thomas AR, Wijeyewickrema LC, Whisstock JC, Boyd SE, Kaiserman D, et al. Elucidation of the substrate specificity of the MASP-2 protease of the lectin complement pathway and identification of the enzyme as a major physiological target of the serpin, C1-inhibitor. Mol Immunol. 2008;45(3):670-7.

134. Gigli I, Mason JW, Colman RW, Austen KF. Interaction of plasma kallikrein with the C1 inhibitor. J Immunol. 1970;104(3):574-81.

135. McConnell DJ. Inhibitors of kallikrein in human plasma. J Clin Invest. 1972;51(7):1611-23.

136. Ratnoff OD, Pensky J, Ogston D, Naff GB. The inhibition of plasmin, plasma kallikrein, plasma permeability factor, and the C'1r subcomponent of the first component of complement by serum C'1 esterase inhibitor. J Exp Med. 1969;129(2):315-31.

137. Cugno M, Bos I, Lubbers Y, Hack CE, Agostoni A. In vitro interaction of C1-inhibitor with thrombin. Blood Coagul Fibrinolysis. 2001;12(4):253-60.

138. Harpel PC, Cooper NR. Studies on human plasma C1 inactivator-enzyme interactions. I. Mechanisms of interaction with C1s, plasmin, and trypsin. J Clin Invest. 1975;55(3):593-604.

139. He S, Sim RB, Whaley K. Mechanism of action of anti-C1-inhibitor autoantibodies: prevention of the formation of stable C1s-C1-inh complexes. Mol Med. 1998;4(2):119-28.

140. Reboul A, Arlaud GJ, Sim RB, Colomb MG. A simplified procedure for the purification of C1-inactivator from human plasma. Interaction with complement subcomponents C1r and C1s. FEBS Lett. 1977;79(1):45-50.

141. Sim RB, Arlaud GJ, Colomb MG. C1 inhibitor-dependent dissociation of human complement component C1 bound to immune complexes. Biochem J. 1979;179(3):449-57.

142. Storm D, Herz J, Trinder P, Loos M. C1 inhibitor-C1s complexes are internalized and degraded by the low density lipoprotein receptor-related protein. J Biol Chem. 1997;272(49):31043-50.

143. Yoshida Y, Kato H, Ikeda Y, Nangaku M. Pathogenesis of Atypical Hemolytic Uremic Syndrome. J Atheroscler Thromb. 2019;26(2):99-110.

144. Raina R, Sethi SK, Dragon-Durey MA, Khooblall A, Sharma D, Khandelwal P, et al. Systematic review of atypical hemolytic uremic syndrome biomarkers. Pediatr Nephrol. 2022;37(7):1479-93.

145. Medjeral-Thomas NR, Pickering MC, Cook HT. Complement and kidney disease, new insights. Curr Opin Nephrol Hypertens. 2021;30(3):310-6.

146. Levi M, Cohn DM. The Role of Complement in Hereditary Angioedema. Transfus Med Rev. 2019;33(4):243-7.

147. Okroj M, Heinegård D, Holmdahl R, Blom AM. Rheumatoid arthritis and the complement system. Ann Med. 2007;39(7):517-30.

148. Weinstein A, Alexander RV, Zack DJ. A Review of Complement Activation in SLE. Curr Rheumatol Rep. 2021;23(3):16. doi: 10.1007/s11926-021-00984-1 [Epub 2021 Feb 10].

149. Réti M, Farkas P, Csuka D, Rázsó K, Schlammadinger Á, Udvardy ML, et al. Complement activation in thrombotic thrombocytopenic purpura. J Thromb Haemost. 2012;10(5):791-8.

150. Daha MR. Role of complement in innate immunity and infections. Crit Rev Immunol. 2010;30(1):47-52.

151. Habibzadeh P, Stoneman EK. The Novel Coronavirus: A Bird's Eye View. Int J Occup Environ Med. 2020;11(2):65-71.

152. Zhu N, Zhang D, Wang W, Li X, Yang B, Song J, et al. A Novel Coronavirus from Patients with Pneumonia in China, 2019. N Engl J Med. 2020;382(8):727-33.

153. World Health Organization (WHO). COVID-19 weekly epidemiological update, update 137 [Internet]. 2023 [last accessed on 2023 Apr 12]. Available from: https://www.who.int/publications/m/item/weekly-epidemiological-update-on-covid-19---6-april-2023.

154. Zhou F, Yu T, Du R, Fan G, Liu Y, Liu Z, et al. Clinical course and risk factors for mortality of adult inpatients with COVID-19 in Wuhan, China: a retrospective cohort study. Lancet. 2020;395(10229):1054-62.

155. Zhou P, Yang XL, Wang XG, Hu B, Zhang L, Zhang W, et al. A pneumonia outbreak associated with a new coronavirus of probable bat origin. Nature. 2020;579(7798):270-3.

156. Hoffmann M, Kleine-Weber H, Schroeder S, Krüger N, Herrler T, Erichsen S, et al. SARS-CoV-2 Cell Entry Depends on ACE2 and TMPRSS2 and Is Blocked by a Clinically Proven Protease Inhibitor. Cell. 2020;181(2):271-80.

157. Kim YM, Shin EC. Type I and III interferon responses in SARS-CoV-2 infection. Exp Mol Med. 2021;53(5):750-60.

158. Gralinski LE, Sheahan TP, Morrison TE, Menachery VD, Jensen K, Leist SR, et al. Complement Activation Contributes to Severe Acute Respiratory Syndrome Coronavirus Pathogenesis. mBio. 2018;9(5): e01753-18. doi: 10.1128/mBio.01753-18 [Epub 2018 Oct 9].

159. Alaiya A, Alshukairi A, Shinwari Z, Al-Fares M, Alotaibi J, AlOmaim W, et al. Alterations in the Plasma Proteome Induced by SARS-CoV-2 and MERS-CoV Reveal Biomarkers for Disease Outcomes for COVID-19 Patients. J Inflamm Res. 2021;14:4313-28.

160. Hamed ME, Naeem A, Alkadi H, Alamri AA, AlYami AS, AlJuryyan A, et al. Elevated Expression Levels of Lung Complement Anaphylatoxin, Neutrophil Chemoattractant Chemokine IL-8, and RANTES in MERS-CoV-Infected Patients: Predictive Biomarkers for Disease Severity and Mortality. J Clin Immunol. 2021;41(7):1607-20.

161. Ali YM, Ferrari M, Lynch NJ, Yaseen S, Dudler T, Gragerov S, et al. Lectin Pathway Mediates Complement Activation by SARS-CoV-2 Proteins. Front Immunol. 2021;12:714511. doi: 10.3389/fimmu.2021.714511 [eCollection 2021].

162. Stravalaci M, Pagani I, Paraboschi EM, Pedotti M, Doni A, Scavello F, et al. Recognition and inhibition of SARS-CoV-2 by humoral innate immunity pattern recognition molecules. Nat Immunol. 2022;23(2):275-86.

163. Holter JC, Pischke SE, de Boer E, Lind A, Jenum S, Holten AR, et al. Systemic complement activation is associated with respiratory failure in COVID-19 hospitalized patients. Proc Natl Acad Sci U S A. 2020;117(40):25018-25.

164. Satyam A, Tsokos MG, Brook OR, Hecht JL, Moulton VR, Tsokos GC. Activation of classical and alternative complement pathways in the pathogenesis of lung injury in COVID-19. Clin Immunol. 2021;226:108716. doi: 10.1016/j.clim.2021.108716 [Epub 2021 Mar 24].

165. Smilowitz NR, Kunichoff D, Garshick M, Shah B, Pillinger M, Hochman JS, et al. C-reactive protein and clinical outcomes in patients with COVID-19. Eur Heart J. 2021;42(23):2270-9.

166. Brunetta E, Folci M, Bottazzi B, De Santis M, Gritti G, Protti A, et al. Macrophage expression and prognostic significance of the long pentraxin PTX3 in COVID-19. Nat Immunol. 2021;22(1):19-24.

167. Yu J, Gerber GF, Chen H, Yuan X, Chaturvedi S, Braunstein EM, et al. Complement dysregulation is associated with severe COVID-19 illness. Haematologica. 2022;107(5):1095-105.

168. Lo MW, Amarilla AA, Lee JD, Albornoz EA, Modhiran N, Clark RJ, et al. SARS-CoV-2 triggers complement activation through interactions with heparan sulfate. Clin Transl Immunology. 2022;11(8):e1413. doi: 10.1002/cti2.1413 [eCollection 2022].

169. Magro C, Mulvey JJ, Berlin D, Nuovo G, Salvatore S, Harp J, et al. Complement associated microvascular injury and thrombosis in the pathogenesis of severe COVID-19 infection: A report of five cases. Transl Res. 2020;220. doi: 10.1016/j.trsl.2020.04.007 [Epub 2020 Apr 15].

170. Gao T, Hu M, Zhang X, Li H, Zhu L, Liu H, et al. Highly pathogenic coronavirus N protein aggravates lung injury by MASP-2-mediated complement over-activation. medRxiv. 2020:2020.03.29.20041962. doi: 10.1101/2020.03.29.20041962v3 [Epub 2020 Jun 18].

171. Niederreiter J, Eck C, Ries T, Hartmann A, Märkl B, Büttner-Herold M, et al. Complement Activation via the Lectin and Alternative Pathway in Patients With Severe COVID-19. Front Immunol. 2022;13:835156. doi: 10.3389/fimmu.2022.835156 [eCollection 2022].

172. Carvelli J, Demaria O, Vély F, Batista L, Chouaki Benmansour N, Fares J, et al. Association of COVID-19 inflammation with activation of the C5a-C5aR1 axis. Nature. 2020;588(7836):146-50.

173. Sinkovits G, Mező B, Réti M, Müller V, Iványi Z, Gál J, et al. Complement Overactivation and Consumption Predicts In-Hospital Mortality in SARS-CoV-2 Infection. Front Immunol. 2021;12:663187. doi: 10.3389/fimmu.2021.663187 [eCollection 2021].

174. Fleischmann C, Scherag A, Adhikari NK, Hartog CS, Tsaganos T, Schlattmann P, et al. Assessment of Global Incidence and Mortality of Hospital-treated Sepsis. Current Estimates and Limitations. Am J Respir Crit Care Med. 2016;193(3):259-72.

175. Bone RC, Balk RA, Cerra FB, Dellinger RP, Fein AM, Knaus WA, et al. Definitions for sepsis and organ failure and guidelines for the use of innovative therapies in sepsis. The ACCP/SCCM Consensus Conference Committee. American College of Chest Physicians/Society of Critical Care Medicine. Chest. 1992;101(6):1644-55.

176. Balk RA. Severe sepsis and septic shock. Definitions, epidemiology, and clinical manifestations. Crit Care Clin. 2000;16(2):179-92.

177. Singer M, Deutschman CS, Seymour CW, Shankar-Hari M, Annane D, Bauer M, et al. The Third International Consensus Definitions for Sepsis and Septic Shock (Sepsis-3). Jama. 2016;315(8):801-10.

178. Huber-Lang M, Sarma VJ, Lu KT, McGuire SR, Padgaonkar VA, Guo RF, et al. Role of C5a in multiorgan failure during sepsis. J Immunol. 2001;166(2):1193-9.

179. Hack CE, Nuijens JH, Felt-Bersma RJ, Schreuder WO, Eerenberg-Belmer AJ, Paardekooper J, et al. Elevated plasma levels of the anaphylatoxins C3a and C4a are associated with a fatal outcome in sepsis. Am J Med. 1989;86(1):20-6.

180. Stöve S, Welte T, Wagner TO, Kola A, Klos A, Bautsch W, et al. Circulating complement proteins in patients with sepsis or systemic inflammatory response syndrome. Clin Diagn Lab Immunol. 1996;3(2):175-83.

181. Furebring M, Håkansson LD, Venge P, Nilsson B, Sjölin J. Expression of the C5a receptor (CD88) on granulocytes and monocytes in patients with severe sepsis. Crit Care. 2002;6(4):363-70.

182. Groeneveld AB, Tacx AN, Bossink AW, van Mierlo GJ, Hack CE. Circulating inflammatory mediators predict shock and mortality in febrile patients with microbial infection. Clin Immunol. 2003;106(2):106-15.

183. Dofferhoff AS, de Jong HJ, Bom VJ, van der Meer J, Limburg PC, de Vries-Hospers HG, et al. Complement activation and the production of inflammatory mediators during the treatment of severe sepsis in humans. Scand J Infect Dis. 1992;24(2):197-204.

184. de Nooijer AH, Kotsaki A, Kranidioti E, Kox M, Pickkers P, Toonen EJM, et al. Complement activation in severely ill patients with sepsis: no relationship with inflammation and disease severity. Crit Care. 2023;27(1):63. doi: 10.1186/s13054-023-04344-6 [Epub 2023 Feb 16].

185. Brandtzaeg P, Mollnes TE, Kierulf P. Complement activation and endotoxin levels in systemic meningococcal disease. J Infect Dis. 1989;160(1):58-65.

186. Fischer MB, Prodeus AP, Nicholson-Weller A, Ma M, Murrow J, Reid RR, et al. Increased susceptibility to endotoxin shock in complement C3- and C4-deficient mice is corrected by C1 inhibitor replacement. J Immunol. 1997;159(2):976-82.

187. Reid RR, Prodeus AP, Khan W, Hsu T, Rosen FS, Carroll MC. Endotoxin shock in antibody-deficient mice: unraveling the role of natural antibody and complement in the clearance of lipopolysaccharide. J Immunol. 1997;159(2):970-5.

188. Ward PA. The dark side of C5a in sepsis. Nat Rev Immunol. 2004;4(2):133-42.

189. Zhao L, Ohtaki Y, Yamaguchi K, Matsushita M, Fujita T, Yokochi T, et al. LPS-induced platelet response and rapid shock in mice: contribution of O-antigen region of LPS and involvement of the lectin pathway of the complement system. Blood. 2002;100(9):3233-9.

190. Sprung CL, Schultz DR, Marcial E, Caralis PV, Gelbard MA, Arnold PI, et al. Complement activation in septic shock patients. Crit Care Med. 1986;14(6):525-8.

191. Marmer DJ, Hurtubise, Paul E. Nephelometric and Turbidimetric Immunoassay. In: Diamandis EP, Christopoulos, Theodore K, [ed.]. Immunoassay. Academic Press. 1996. p. 363-87.

192. Mancini G, Carbonara AO, Heremans JF. Immunochemical quantitation of antigens by single radial immunodiffusion. Immunochemistry. 1965;2(3):235-54.

193. Ouchterlony O. In vitro method for testing the toxin-producing capacity of diphtheria bacteria. Acta Pathol Microbiol Scand. 1948;25(1-2):186-91.

194. Milgrom F, Tuggac ZM, Campbell WA. Analysis of antigen-antibody complexes by immunoelectrophoresis. Immunology. 1965;8(4):406-10.

195. Terstappen LW, Nguyen M, Lazarus HM, Medof ME. Expression of the DAF (CD55) and CD59 antigens during normal hematopoietic cell differentiation. J Leukoc Biol. 1992;52(6):652-60.

196. Petersen SV, Thiel S, Jensen L, Steffensen R, Jensenius JC. An assay for the mannan-binding lectin pathway of complement activation. J Immunol Methods. 2001;257(1-2):107-16.

197. Prohászka Z, Frazer-Abel A. Complement multiplex testing: Concept, promises and pitfalls. Mol Immunol. 2021;140:120-6.

198. Lai Y, Zhang G, Zhou Z, Inhaber N, Bernstein JA, Chockalingam PS, et al. A novel functional C1 inhibitor activity assay in dried blood spot for diagnosis of Hereditary angioedema. Clin Chim Acta. 2020;504:155-62.

199. Willems E, Lorés-Motta L, Zanichelli A, Suffritti C, van der Flier M, van der Molen RG, et al. Quantitative multiplex profiling of the complement system to diagnose complement-mediated diseases. Clin Transl Immunology. 2020;9(12):e1225. doi: 10.1002/cti2.1225 [eCollection 2020].

200. Mayer MM. Complement and complement fixation. In: Kabat EA, Mayer MM [ed.]. Experimental Immunochemistry. 2nd edition: R Thomas: Springfield. 1967. p. 133-240.

201. Nilsson UR, Nilsson B. Simplified assays of hemolytic activity of the classical and alternative complement pathways. J Immunol Methods. 1984;72(1):49-59.

202. Masaki T, Okada N, Yasuda R, Okada H. Assay of complement activity in human serum using large unilamellar liposomes. J Immunol Methods. 1989;123(1):19-24.

203. Jaskowski TD, Martins TB, Litwin CM, Hill HR. Comparison of three different methods for measuring classical pathway complement activity. Clin Diagn Lab Immunol. 1999;6(1):137-9.

204. Platts-Mills TA, Ishizaka K. Activation of the alternate pathway of human complements by rabbit cells. J Immunol. 1974;113(1):348-58.

205. Martin A, Lachmann PJ, Halbwachs L, Hobart MJ. Haemolytic diffusion plate assays for factors B and D of the alternative pathway of complement activation. Immunochemistry. 1976;13(4):317-24.

206. Des Prez RM, Bryan CS, Hawiger J, Colley DG. Function of the classical and alternate pathways of human complement in serum treated with ethylene glycol tetraacetic acid and $MgCl_2$-ethylene glycol tetraacetic acid. Infect Immun. 1975;11(6):1235-43.

207. Roos A, Bouwman LH, Munoz J, Zuiverloon T, Faber-Krol MC, Fallaux-van den Houten FC, et al. Functional characterization of the lectin pathway of complement in human serum. Mol Immunol. 2003;39(11):655-68.

208. Seelen MA, Roos A, Wieslander J, Mollnes TE, Sjöholm AG, Wurzner R, et al. Functional analysis of the classical, alternative, and MBL pathways of the complement system: standardization and validation of a simple ELISA. J Immunol Methods. 2005;296(1-2):187-98.

209. Zwirner J, Felber E, Reiter C, Riethmüller G, Feucht HE. Deposition of complement activation products on plastic-adsorbed immunoglobulins. A simple ELISA technique for the detection of defined complement deficiencies. J Immunol Methods. 1989;124(1):121-9.

210. Lachmann PJ. Preparing serum for functional complement assays. J Immunol Methods. 2010;352(1-2):195-7.

211. Mutti M, Ramoni K, Nagy G, Nagy E, Szijártó V. A New Tool for Complement Research: In vitro Reconstituted Human Classical Complement Pathway. Front Immunol. 2018;9:2770. doi: 10.3389/fimmu.2018.02770 [eCollection 2018].

212. Li HH, Busse P, Lumry WR, Frazer-Abel A, Levy H, Steele T, et al. Comparison of chromogenic and ELISA functional C1 inhibitor tests in diagnosing hereditary angioedema. J Allergy Clin Immunol Pract. 2015;3(2):200-5.

213. Zubler RH, Lange G, Lambert PH, Miescher PA. Detection of immune complexes in unheated sera by modified 125I-Clq binding test. Effect of heating on the binding of Clq by immune complexes and application of the test to systemic lupus erythematosus. J Immunol. 1976;116(1):232-5.

214. Rossen RD, Reisberg MA, Hersh EM, Gutterman JU. The C1q binding test for soluble immune complexes: clinical correlations obtained in patients with cancer. J Natl Cancer Inst. 1977;58(5):1205-15.

215. Noris M, Remuzzi G. Overview of complement activation and regulation. Semin Nephrol. 2013;33(6):479-92.

216. Takeda J, Kinoshita T, Takata Y, Kozono H, Tanaka E, Hong K, et al. Rapid and simple measurement of human C5a-des-Arg level in plasma or serum using monoclonal antibodies. J Immunol Methods. 1987;101(2):265-70.

217. Aguado MT, Lambris JD, Tsokos GC, Burger R, Bitter-Suermann D, Tamerius JD, et al. Monoclonal antibodies against complement 3 neoantigens for detection of immune complexes and complement activation. Relationship between immune complex levels, state of C3, and numbers of receptors for C3b. J Clin Invest. 1985;76(4):1418-26.

218. Garred P, Mollnes TE, Lea T. Quantification in enzyme-linked immunosorbent assay of a C3 neoepitope expressed on activated human complement factor C3. Scand J Immunol. 1988;27(3):329-35.

219. Mollnes TE, Lea T, Frøland SS, Harboe M. Quantification of the terminal complement complex in human plasma by an enzyme-linked immunosorbent assay based on monoclonal antibodies against a neoantigen of the complex. Scand J Immunol. 1985;22(2):197-202.

220. Mayes JT, Schreiber RD, Cooper NR. Development and application of an enzyme-linked immunosorbent assay for the quantitation of alternative complement pathway activation in human serum. J Clin Invest. 1984;73(1):160-70.

221. Nielsen EW, Johansen HT, Gaudesen O, Osterud B, Olsen JO, Høgåsen K, et al. C3 is activated in hereditary angioedema, and C1/C1-inhibitor complexes rise during physical stress in untreated patients. Scand J Immunol. 1995;42(6):679-85.

222. Kajdácsi E, Jandrasics Z, Veszeli N, Makó V, Koncz A, Gulyás D, et al. Patterns of C1-Inhibitor/Plasma Serine Protease Complexes in Healthy Humans and in Hereditary Angioedema Patients. Front Immunol. 2020;11:794. doi: 10.3389/fimmu.2020.00794 [eCollection 2020].

223. Waldo FB, West CD. Quantitation of (C1INH)2 C1r-C1s complexes in glomerulonephritis as an indicator of C1 activation. Clin Immunol Immunopathol. 1987;42(2):239-49.

224. Auda G, Holme ER, Davidson JE, Zoma A, Veitch J, Whaley K. Measurement of complement activation products in patients with chronic rheumatic diseases. Rheumatol Int. 1990;10(5):185-9.

225. Füst G, Ujhelyi E, Hidvégi T, Pálóczi K, Mihalik R, Hollán S, et al. The complement system in HIV disease. Immunol Invest. 1991;20(2):231-41.

226. Hansen CB, Csuka D, Munthe-Fog L, Varga L, Farkas H, Hansen KM, et al. The Levels of the Lectin Pathway Serine Protease MASP-1 and Its Complex Formation with C1 Inhibitor Are Linked to the Severity of Hereditary Angioedema. J Immunol. 2015;195(8):3596-604.

227. Dobó J, Harmat V, Sebestyén E, Beinrohr L, Závodszky P, Gál P. Purification, crystallization and preliminary X-ray analysis of human mannose-binding lectin-associated serine protease-1 (MASP-1) catalytic region. Acta Crystallogr Sect F Struct Biol Cryst Commun. 2008;64(Pt 9):781-4.

228. Megyeri M, Harmat V, Major B, Végh Á, Balczer J, Héja D, et al. Quantitative characterization of the activation steps of mannan-binding lectin (MBL)-associated serine proteases (MASPs) points to the central role of MASP-1 in the initiation of the complement lectin pathway. J Biol Chem. 2013;288(13):8922-34.

229. Kardos J, Gál P, Szilágyi L, Thielens NM, Szilágyi K, Lõrincz Z, et al. The role of the individual domains in the structure and function of the catalytic region of a modular serine protease, C1r. J Immunol. 2001;167(9):5202-8.

230. Jensenius JC, Jensen PH, McGuire K, Larsen JL, Thiel S. Recombinant mannan-binding lectin (MBL) for therapy. Biochem Soc Trans. 2003;31(Pt 4):763-7.

231. Trojnar E, Józsi M, Szabó Z, Réti M, Farkas P, Kelen K, et al. Elevated Systemic Pentraxin-3 Is Associated With Complement Consumption in the Acute Phase of Thrombotic Microangiopathies. Front Immunol. 2019;10:240. doi: 10.3389/fimmu.2019.00240 [eCollection 2019].

232. Bergamaschi L, Mescia F, Turner L, Hanson AL, Kotagiri P, Dunmore BJ, et al. Longitudinal analysis reveals that delayed bystander CD8+ T cell activation and early immune pathology distinguish severe COVID-19 from mild disease. Immunity. 2021;54(6):1257-75.

233. Huber S, Massri M, Grasse M, Fleischer V, Kellnerová S, Harpf V, et al. Systemic Inflammation and Complement Activation Parameters Predict Clinical Outcome of Severe SARS-CoV-2 Infections. Viruses. 2021;13(12):2376. doi: 10.3390/v13122376 [Epub 2021 Nov 26].

234. Huber S. Advanced pathogen detection in bloodstream infections [PhD thesis]. Innsbruck, Austria: Medical University Innsbruck, Institute of Hygiene and Medical Microbiology. 2022.

235. Würzner R, Xu H, Franzke A, Schulze M, Peters JH, Götze O. Blood dendritic cells carry terminal complement complexes on their cell surface as detected by newly developed neoepitope-specific monoclonal antibodies. Immunology. 1991;74(1):132-8.

236. Gál P, Závodszky P. Structure and function of the serine-protease subcomponents of C1: protein engineering studies. Immunobiology. 1998;199(2):317-26.

237. Ambrus G, Gál P, Kojima M, Szilágyi K, Balczer J, Antal J, et al. Natural substrates and inhibitors of mannan-binding lectin-associated serine protease-1 and -2: a study on recombinant catalytic fragments. J Immunol. 2003;170(3):1374-82.

238. Defendi F, Leroy C, Epaulard O, Clavarino G, Vilotitch A, Le Marechal M, et al. Complement Alternative and Mannose-Binding Lectin Pathway Activation Is Associated With COVID-19 Mortality. Front Immunol. 2021;12:742446. doi: 10.3389/fimmu.2021.742446 [eCollection 2021].

239. Eichhorn T, Huber S, Weiss R, Ebeyer-Masotta M, Lauková L, Emprechtinger R, et al. Infection with SARS-CoV-2 Is Associated with Elevated Levels of IP-10, MCP-1, and IL-13 in Sepsis Patients. Diagnostics (Basel). 2023;13(6). doi: 10.3390/diagnostics13061069 [Epub 2023 Mar 11].

240. Ricklin D, Reis ES, Lambris JD. Complement in disease: a defence system turning offensive. Nat Rev Nephrol. 2016;12(7):383-401.

241. Aukrust P, Gullestad L, Lappegård KT, Ueland T, Aass H, Wikeby L, et al. Complement activation in patients with congestive heart failure: effect of high-dose intravenous immunoglobulin treatment. Circulation. 2001;104(13):1494-500.

242. Weetman AP, Cohen SB, Oleesky DA, Morgan BP. Terminal complement complexes and C1/C1 inhibitor complexes in autoimmune thyroid disease. Clin Exp Immunol. 1989;77(1):25-30.

243. Nagy G, Brózik M, Varga L, Füst G, Kirschfink M, Kiss E, et al. Usefulness of detection of complement activation products in evaluating SLE activity. Lupus. 2000;9(1):19-25.

244. Messias-Reason IJ, Hayashi SY, Nisihara RM, Kirschfink M. Complement activation in infective endocarditis: correlation with extracardiac manifestations and prognosis. Clin Exp Immunol. 2002;127(2):310-5.

245. Locke DP, Hillier LW, Warren WC, Worley KC, Nazareth LV, Muzny DM, et al. Comparative and demographic analysis of orang-utan genomes. Nature. 2011;469(7331):529-33.

246. Prohászka Z, Nilsson B, Frazer-Abel A, Kirschfink M. Complement analysis 2016: Clinical indications, laboratory diagnostics and quality control. Immunobiology. 2016;221(11):1247-58.

247. Frazer-Abel A, Kirschfink M, Prohászka Z. Expanding Horizons in Complement Analysis and Quality Control. Front Immunol. 2021;12:697313. doi: 10.3389/fimmu.2021.697313 [eCollection 2021].

248. Prohászka Z, Kirschfink M, Frazer-Abel A. Complement analysis in the era of targeted therapeutics. Mol Immunol. 2018;102:84-8.

249. Sinosich MJ, Teisner B, Brandslund I, Fisher M, Grudzinskas JG. Influence of time, temperature and coagulation on the measurement of C3, C3 split products and C4. J Immunol Methods. 1982;55(1):107-14.

250. Vercauteren KOA, Lambrecht S, Delanghe J. Preanalytical classical and alternative complement pathway activity loss. Biochem Med (Zagreb). 2019;29(3):030701. doi: 10.11613/BM.2019.030701 [Epub 2019 Aug 5].

251. Wuillemin WA, te Velthuis H, Lubbers YT, de Ruig CP, Eldering E, Hack CE. Potentiation of C1 inhibitor by glycosaminoglycans: dextran sulfate species are effective inhibitors of in vitro complement activation in plasma. J Immunol. 1997;159(4):1953-60.

252. Blondin C, Fischer E, Boisson-Vidal C, Kazatchkine MD, Jozefonvicz J. Inhibition of complement activation by natural sulfated polysaccharides (fucans) from brown seaweed. Mol Immunol. 1994;31(4):247-53.

253. Sahu A, Pangburn MK. Identification of multiple sites of interaction between heparin and the complement system. Mol Immunol. 1993;30(7):679-84.

254. Presanis JS, Hajela K, Ambrus G, Gál P, Sim RB. Differential substrate and inhibitor profiles for human MASP-1 and MASP-2. Mol Immunol. 2004;40(13):921-9.

255. Sim RB, Arlaud GJ, Colomb MG. Kinetics of reaction of human C1-inhibitor with the human complement system proteases C1r and C1s. Biochim Biophys Acta. 1980;612(2):433-49.

256. Dobó J, Harmat V, Beinrohr L, Sebestyén E, Závodszky P, Gál P. MASP-1, a promiscuous complement protease: structure of its catalytic region reveals the basis of its broad specificity. J Immunol. 2009;183(2):1207-14.

257. Villiers CL, Arlaud GJ, Painter RH, Colomb MG. Calcium binding properties of the C1 subcomponents C1q, C1r and C1s. FEBS Lett. 1980;117(1):289-94.

258. Pfeifer PH, Kawahara MS, Hugli TE. Possible mechanism for in vitro complement activation in blood and plasma samples: futhan/EDTA controls in vitro complement activation. Clin Chem. 1999;45(8 Pt 1):1190-9.

259. Gingras AR, Girija UV, Keeble AH, Panchal R, Mitchell DA, Moody PC, et al. Structural basis of mannan-binding lectin recognition by its associated serine protease MASP-1: implications for complement activation. Structure. 2011;19(11):1635-43.

260. Brandwijk R, Michels M, van Rossum M, de Nooijer AH, Nilsson PH, de Bruin WCC, et al. Pitfalls in complement analysis: A systematic literature review of assessing complement activation. Front Immunol. 2022;13:1007102. doi: 10.3389/fimmu.2022.1007102 [eCollection 2022].

261. Yang S, McGookey M, Wang Y, Cataland SR, Wu HM. Effect of blood sampling, processing, and storage on the measurement of complement activation biomarkers. Am J Clin Pathol. 2015;143(4):558-65.

262. Csuka D, Füst G, Farkas H, Varga L. Parameters of the classical complement pathway predict disease severity in hereditary angioedema. Clin Immunol. 2011;139(1):85-93.

263. Fearon DT, Austen KF. Activation of the alternative complement pathway due to resistance of zymosan-bound amplification convertase to endogenous regulatory mechanisms. Proc Natl Acad Sci U S A. 1977;74(4):1683-7.

264. Super M, Levinsky RJ, Turner MW. The level of mannan-binding protein regulates the binding of complement-derived opsonins to mannan and zymosan at low serum concentrations. Clin Exp Immunol. 1990;79(2):144-50.

265. Schenkein HA, Ruddy S. The role of immunoglobulins in alternative complement pathway activation by zymosan. I. Human IgG with specificity for Zymosan enhances alternative pathway activation by zymosan. J Immunol. 1981;126(1):7-10.

266. Schifferli JA, Taylor RP. Physiological and pathological aspects of circulating immune complexes. Kidney Int. 1989;35(4):993-1003.

267. Manderson AP, Pickering MC, Botto M, Walport MJ, Parish CR. Continual low-level activation of the classical complement pathway. J Exp Med. 2001;194(6):747-56.

268. Nilsson T, Bäck O. Determination of C1s-C1 inhibitor complexes in plasma by means of an enzyme linked immunosorbent assay. Clin Exp Immunol. 1985;60(1):178-82.

269. Mollnes TE, Høgåsen K, De Carolis C, Vaquero E, Nielsen EW, Fontana L, et al. High-dose intravenous immunoglobulin treatment activates complement in vivo. Scand J Immunol. 1998;48(3):312-7.

270. Füst Á, Csuka D, Imre L, Bausz M, Nagymihály A, Füst G, et al. The role of complement activation in the pathogenesis of Fuchs' dystrophy. Mol Immunol. 2014;58(2):177-81.

271. Kerényi A, Nagy G, Veres A, Varga L, Füst A, Nagymihány A, et al. C1r-C1s-C1inhibitor (C1rs-C1inh) complex measurements in tears of patients before and after penetrating keratoplasty. Curr Eye Res. 2002;24(2):99-104.

272. Horváth Z, Csuka D, Vargova K, Kovács A, Molnár A, Gulácsi-Bárdos P, et al. Elevated C1rC1sC1inh levels independently predict atherosclerotic coronary heart disease. Mol Immunol. 2013;54(1):8-13.

273. Adamek M, Heyder J, Heinold A, Fiedler G, Opelz G, Tran TH. Characterization of mannose-binding lectin (MBL) variants by allele-specific sequencing of MBL2 and determination of serum MBL protein levels. Tissue Antigens. 2013;82(6):410-5.

274. Dobó J, Schroeder V, Jenny L, Cervenak L, Závodszky P, Gál P. Multiple roles of complement MASP-1 at the interface of innate immune response and coagulation. Mol Immunol. 2014;61(2):69-78.

275. Dobó J, Pál G, Cervenak L, Gál P. The emerging roles of mannose-binding lectin-associated serine proteases (MASPs) in the lectin pathway of complement and beyond. Immunol Rev. 2016;274(1):98-111.

276. Hess K, Ajjan R, Phoenix F, Dobó J, Gál P, Schroeder V. Effects of MASP-1 of the complement system on activation of coagulation factors and plasma clot formation. PLoS One. 2012;7(4):e35690. doi: 10.1371/journal.pone.0035690 [Epub 2012 Apr 20].

277. Gaya da Costa M, Poppelaars F, van Kooten C, Mollnes TE, Tedesco F, Würzner R, et al. Age and Sex-Associated Changes of Complement Activity and Complement Levels in a Healthy Caucasian Population. Front Immunol. 2018;9:2664. doi: 10.3389/fimmu.2018.02664 [eCollection 2018].

278. Bergseth G, Ludviksen JK, Kirschfink M, Giclas PC, Nilsson B, Mollnes TE. An international serum standard for application in assays to detect human complement activation products. Mol Immunol. 2013;56(3):232-9.

279. Troldborg A, Hansen A, Hansen SW, Jensenius JC, Stengaard-Pedersen K, Thiel S. Lectin complement pathway proteins in healthy individuals. Clin Exp Immunol. 2017;188(1):138-47.

280. Diurno F, Numis FG, Porta G, Cirillo F, Maddaluno S, Ragozzino A, et al. Eculizumab treatment in patients with COVID-19: preliminary results from real life ASL Napoli 2 Nord experience. Eur Rev Med Pharmacol Sci. 2020;24(7):4040-7.

281. Mastaglio S, Ruggeri A, Risitano AM, Angelillo P, Yancopoulou D, Mastellos DC, et al. The first case of COVID-19 treated with the complement C3 inhibitor AMY-101. Clin Immunol. 2020;215:108450. doi: 10.1016/j.clim.2020.108450 [Epub 2020 Apr 29].

282. Mastellos DC, Pires da Silva BGP, Fonseca BAL, Fonseca NP, Auxiliadora-Martins M, Mastaglio S, et al. Complement C3 vs C5 inhibition in severe COVID-19: Early clinical findings reveal differential biological efficacy. Clin Immunol. 2020;220:108598. doi: 10.1016/j.clim.2020.108598 [Epub 2020 Sep 19].

283. Zelek WM, Cole J, Ponsford MJ, Harrison RA, Schroeder BE, Webb N, et al. Complement Inhibition with the C5 Blocker LFG316 in Severe COVID-19. Am J Respir Crit Care Med. 2020;202(9):1304-8.

284. Vlaar APJ, Lim EHT, de Bruin S, Rückinger S, Pilz K, Brouwer MC, et al. The anti-C5a antibody vilobelimab efficiently inhibits C5a in patients with severe COVID-19. Clin Transl Sci. 2022;15(4):854-8.

285. Vlaar APJ, Witzenrath M, van Paassen P, Heunks LMA, Mourvillier B, de Bruin S, et al. Anti-C5a antibody (vilobelimab) therapy for critically ill, invasively mechanically ventilated patients with COVID-19 (PANAMO): a multicentre, double-blind, randomised, placebo-controlled, phase 3 trial. Lancet Respir Med. 2022;10(12):1137-46.

286. Rambaldi A, Gritti G, Micò MC, Frigeni M, Borleri G, Salvi A, et al. Endothelial injury and thrombotic microangiopathy in COVID-19: Treatment with the lectin-pathway inhibitor narsoplimab. Immunobiology. 2020;225(6):152001. doi: 10.1016/j.imbio.2020.152001 [Epub 2020 Aug 9].

287. Smith K, Pace A, Ortiz S, Kazani S, Rottinghaus S. A Phase 3 Open-label, Randomized, Controlled Study to Evaluate the Efficacy and Safety of Intravenously Administered Ravulizumab Compared with Best Supportive Care in Patients with COVID-19 Severe Pneumonia, Acute Lung Injury, or Acute Respiratory Distress Syndrome: A structured summary of a study protocol for a randomised controlled trial. Trials. 2020;21(1):639. doi: 10.1186/s13063-020-04548-z [Epub 2020 Jul 13].

288. Vlaar APJ, de Bruin S, Busch M, Timmermans S, van Zeggeren IE, Koning R, et al. Anti-C5a antibody IFX-1 (vilobelimab) treatment versus best supportive care for patients with severe COVID-19 (PANAMO): an exploratory, open-label, phase 2 randomised controlled trial. Lancet Rheumatol. 2020;2(12):e764-e73.

289. Yu J, Yuan X, Chen H, Chaturvedi S, Braunstein EM, Brodsky RA. Direct activation of the alternative complement pathway by SARS-CoV-2 spike proteins is blocked by factor D inhibition. Blood. 2020;136(18):2080-9.

290. Siggins MK, Davies K, Fellows R, Thwaites RS, Baillie JK, Semple MG, et al. Alternative pathway dysregulation in tissues drives sustained complement activation and predicts outcome across the disease course in COVID-19. Immunology. 2023;168(3):473-492.

291. Götz MP, Skjoedt MO, Bayarri-Olmos R, Hansen CB, Pérez-Alós L, Jarlhelt I, et al. Lectin Pathway Enzyme MASP-2 and Downstream Complement Activation in COVID-19. J Innate Immun. 2022. doi: 10.1159/000525508 [Epub ahead of print 2022 Jul 11].

292. Gao T, Zhu L, Liu H, Zhang X, Wang T, Fu Y, et al. Highly pathogenic coronavirus N protein aggravates inflammation by MASP-2-mediated lectin complement pathway overactivation. Signal Transduct Target Ther. 2022;7(1):318. doi: 10.1038/s41392-022-01133-5 [Epub 2022 Sep 14].

293. Ip WK, Chan KH, Law HK, Tso GH, Kong EK, Wong WH, et al. Mannose-binding lectin in severe acute respiratory syndrome coronavirus infection. J Infect Dis. 2005;191(10):1697-704.

294. Zhou Y, Lu K, Pfefferle S, Bertram S, Glowacka I, Drosten C, et al. A single asparagine-linked glycosylation site of the severe acute respiratory syndrome coronavirus spike glycoprotein facilitates inhibition by mannose-binding lectin through multiple mechanisms. J Virol. 2010;84(17):8753-64.

295. Zhang H, Zhou G, Zhi L, Yang H, Zhai Y, Dong X, et al. Association between mannose-binding lectin gene polymorphisms and susceptibility to severe acute respiratory syndrome coronavirus infection. J Infect Dis. 2005;192(8):1355-61.

296. Tu X, Chong WP, Zhai Y, Zhang H, Zhang F, Wang S, et al. Functional polymorphisms of the CCL2 and MBL genes cumulatively increase susceptibility to severe acute respiratory syndrome coronavirus infection. J Infect. 2015;71(1):101-9.

297. Yuan FF, Tanner J, Chan PK, Biffin S, Dyer WB, Geczy AF, et al. Influence of FcgammaRIIA and MBL polymorphisms on severe acute respiratory syndrome. Tissue Antigens. 2005;66(4):291-6.

298. Asselta R, Paraboschi EM, Stravalaci M, Invernizzi P, Bonfanti P, Biondi A, et al. Reply to: Hultström et al., Genetic determinants of mannose-binding lectin activity predispose to thromboembolic complications in critical COVID-19. Mannose-binding lectin genetics in COVID-19. Nat Immunol. 2022;23(6):865-7.

299. Malaquias MAS, Gadotti AC, Motta-Junior JDS, Martins APC, Azevedo MLV, Benevides APK, et al. The role of the lectin pathway of the complement system in SARS-CoV-2 lung injury. Transl Res. 2021;231:55-63.

300. Hultström M, Frithiof R, Grip J, Lindelöf L, Rooijackers O, Pigazzini S, et al. Genetic determinants of mannose-binding lectin activity predispose to thromboembolic complications in critical COVID-19. Nat Immunol. 2022;23(6):861-4.

301. Medetalibeyoglu A, Bahat G, Senkal N, Kose M, Avci K, Sayin GY, et al. Mannose binding lectin gene 2 (rs1800450) missense variant may contribute to development and severity of COVID-19 infection. Infect Genet Evol. 2021;89:104717. doi: 10.1016/j.meegid.2021.104717 [Epub 2021 Jan 27].

302. Speletas M, Dadouli K, Syrakouli A, Gatselis N, Germanidis G, Mouchtouri VA, et al. MBL deficiency-causing B allele (rs1800450) as a risk factor for severe COVID-19. Immunobiology. 2021;226(6):152136. doi: 10.1016/j.imbio.2021.152136 [Epub 2021 Sep 24].

303. Ezekowitz RA, Day LE, Herman GA. A human mannose-binding protein is an acute-phase reactant that shares sequence homology with other vertebrate lectins. J Exp Med. 1988;167(3):1034-46.

304. Thiel S, Holmskov U, Hviid L, Laursen SB, Jensenius JC. The concentration of the C-type lectin, mannan-binding protein, in human plasma increases during an acute phase response. Clin Exp Immunol. 1992;90(1):31-5.

305. Neth O, Hann I, Turner MW, Klein NJ. Deficiency of mannose-binding lectin and burden of infection in children with malignancy: a prospective study. Lancet. 2001;358(9282):614-8.

306. Arai T, Tabona P, Summerfield JA. Human mannose-binding protein gene is regulated by interleukins, dexamethasone and heat shock. Q J Med. 1993;86(9):575-82.

307. Messner CB, Demichev V, Wendisch D, Michalick L, White M, Freiwald A, et al. Ultra-High-Throughput Clinical Proteomics Reveals Classifiers of COVID-19 Infection. Cell Syst. 2020;11(1):11-24.

308. Keshavarz F, Ghalamfarsa F, Javdansirat S, Hasanzadeh S, Azizi A, Sabz G, et al. Patients with Covid 19 have significantly reduced CH50 activity. Virusdisease. 2021;32(4):681-9.

309. Garcia-Vidal C, Sanjuan G, Moreno-García E, Puerta-Alcalde P, Garcia-Pouton N, Chumbita M, et al. Incidence of co-infections and superinfections in hospitalized patients with COVID-19: a retrospective cohort study. Clin Microbiol Infect. 2021;27(1):83-8.

310. Feldman C, Anderson R. The role of co-infections and secondary infections in patients with COVID-19. Pneumonia (Nathan). 2021;13(1):5. doi: 10.1186/s41479-021-00083-w [Epub 2021 Apr 25].

311. Hammad NM, El Badawy NE, Ghramh HA, Al Kady LM. Mannose-Binding Lectin: A Potential Therapeutic Candidate against Candida Infection. Biomed Res Int. 2018;2018:2813737. doi: 10.1155/2018/2813737 [eCollection 2018].

312. Ying SC, Gewurz AT, Jiang H, Gewurz H. Human serum amyloid P component oligomers bind and activate the classical complement pathway via residues 14-26 and 76-92 of the A chain collagen-like region of C1q. J Immunol. 1993;150(1):169-76.

313. Behrens NE, Lipke PN, Pilling D, Gomer RH, Klotz SA. Serum Amyloid P Component Binds Fungal Surface Amyloid and Decreases Human Macrophage Phagocytosis and Secretion of Inflammatory Cytokines. mBio. 2019;10(2): e00218-19. doi: 10.1128/mBio.00218-19 [Epub 2019 Mar 12].

314. Li K, Sacks SH, Sheerin NS. The classical complement pathway plays a critical role in the opsonisation of uropathogenic Escherichia coli. Mol Immunol. 2008;45(4):954-62.

315. Ma YJ, Doni A, Hummelshøj T, Honoré C, Bastone A, Mantovani A, et al. Synergy between ficolin-2 and pentraxin 3 boosts innate immune recognition and complement deposition. J Biol Chem. 2009;284(41):28263-75.

316. Moalli F, Doni A, Deban L, Zelante T, Zagarella S, Bottazzi B, et al. Role of complement and Fc{gamma} receptors in the protective activity of the long pentraxin PTX3 against Aspergillus fumigatus. Blood. 2010;116(24):5170-80.

317. Dumestre-Pérard C, Lamy B, Aldebert D, Lemaire-Vieille C, Grillot R, Brion JP, et al. Aspergillus conidia activate the complement by the mannan-binding lectin C2 bypass mechanism. J Immunol. 2008;181(10):7100-5.

318. Rambach G, Dum D, Mohsenipour I, Hagleitner M, Würzner R, Lass-Flörl C, et al. Secretion of a fungal protease represents a complement evasion mechanism in cerebral aspergillosis. Mol Immunol. 2010;47(7-8):1438-49. doi: 10.1016/j.molimm.2010.02.010 [Epub 2010 Mar 19].

319. Mannes M, Schmidt CQ, Nilsson B, Ekdahl KN, Huber-Lang M. Complement as driver of systemic inflammation and organ failure in trauma, burn, and sepsis. Semin Immunopathol. 2021;43(6):773-88.

320. Homann C, Varming K, Høgåsen K, Mollnes TE, Graudal N, Thomsen AC, et al. Acquired C3 deficiency in patients with alcoholic cirrhosis predisposes to infection and increased mortality. Gut. 1997;40(4):544-9.

321. Hartemink KJ, Groeneveld AB. The hemodynamics of human septic shock relate to circulating innate immunity factors. Immunol Invest. 2010;39(8):849-62.

322. Flierl MA, Rittirsch D, Nadeau BA, Day DE, Zetoune FS, Sarma JV, et al. Functions of the complement components C3 and C5 during sepsis. Faseb j. 2008;22(10):3483-90.

323. León C, Rodrigo MJ, Tomasa A, Gallart MT, Latorre FJ, Rius J, et al. Complement activation in septic shock due to gram-negative and gram-positive bacteria. Crit Care Med. 1982;10(5):308-10.

324. Huson MA, Wouters D, van Mierlo G, Grobusch MP, Zeerleder SS, van der Poll T. HIV Coinfection Enhances Complement Activation During Sepsis. J Infect Dis. 2015;212(3):474-83.

325. Bronkhorst MW, Lomax MA, Vossen RH, Bakker J, Patka P, van Lieshout EM. Risk of infection and sepsis in severely injured patients related to single nucleotide polymorphisms in the lectin pathway. Br J Surg. 2013;100(13):1818-26.

326. Ghebrehiwet B, Randazzo BP, Kaplan AP. Studies of complement autoactivatability in hereditary angioedema: direct relationship to functional C-1-INA and the effect of classical pathway activators. Clin Immunol Immunopathol. 1984;32(1):101-10.

327. Sinkovits G, Schnur J, Hurler L, Kiszel P, Prohászka ZZ, Sík P, et al. Evidence, detailed characterization and clinical context of complement activation in acute multisystem inflammatory syndrome in children. Sci Rep. 2022;12(1):19759. doi: 10.1038/s41598-022-23806-5 [Epub 2022 Nov 17].

328. Röth A, Barcellini W, D'Sa S, Miyakawa Y, Broome CM, Michel M, et al. Sutimlimab in Cold Agglutinin Disease. N Engl J Med. 2021;384(14):1323-34.

329. Roth A, Barcellini W, D'Sa S, Miyakawa Y, Broome CM, Michel M, et al. Complement C1s inhibition with sutimlimab results in durable response in cold agglutinin disease: CARDINAL study 1-year interim follow-up results. Haematologica. 2022;107(7):1698-702.

330. Dhillon S. Sutimlimab: First Approval. Drugs. 2022;82(7):817-23.

331. Röth A, Broome CM, Barcellini W, Jilma B, Hill QA, Cella D, et al. Sutimlimab provides clinically meaningful improvements in patient-reported outcomes in patients with cold agglutinin disease: Results from the randomised, placebo-controlled, Phase 3 CADENZA study. Eur J Haematol. 2023;110(3):280-288. doi:10.1111/ejh.13903 [Epub 2022 Dec 9].

332. Broome CM, Röth A, Kuter DJ, Scully M, Smith R, Wang J, et al. Safety and Efficacy of Classical Complement Pathway Inhibition with Sutimlimab in Chronic Immune Thrombocytopenia. Blood Adv. 2023;7(6):987-996.

333. Mühlbacher J, Jilma B, Wahrmann M, Bartko J, Eskandary F, Schörgenhofer C, et al. Blockade of HLA Antibody-Triggered Classical Complement Activation in Sera From Subjects Dosed With the Anti-C1s Monoclonal Antibody TNT009-Results from a Randomized First-in-Human Phase 1 Trial. Transplantation. 2017;101(10):2410-8.

334. Eskandary F, Jilma B, Mühlbacher J, Wahrmann M, Regele H, Kozakowski N, et al. Anti-C1s monoclonal antibody BIVV009 in late antibody-mediated kidney allograft rejection-results from a first-in-patient phase 1 trial. Am J Transplant. 2018;18(4):916-26.

335. Freire PC, Muñoz CH, Derhaschnig U, Schoergenhofer C, Firbas C, Parry GC, et al. Specific Inhibition of the Classical Complement Pathway Prevents C3 Deposition along the Dermal-Epidermal Junction in Bullous Pemphigoid. J Invest Dermatol. 2019;139(12):2417-24.

336. Kapferer-Seebacher I, Pepin M, Werner R, Aitman TJ, Nordgren A, Stoiber H, et al. Periodontal Ehlers-Danlos Syndrome Is Caused by Mutations in C1R and C1S, which Encode Subcomponents C1r and C1s of Complement. Am J Hum Genet. 2016;99(5):1005-14.

337. Ajona D, Pajares MJ, Corrales L, Perez-Gracia JL, Agorreta J, Lozano MD, et al. Investigation of complement activation product c4d as a diagnostic and prognostic biomarker for lung cancer. J Natl Cancer Inst. 2013;105(18):1385-93.

338. Klikovits T, Stockhammer P, Laszlo V, Dong Y, Hoda MA, Ghanim B, et al. Circulating complement component 4d (C4d) correlates with tumor volume, chemotherapeutic response and survival in patients with malignant pleural mesothelioma. Sci Rep. 2017;7(1):16456. doi: 10.1038/s41598-017-16551-7 [Epub 2017 Nov 28].

339. Khaled SK, Claes K, Goh YT, Kwong YL, Leung N, Mendrek W, et al. Narsoplimab, a Mannan-Binding Lectin-Associated Serine Protease-2 Inhibitor, for the Treatment of Adult Hematopoietic Stem-Cell Transplantation-Associated Thrombotic Microangiopathy. J Clin Oncol. 2022;40(22):2447-57.

340. Lafayette RA, Rovin BH, Reich HN, Tumlin JA, Floege J, Barratt J. Safety, Tolerability and Efficacy of Narsoplimab, a Novel MASP-2 Inhibitor for the Treatment of IgA Nephropathy. Kidney Int Rep. 2020;5(11):2032-41.

8 PUBLICATIONS

8.1 Publications included in the PhD dissertation of the candidate

1) **Hurler L**, Toonen EJM, Kajdácsi E, van Bree B, Brandwijk RJMGE, de Bruin W, Lyons PA, Bergamaschi L; Cambridge Institute of Therapeutic Immunology and Infectious Disease-National Institute of Health Research (CITIID-NIHR) COVID BioResource Collaboration, Sinkovits G, Cervenak L, Würzner R, Prohászka Z. Distinction of early complement classical and lectin pathway activation via quantification of C1s/C1-INH and MASP-1/C1-INH complexes using novel ELISAs. Front Immunol. 2022 Nov 4;13:1039765. doi: 10.3389/fimmu.2022.1039765. PMID: 36420270; PMCID: PMC9677118.

IF: 8.787*****

2) **Hurler L**, Szilágyi Á, Mescia F, Bergamaschi L, Mező B, Sinkovits G, Réti M, Müller V, Iványi Z, Gál J, Gopcsa L, Reményi P, Szathmáry B, Lakatos B, Szlávik J, Bobek I, Prohászka ZZ, Förhécz Z, Csuka D, Kajdácsi E, Cervenak L, Kiszel P, Masszi T, Vályi-Nagy I, Würzner R, Cambridge Institute of Therapeutic Immunology and Infectious Disease-National Institute of Health Research (CITIID-NIHR) COVID BioResource Collaboration, Lyons PA, Toonen EJM, and Prohászka Z (2023). Complement lectin pathway activation is associated with COVID-19 disease severity, independent of *MBL2* genotype subgroups. Front Immunol. 2023 Mar 27;14:1162171. doi: 10.3389/fimmu.2023.1162171. PMID: 37051252; PMCID: PMC10084477.

IF: 8.787*****

Cumulative impact factor of publications related to the PhD dissertation of the candidate: **17.574**

* expected IF value

8.2 Publications independent of the PhD dissertation of the candidate

1) Sinkovits G, Mező B, Réti M, Müller V, Iványi Z, Gál J, Gopcsa L, Reményi P, Szathmáry B, Lakatos B, Szlávik J, Bobek I, Prohászka ZZ, Förhécz Z, Csuka D, **Hurler L**, Kajdácsi E, Cervenak L, Kiszel P, Masszi T, Vályi-Nagy I, Prohászka Z. Complement Overactivation and Consumption Predicts In-Hospital Mortality in SARS-CoV-2 Infection. Front Immunol. 2021 Mar 25;12:663187. doi: 10.3389/fimmu.2021.663187. PMID: 33841446; PMCID: PMC8027327

IF: 8.787

2) Henry BM, Sinkovits G, Szergyuk I, de Oliveira MHS, Lippi G, Benoit JL, Favaloro EJ, Pode-Shakked N, Benoit SW, Cooper DS, Müller V, Iványi Z, Gál J, Réti M, Gopcsa L, Reményi P, Szathmáry B, Lakatos B, Szlávik J, Bobek I, Prohászka ZZ, Förhécz Z, Csuka D, **Hurler L**, Kajdácsi E, Cervenak L, Mező B, Kiszel P, Masszi T, Vályi-Nagy I, Prohászka Z. Complement Levels at Admission Reflecting Progression to Severe Acute Kidney Injury (AKI) in Coronavirus Disease 2019 (COVID-19): A Multicenter Prospective Cohort Study. Front Med (Lausanne). 2022 Apr 29;9:796109. doi: 10.3389/fmed.2022.796109. PMID: 35572977; PMCID: PMC9100416.

IF: 5.058*****

3) Sinkovits G, Réti M, Müller V, Iványi Z, Gál J, Gopcsa L, Reményi P, Szathmáry B, Lakatos B, Szlávik J, Bobek I, Prohászka ZZ, Förhécz Z, Mező B, Csuka D, **Hurler L**, Kajdácsi E, Cervenak L, Kiszel P, Masszi T, Vályi-Nagy I, Prohászka Z. Associations between the von Willebrand Factor-ADAMTS13 Axis, Complement Activation, and COVID-19 Severity and Mortality. Thromb Haemost. 2022 Feb;122(2):240-256. doi: 10.1055/s-0041-1740182. Epub 2022 Jan 21. PMID: 35062036; PMCID: PMC8820843.

IF: 6.830*****

4) Sinkovits G, Schnur J, **Hurler L**, Kiszel P, Prohászka ZZ, Kajdácsi E, Cervenak L, Maráczi V, Dávid M, Zsigmond B, Rimanóczy É, Bereczki C, Willems L, Toonen EJM, Prohászka Z. Evidence, detailed characterization and clinical context of complement activation in acute multisystem inflammatory syndrome in children. Sci Rep. 2022 Nov 17;12(1):19759. doi: 10.1038/s41598-022-23806-5. PMID: 36396679; PMCID: PMC9670087.

IF: 4.997*

Cumulative impact factor of publications independent of the PhD dissertation of the candidate: **25.672**

Total cumulative impact factor of the candidate: 43.246

9 ACKNOWLEDGEMENTS

At this point, I would like to take the opportunity and thank the multitude of individuals who provided me with their support and valuable guidance throughout the completion of my PhD project, and without whom this work would not have been possible.

First of all, I would like to express my sincere gratitude to my main supervisor Prof. Zoltán Prohászka from Semmelweis University Budapest, for welcoming me with open arms in Hungary as well as in his complement lab, for being a great mentor, and for all the encouragement, motivation, and support I've received throughout my project. Nagyon szépen köszönöm!
Deepest thanks also to my co-supervisor Prof. Reinhard Würzner from Medical University Innsbruck, for his continuous support and much valued input and advice on my project, as well as for bringing CORVOS into being.

Sincere gratitude also to everyone hosting me during secondments, with special thanks to Dr. Erik JM Toonen, Loek Willems and Bregje van Bree from Hycult Biotech. It was a great pleasure to gain a deep insight into the non-academic sector, and to see the developed C1-INH complex assays entering the market. Erik, thank you for being my bonus-supervisor, for initiating great and fruitful collaborations, and for trying to improve my scientific writing.

In addition, I'd like to thank the whole CORVOS consortium and all of my colleagues and lab mates from Budapest and Innsbruck for their input, assistance and technical, personal, and administrative support at every stage during my PhD time, as well as Prof. Paul A Lyons and co-workers from the University of Cambridge for the collaboration on our COVID-19 studies. Special thanks to Dr. Erika Kajdacsi, Dr. Ágnes Szilagyi, Dr. György Sinkovits, Dr. Petra Kiszel, Dr. Laszlo Cervenak, Dr. Dorottya Csuka, as well as everyone else from the Research Lab for helping me navigate through the demands of everyday lab-life in Budapest and for creating a great working atmosphere.

I am further grateful for research funding by the EU MSCA project CORVOS 860044, as well as by the Austrian Science Fund (FWF), HOROS W-1253. Additionally, I would also like to thank Prof. Heribert Stoiber and Prof. Doris Wilflingseder (MUI PhD committee), as well as Dr. Nóra Veszeli (internal reviewer) for valuable input on my thesis, as well as Prof. Tamás Németh and Prof. Doris Wilflingseder for accepting the tasks of being my official thesis reviewers.

Finally, getting through my PhD studies required more than only academic support. Therefore, I would like to thank my parents Helga and Erwin, my sisters Anna and Marlene, as well as my whole family and all of my friends, who accompanied and supported me throughout my studies and beyond. I clearly could not ask for better people in my life.